

Stress-laminated timber T-beam and box-beam bridges



Master's Thesis in the International Master's programme in Structural Engineering

AGNIESZKA GILUŃ

JULIA MERONK

Department of Civil and Environmental Engineering

Division of Structural Engineering

Steel and Timber Structures

CHALMERS UNIVERSITY OF TECHNOLOGY

Göteborg, Sweden 412 96

Master's Thesis 2016:2



MASTER'S THESIS 2006:2


Stress-laminated timber T-beam and box-beam bridges

Master's Thesis in the International Master's programme in Structural Engineering

AGNIESZKA GILUŃ

JULIA MERONK

Department of Civil and Environmental Engineering
Division of Structural Engineering
Steel and Timber Structures
CHALMERS UNIVERSITY OF TECHNOLOGY
Göteborg, Sweden 2006

 ss-laminated timber T-beam and box-beam bridges

Master's Thesis in the International Master's programme in Structural Engineering

AGNIESZKA GILUŃ

JULIA MERONK

©  NIESZKA GILUŃ & JULIA MERONK, 2006

Master's Thesis 2006:2

Department of Civil and Environmental Engineering

Division of Structural Engineering

Steel and Timber Structures

Chalmers University of Technology

SE-412 96 Göteborg

Sweden

Telephone: + 46 (0)31-772 1000

Cover:

Top left: Prefabricated T-beam bridge (Moelven Töreboda)

Top right: Lusbäcken bridge in Borlänge in Sweden (box-beam bridge)

Bottom left: Front view of a T-beam bridge

Bottom right: Cross-section of a box-beam bridge

 Department of Civil and Environmental Engineering
Göteborg, Sweden 2006

Stress-laminated timber T-beam and box-beam bridges

Master's Thesis in the International Master's programme in Structural Engineering

AGNIESZKA GILUŃ

JULIA MERONK

Department of Civil and Environmental Engineering

Division of Structural Engineering

Steel and Timber Structures

Chalmers University of Technology

ABSTRACT

Stress-laminated glulam decks with rectangular cross-section have been successfully used since 1989. Since that time, the concept of stress-laminating has received a great deal of attention and hundreds of bridges have been built. In 90s to meet the need for longer spans, researchers shifted their emphasis to new types of cross-section for superstructures. Two types of experimental bridge that have demonstrated very good performance are T-beam and box-beam bridges.

The composite action between the web and the flange in these bridges is developed through friction by stressing the section with high-strength steel bars through the flanges and webs. Box-beam bridge has higher moment of inertia due to additional flanges and stressing bars in the bottom.

This thesis deals with the design of T-beam and box-beam bridges. Every analysed model has one span loaded with one-way road traffic (without pedestrian traffic).

Due to the lack of design regulations in national codes for such bridges the thesis tries to clarify many important issues concerning design. Special attention is paid on the mechanism of load distribution among deck and beams, especially in the case of unsymmetrical load. Load distribution factors and effective flange widths are determined. Other aspects, like local effect of the wheel load including estimation of dispersion angles are also discussed.

Based on the Finite Element Method analyses performed with I-DEAS software, design guidelines proposed by West Virginia University were verified. The hand calculation method seems to give promising results but more evaluation of some formulas is needed.

Finally the thesis gives some recommendations concerning design and construction of the discussed bridges.

Key words: T-beam bridge, box-beam bridge, glulam, stress-laminated decks, timber bridge

Drewniane mosty sprężane poprzecznie o przekroju teowym i skrzynkowym

Praca magisterska w ramach międzynarodowych studiów magisterskich na kierunku Konstrukcje Inżynierskie

AGNIESZKA GILUŃ

JULIA MERONK

Wydział Inżynierii Lądowej i Środowiska

Division of Structural Engineering

Steel and Timber Structures

Chalmers University of Technology

ABSTRAKT

Mosty płytowe poprzecznie sprężane wykonywane z drewna klejonego warstwowo są używane z powodzeniem od 1989 roku. Od tego czasu koncepcja sprężenia mostu zyskała powszechne uznanie i wybudowano wiele tego typu mostów. W latach dziewięćdziesiątych ze względu na zapotrzebowanie na dłuższe przęsła naukowcy zajęli się nowymi rozwiązaniami przekroju poprzecznego mostu. Podczas badań dwa typy mostów wykazały się wyjątkowo dobrą nośnością: most o przekroju teowym i most o przekroju skrzynkowym.

Praca zespolona pomiędzy środkiem a półką w tych mostach jest uzyskana dzięki tarcii, powstałemu na skutek sprężenia poprzecznego przekroju prętami ze stali wysokowytrzymałej. Mosty o przekroju skrzynkowym mają większy moment bezwładności dzięki dodatkowej półce dolnej, która również jest sprężana.

Ta praca magisterka dotyczy projektowania mostów o przekroju teowym i skrzynkowym. Wszystkie analizowane modele to mosty jednoprzęsłowe, jednokierunkowe, z przeznaczeniem dla transportu samochodowego.

Ze względu na brak usystematyzowanych wytycznych do projektowania takich mostów w normach państwowych, praca próbuje wyjaśnić istotę ważnych aspektów potrzebnych w projektowaniu. W pracy szczególny nacisk położono na analizę rozdziału obciążenia pomiędzy dźwigarami, szczególnie w przypadku obciążenia niesymetrycznego. Wyznaczono współczynniki rozdziału obciążenia i długość efektywną półki. W pracy dokonano również przeglądu innych zagadnień takich jak lokalny wpływ koła - w tym określenie kąta rozproszenia obciążenia.

Na podstawie analizy Metodą Elementów Skończonych przeprowadzonej za pomocą programu I-DEAS, zostały zweryfikowane zalecenia do projektowania proponowane przez West Virginia University. Badania metodami numerycznymi wykazały, że niektóre wzory empiryczne wymagają korekt i poprawek.

Ostatecznie osiągnięto cel pracy, jakim było ustanowienie zaleceń i wytycznych dla potrzeb projektowania i wykonawstwa rozpatrywanych mostów drewnianych

Słowa kluczowe: most teowy, most skrzynkowy, drewno klejone warstwowo, mosty drewniane, płyta sprężona poprzecznie

Contents

ABSTRACT	I
ABSTRAKT	III
CONTENTS	V
PREFACE	IX
NOTATIONS	X
1 INTRODUCTION	1
1.1 Stress-laminated bridges	1
1.1.1 General information	1
1.1.2 Types of deck system	1
1.2 Problem description	4
1.2.1 Aim and scope	4
1.2.2 Limitations	5
1.2.3 Method	5
1.2.4 Outline	6
1.3 Examples of existing T-beam and box-beam stress-laminated bridges	6
2 ELEMENTS OF STRESS-LAMINATED BRIDGES	10
2.1 Stress-laminated deck	10
2.2 Prestressing system	11
2.2.1 Prestressing elements and anchorage	11
2.2.2 Stress loss and prevention	12
3 BRIDGE CONSTRUCTION	14
3.1 General description	14
3.2 Stressing methods	16
3.3 Features of stress-laminated bridges	18
3.3.1 Advantages	18
3.3.2 Disadvantages	18
4 MATERIAL DESCRIPTION	19
4.1 Characteristic strength and stiffness parameters	20
4.2 Design values of material properties [EC5 (1993)]	21
4.2.1 Partial factor for material properties γ_M	21
4.2.2 Service classes	22
4.2.3 Load-duration classes	22
4.2.4 Stiffness parameters in the serviceability limit state.	22
5 LOAD ANALYSIS	24

5.1	Actions on the bridge	24
5.1.1	Permanent loads	24
5.1.2	Variable load	25
5.2	Load combinations	25
5.2.1	Combination in Serviceability Limit State	26
5.2.2	Combination in Ultimate Limit State	26
6	DEVELOPMENT OF HAND CALCULATION - WVU DESIGN METHOD (DAVALOS AND SALIM 1993, TAYLOR ET AL. 2000)	27
6.1	Determination of the effective flange width	27
6.2	Determination of wheel load distribution factors (W_f)	29
6.3	Design the deck for the local effects	31
6.3.1	Maximum local deflection	31
6.3.2	The maximum local transverse stress	31
6.4	Global analysis	32
6.4.1	Bending stresses	32
6.4.2	Maximum shear stresses	33
6.4.3	Maximum punching shear stress	34
6.4.4	Maximum shear in the surface between web and flange	35
6.5	Check of the deflection	36
6.5.1	Live load deflection	36
6.5.2	Dead-load deflection (Initial stage)	38
6.5.3	Long-term deflection	38
6.6	Check of Vibrations according to BRO 2004	39
7	FINITE ELEMENT ANALYSIS	40
7.1	Description of Model 1	40
7.1.1	Mesh	40
7.1.2	Boundary conditions	41
7.1.3	Material properties	41
7.2	Description of Model 2	42
7.2.1	Mesh	42
7.2.2	Boundary conditions	42
7.2.3	Material properties	43
7.3	Determination of effective flange width	43
7.3.1	Acting load	45
7.3.2	Method	45
7.3.3	Results	46
7.3.4	Comparison of finite element method and hand calculation	50
7.4	Transversal load distribution	52
7.4.1	Description of the analysis	52
7.4.2	Comparison of the results and conclusions	54
7.4.3	Check of the uplifting force for T-beam bridge	65
7.5	Local effect of the wheel load	66

7.5.1	Wheel load between the webs	67
7.5.2	Dispersion of a concentrated load	72
7.6	Global analysis of the bridge performed by FEM	76
7.6.1	General description	76
7.6.2	Load combinations	76
7.6.3	Comparison of the results from FEM and hand calculation	78
7.6.4	Analysis of the T-beam and box-beam bridge in the ULS	79
7.7	Dynamic analysis	83
8	FINAL REMARKS	85
8.1	Discussion	85
8.2	Conclusions from the studies	85
8.3	General recommendations after literature study	86
9	REFERENCES:	88
	APPENDIX A – MATHCAD FILE TO PERFORM AN ANALYSIS OF A T-BEAM BRIDGE DECK	90
	APPENDIX B – MATHCAD FILE TO PERFORM AN ANALYSIS OF A BOX-BEAM BRIDGE DECK	105
	APPENDIX C – COMPARISON OF MAXIMUM VALUES OF STRESS AND DEFLECTION OF THE BRIDGE FOR DIFFERENT CONFIGURATIONS OF MODEL 1	119
	APPENDIX D – MATHCAD FILE TO CALCULATE SHEAR STRESSES IN A T-BEAM BRIDGE DECK	123

Preface

This master's project deals with the design of stress-laminated timber T-beam and box-beam bridges. The work has been carried out from September 2005 to January 2006 at the Division of Structural Engineering, Department of Civil and Environmental Engineering at Chalmers University of Technology. The thesis completes the authors' International Master's Programme in Structural Engineering at Chalmers University of Technology.

At the beginning we would like to thank our supervisor Dr. Eng. Roberto Crocetti, engineer at MOELVEN Töreboda, Sweden, for proposing the subject of the thesis and constant assistance throughout the work. Additionally we would like to thank him for the possibility of visiting the factory of glulam and seeing the bridges completely assembled there, what widened our perspective on the topic

Secondly we would like to thank Professor Robert Kliger, the examiner, for his important remarks, support and help in getting literature in the field.

We would also like to thank Assistant Professor Mohammad Al-Emrani for his great help especially with software problems.

We also appreciate the valuable comments of our opponent Abu Thomas Zachariah.

To reach the aim of the master's project it was very important to perform an extensive literature study at the beginning. The source of the greatest importance ('Design of Stress-Laminated T-system Timber Bridges' Davalos, J. and H. Salim 1992) was obtained from the Constructed Facilities Centre at West Virginia University. The second very useful report 'Evaluation of Stress-Laminated Wood T-Beam and Box-Beam Bridge Superstructures' could have been studied thanks to Steven Taylor, professor of Auburn University and the main author of the report.

Göteborg January 2006

Agnieszka Giluń
Julia Meronk

Notations

Roman upper case letters

A	Area of cross-section
B	One-half clear distance between the webs
D	Depth of portion of web that is outside the deck
E_{Lf}	Longitudinal modulus of elasticity of the flange
E_{Lw}	Longitudinal modulus of elasticity of the web
E_{Tf}	Transverse modulus of elasticity of the flange
E_{Tw}	Transverse modulus of elasticity of the web
F	Point load
$F_{v.Ed}$	Design shear force per unit length
G_0	Shear modulus
I	Moment of inertia of the transformed section
I_{ex}	Composite moment of inertia of the edge beam plus the overhanging flange width
L	Length of the bridge span
M	Live load bending moment
M_g	Dead load bending moment
N_L	Number of traffic lanes
P_k	Wheel point force, characteristic value
S	Spacing of webs
S_c	Clear distance between the webs
S_x	First moment of area of the shear plane at the level of consideration
V	Shear force
V_{res}	Resisting frictional force
W	Width of the bridge
W_f	Wheel distribution factor

Y Distance from T-beam neutral axis to the top or bottom fibres

Roman lower case letters

a_{RMS}	Vertical acceleration
b	Centre to centre distance between exterior webs
b_{ef}	Effective width of the flange
b_m	Overhanging flange width
b_l	Tire contact length in the direction of span
b_w	Width of the load area on the contact surface of the deck plate
$b_{w,middle}$	Width of the load area referred to the middle lane of the deck plate
b_x	Width of exterior flange
e	Distance from flange mid-surface to transformed section neutral axis
f_{cd}	Design value of the compression stress perpendicular to the grain
f_{md}	Design value of the bending stress parallel to the grain
f_n	Natural frequency
f_p	Final pre-stress level
f_{td}	Design value of the tensile stress parallel to the grain
f_{t90d}	Design value of the tensile stress perpendicular to the grain
f_{vd}	Design value of the longitudinal shear stress
g_1	Self-weight load
g_2	Surface load
h_w	Height of the web
k_{def}	Factor taking into account the increase in deformation with time
k_{mod}	Modification factor for duration of load and moisture content
n	Number of webs across the bridge width
n_w	Number of webs
m	Total mass of the bridge per unit length

q_{1Bk}	Uniformly distributed traffic load, characteristic value
s_1	Wearing layer thickness
s_2	Deck thickness
t	Width of a lamina
t_f	Thickness of the flange
t_w	Thickness of the web
v	Velocity of the vehicle

Roman lower case letters

α	Aspect ratio b / L
β	Dispersion angle of concentrated loads
γ	Load coefficient
γ_M	Partial factor for material properties
δ	Deflection
λ	Aspect ratio S / t_f
μ	Coefficient of friction
ν_0	Poisson's ratio
ρ	Density
σ	Bending stress
$\sigma_{p,min}$	The minimum long-term residual compressive stress due to prestressing
τ	Shear stress

1 Introduction

1.1 Stress-laminated bridges

1.1.1 General information

Stress-laminating is one of the newest techniques used in modern timber bridge construction. The concept originated in Canada in the mid-1970s as a rehabilitation method for nail-laminated timber bridges. In the 1980s the concept was adapted for the construction of new bridges and numerous structures in Canada were successfully built or rehabilitated using the stress-laminating concept. Since that time several hundred stress-laminated timber bridges have been constructed, mainly on low-volume roads. Although most of these types of bridges are plate deck systems made from sawn timber or glulam, the technology has been extended to stress-laminated T-beam, box-beam and cellular sections.

Stress-laminated timber bridges are constructed by compressing edgewise placed timber components together with high-strength steel bars to create large structural assemblies. The bar force, which typically ranges from 111 to 356kN squeezes the laminations together so that the stressed deck acts as a solid wood plane. In contrast to longitudinal glued-laminated assemblies, which achieve load transfer among laminations by structural adhesives or mechanical fasteners, the load transfer between laminations is developed through compression and interlaminar friction. This interlaminar friction is created by the high-strength steel stressing elements typically used in prestressed concrete. The most critical factor for the design is to achieve adequate prestress force between the laminates so that the orthotropic plate action is maintained.

1.1.2 Types of deck system

1.1.2.1 Plate decks

Since 1980s only in the USA over 150 stress-laminated bridges using sawn timber laminations have been built. A specification for the design of these kinds of bridges was published by the American Association of State Highway and Transportation Officials.

In the 1989, the concept of stress-laminated decks was expanded to use glulam beams, rather than sawn timber, as deck laminations. The reason was a need for greater depth than could be provided by sawn timber. The first known example of this type of construction was the Teal River Bridge constructed in 1992 in Wisconsin in USA.

In Sweden, based on the Nordic Timber Bridge Program, two hundred timber bridges have been erected since 1994. About half of them are stress-laminated decks.

Typical stress-laminated deck bridge is shown in Figure 1.1

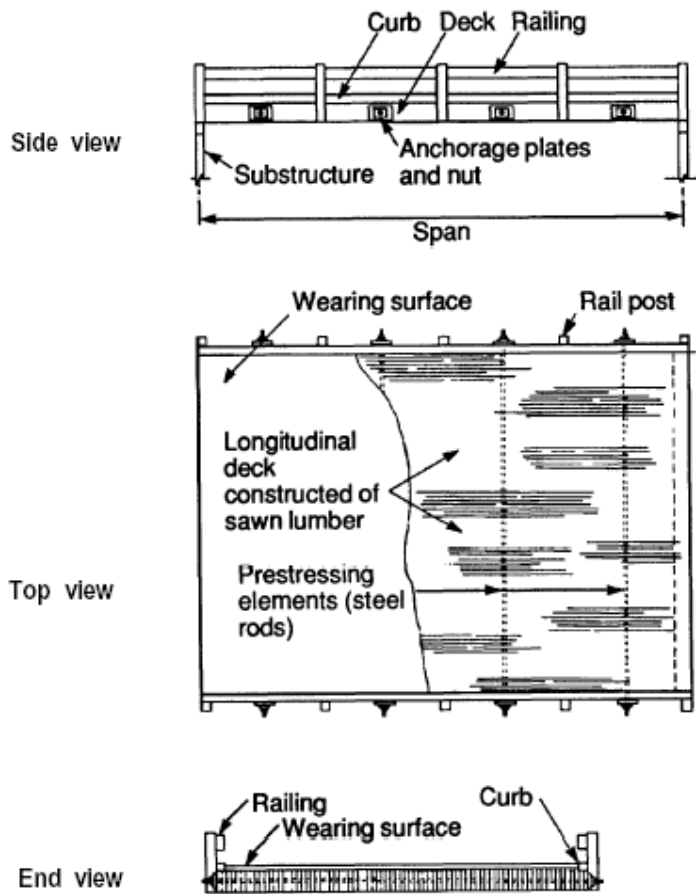


Figure 1.1 Configuration of a longitudinal stress-laminated deck. [Ritter (1992)]

Stress-laminated decks are also often used in modern truss bridges. Use of such a deck in for example King-Post truss bridge (see Figure 1.2) assures more uniform distribution of traffic load on the cross-girders and then on the truss.

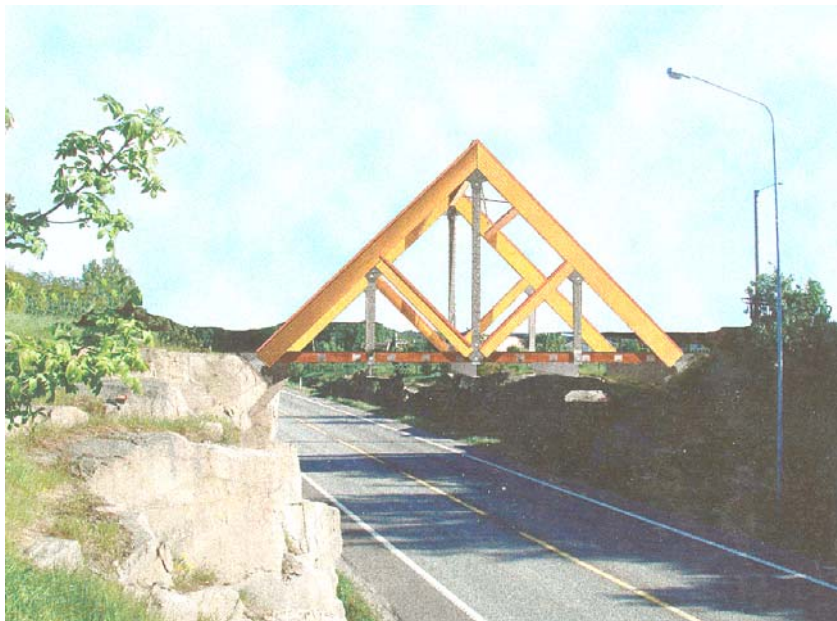


Figure 1.2 A King-Post truss bridge. [Cesaro and Piva (2003)]

Bridges using glulam in stress-laminated deck have demonstrated very good performance. They are more attractive than bridges with sawn timber decks especially for low-volume roads. Thanks to finger joints, glulam can be produced to be continuous over the bridge length. Therefore butt joints that can reduce the bridge strength and serviceability are not required.

However as the clear span of stress-laminated decks is limited by the design and economical limitations on the bridge depth, other options have been investigated.

1.1.2.2 Built-up decks

Because of the limitations of the plate decks, as mentioned in the previous section, stress-laminating has been extended to T-beam and box-beam bridges. The structure of such bridges consists of glulam web members and glulam flanges, see Figure 1.3. The box-beam bridge section is almost the same as the T-beam one, but the flanges and stressing bars are added to create a higher moment of inertia. The composite action between the flange and the web is developed through friction by prestressing the section with stressing bars through the flange and the webs. The potential advantage of these bridges is their improved stiffness, which allows for longer spans than a homogeneous plate without a corresponding increase of the wood volume.

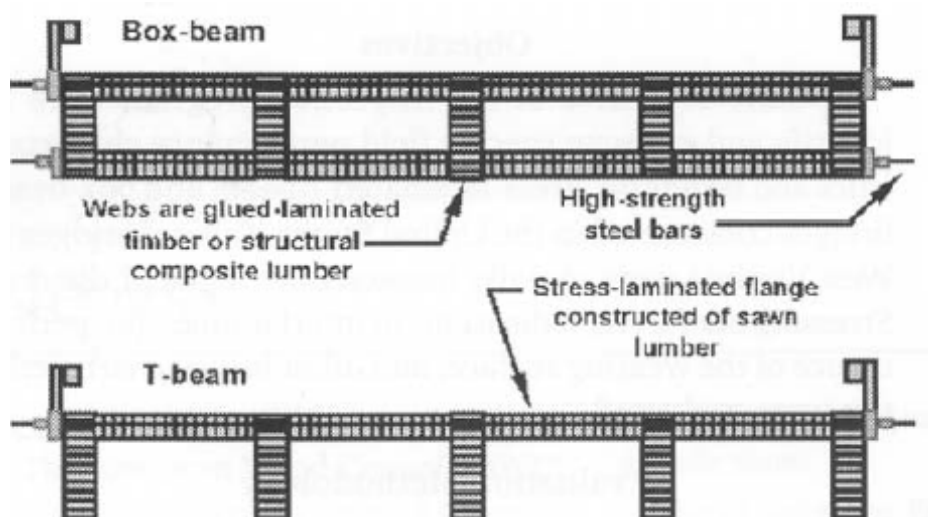


Figure 1.3 Schematics of stress-laminated T-beam and box-beam bridges. [Taylor et al. (2002)]

The first stress-laminated T-beam bridge in the world is a 75-foot (~2.9m), single-lane structure built in Charleston, West Virginia in 1988. The next stress-laminated T-beam bridges were constructed after 1992 with spans up to 119ft (~36.3m). However, the recommended lengths of spans are shorter than the ones of the bridges built in USA. For T-beam decks the span varies from 10m for road bridges, to approximately 15m for pedestrian bridges and for box-beam decks the spans are 15-25m long for road bridges, and up to 30m for foot-bridges (Pousette et al. 2001).

In Australia cellular decks similar in concept to the box-beam were also developed. The difference is that, in cellular deck the webs are spaced more closely and are thinner, see Figure 1.4. The spacing between the webs should not exceed 500mm. The webs typically are made from LVL with thickness from 45 to 63mm.

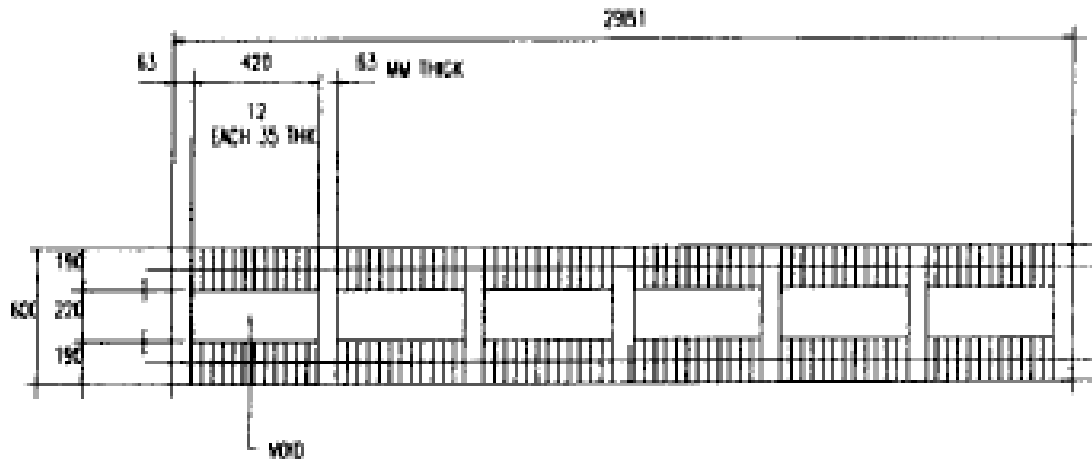


Figure 1.4 Schematics of stress-laminated cellular deck. [Crews (1996)]

1.2 Problem description

The design guidelines for a stress-laminated deck are included in AASHTO (1991) as well as they can be found in Ritter (1992).

However, the design and manufacturing of the bridges with build-up decks is considerably more complicated than for a solid plate. That's why in spite of numerous stress-laminated T-beam and box-beam bridges have been built, design specifications for these bridges are not in the AASHTO specifications and any other national code yet. They are still considered experimental as many unanswered questions about load distribution characteristics and economics remain.

1.2.1 Aim and scope

The aim of the thesis is to develop a relatively simple routine that enables design of T-beam and box-beam bridges by means of hand calculations. The proposed design method is based on the design guidelines for stress-laminated bridge decks found in EC5 (2004) and the design recommendations by West Virginia Division of Highways.

Special attention is paid on the mechanism of load distribution among deck and beams, especially in the case of unsymmetrical load. The research tries to clarify issues about load distribution factors and effective flange width.

Other aspects, like local effect of the wheel load are also analysed. Finally the global analysis of the bridge is performed.

Furthermore the utilization of analysed models of T-beam and Box-beam bridges was investigated and compared.

An assessment of the proposed design method is made by comparing its results to those given by independent models performed by Finite Element Method in I-DEAS, commercially available software.

Additionally in the beginning of the thesis general information about build-up decks especially regarding construction methods and durability was gathered.

1.2.2 Limitations

The models that are studied in the thesis are T-beam and box-beam bridges, other types of bridge deck system were not considered in the calculations.

The thesis contains only analysis of the bridge deck; it does not include any study of abutments, columns or foundation.

The analysis is only carried out on the structure when adequate prestress force between the laminations is induced so the composite action between flange and web can be assumed. This assumption seems to be accurate because after monitoring number of bridges in USA, only in one, structural problems due to the loss of the force in stressing bars below minimum limits was detected. Vertical slip of the laminations was caused by heavy traffic. After slip occurred, the bridge continued to carry traffic at a reduced load level until it was restressed and subsequently repaired. When slip of this type occurs, the stressing bars act as dowels among laminations; the failure primarily affects serviceability and is very evident. Therefore the monitoring of the bridge should be performed to made appropriate repair before further problems develop. (Ritter et al. 1995) The slip between lamellas is not considered in this thesis.

1.2.3 Method

To reach the aim of the master's project it was very important to perform an extensive literature study at the beginning. During this study two sources of the design guidelines for hand calculation of build-up bridges (Davalos, Salim 1992; Taylor et al. 2000) were found. To verify these methods by comparing with the results of Finite Element Method analysis, 15m long single span bridge with the width of 4.5m was modelled (Crocetti 2005). The model in Figure 1.5 was analysed with different geometrical configurations of the cross-section depending on number of webs and also with a box-beam cross-section.

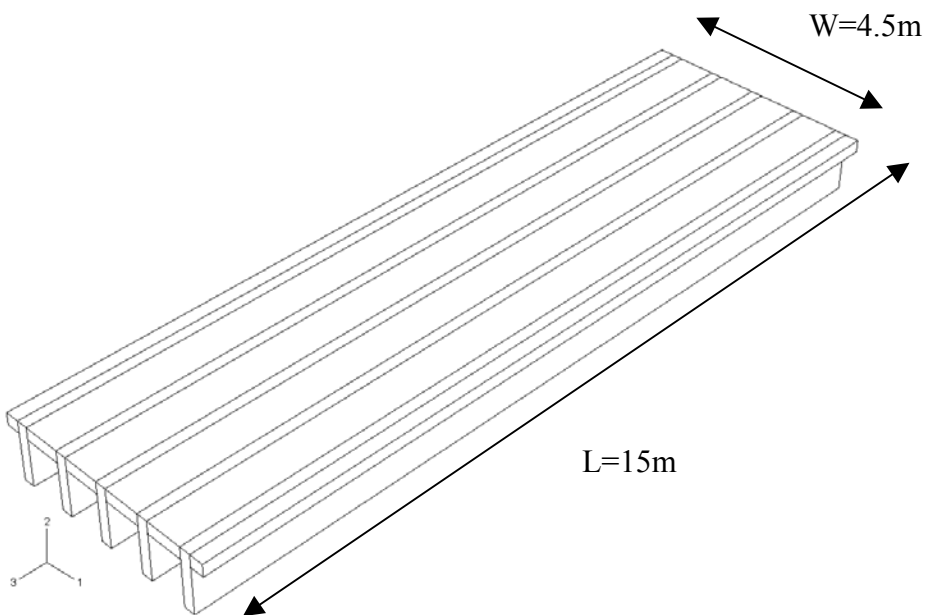


Figure 1.5 Sketch of the analysed model of the bridge

After performing hand calculation in MathCAD, the Finite Element Method analysis of different models was conducted in I-DEAS. Based on the comparison between the results of hand calculation and FEM analysis the conclusions about accuracy of the formulas found in literature were drawn.

1.2.4 Outline

Background of the thesis, description of the problem and examples of existing T-beam and box-beam stress-laminated bridges can be found in Chapter 1. A detailed description of parts of the stress-laminated bridges is included in the Chapter 2. The procedure of the bridge assembly and the reasons for using stress-laminated bridges as well as the disadvantages of such constructions are presented in Chapter 3. Description of glulam, as it is the most common material for stress-laminated decks is in Chapter 4. The description of the analysis of the models starts in Chapter 5 with the presentation of loads acting on the structure. The development of hand calculation can be found in Chapter 6. Finite Element Method analysis as well as the comparison of its results with the hand calculation is included in Chapter 7. Final conclusions can be found in Chapter 8.

1.3 Examples of existing T-beam and box-beam stress-laminated bridges

The biggest number of T-beam and box-beam stress-laminated bridges was erected in USA, Australia and Nordic countries. A few of these existing bridges have been chosen to present below with some general information and design configuration.

- **Väg 50 Borlänge-Falun, Sweden**



Structure type	T-beam stress-laminated glulam bridge
Year of construction	2004
Number of spans	2
Bridge type	Pedestrian

Total length 50m
Width 4,035m

- **North Siwell bridge in Mississippi in USA**



Structure type T-beam bridge, stress-laminated glulam webs and sawn timber butt jointed flanges
Year of construction 1994
Number of spans 1
Bridge type vehicle
Total Length 9,1m
Width 8,8m

- **Lusbäcken bridge in Borlänge in Sweden**



Structural system	Box-beam stress-laminated glulam bridge
Year of construction	1998
Number of spans	1
Bridge type	vehicle
Total length	21m
Width	8m

- **Alsterån bridge in Uppvidinge in Sweden**



Structural system	Box-beam stress-laminated glulam bridge
Year of construction	2000
Number of spans	1
Bridge type	vehicle
Total length	23m
Width	4,5m

- **Spearfish Creek bridge in South Dakota in USA**



Structural system	Box-beam stress-laminated glulam bridge
Year of construction	1992
Number of spans	1
Bridge type	vehicle
Length	19,8m
Width	11,3m

2 Elements of stress-laminated bridges

2.1 Stress-laminated deck

As previously stated stress-laminated decks are constructed by laminating together pieces of timber, which have been placed on the edge, until the desired width is achieved. Later timber members are compressed through application of a post-tensioned prestress in the transverse direction.

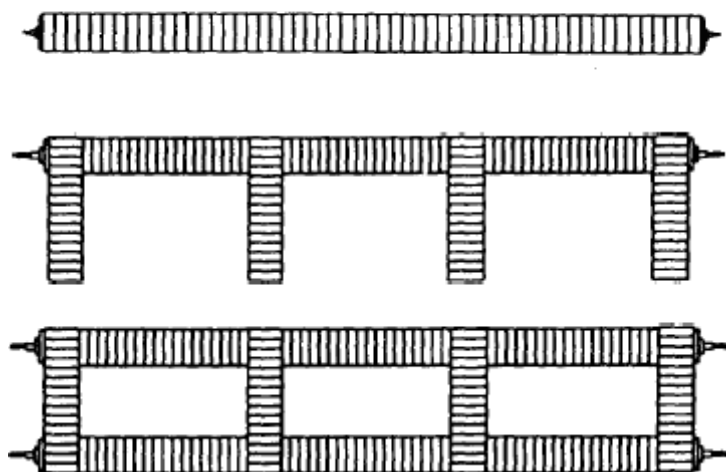


Figure 2.1 Typical cross-sections of stress-laminated bridges. [Ritter et al. (1994)]

Stress-laminated decks behave as orthotropic plates. That means they have different properties in the longitudinal and transverse directions. When the wheel load is applied, the entire deck deflects with different displacements in both longitudinal and transverse directions. Five features determine the bending moment that cause the deflection and bending stress: load magnitude, deck span, deck width, longitudinal and transverse deck stiffness.

When the wheel load is placed at any point of the deck, two actions of deterioration of the plate can appear. Transverse bending moment can produce a tendency for opening between the laminations on the deck underside. Secondly, transverse shear force may develop a tendency for laminations to slip vertically, see Figure 2.2. To avoid that the sufficient prestress level must be held in the deck during the lifetime.

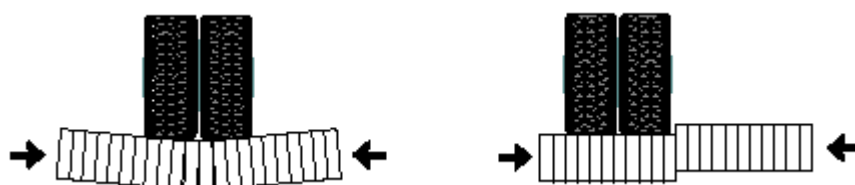


Figure 2.2 Load transfer between laminates in the stress-laminated deck. [Ritter (1992)]

Maintaining the compressive stress in the deck is one of the most important aspects of this type of construction. For acceptable performance, this compression must be sufficient to prevent vertical slip and opening between laminations. Therefore current design procedures recommend a minimum interlaminar compression of 0,69MPa at the time of bridge construction. Research has shown that slip between the laminations does not begin until the interlaminar compression has been reduced to 0,165MPa. (Ritter et al. 1995)

2.2 Prestressing system

2.2.1 Prestressing elements and anchorage

Due to the fact that the prestressing system holds the bridge together and develops necessary friction, it is one of the most important parts of stress-laminated bridges. The system consists of prestressing elements and anchorages.

Prestressing elements are placed transverse to the bridge span and are stressed in tension with the force up to 356kN. The high strength and corrosion resistance steel should be used. One of the possible methods of protecting the rods from corrosion is galvanizing them during manufacturing process. This method avoids embrittlement and strength loss in the steel. Other possibility used successfully in Canada is a plastic pipe that is placed over the rods and filled with grease.

The second part of the prestressing system is anchorage. Main function of anchorage is to transfer the required stress to the laminations without causing wood crushing in the outside timber parts. It also must be capable of developing the full capacity of prestressing elements. The rod is placed through the steel plates and anchored with a nut. Two different types of anchorage are proposed (Ritter 1992).

First one considers the rehabilitation of existing deck. In this case the rods are placed externally over and under laminations and the continuous channel along the deck edges is proposed, see Figure 2.3.

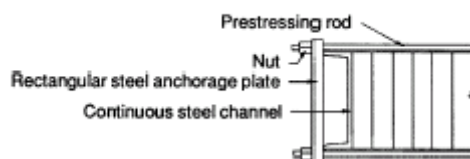


Figure 2.3 External channel bulkhead anchorage configuration. [Ritter (1992)]

For the new bridges where the rods are placed internally through the holes in laminations two solution are possible, see Figure 2.4 and Figure 2.5.



Figure 2.4 Channel bulkhead anchorage configuration. [Ritter (1992)]



Figure 2.5 Channel bearing plate anchorage configuration. [Ritter (1992)]

Recently, mainly the second type of anchorage with rectangular steel bearing plate and a smaller outside plate has been used.

2.2.2 Stress loss and prevention

For acceptable performance of the bridge, all bars must have sufficient level of uniform, compressive stress. During the initial prestressing, the stress loss can be affected by creep in the wood and the variation in moisture content.

Studies in Ontario in Canada (Ritter 1992) showed that the loss of compression in timber caused by creep increased when the cross-sectional area of the steel prestressing components increased. During this research it was found also that using high-strength steel rods that can carry the large prestressing force with a minimum cross-section of steel could reduce this effect. The amount of creep is directly related to the number of times the deck is stressed. If the deck is stressed only once during construction, 80 percent or more of initial compression may be loss in creep. If the deck is restressed within a relatively short period the stress loss is less.

Changes in moisture content of wood can affect strength, stiffness and dimension stability. Below fibre saturation point at approximately 30 percent, wood will expand as moisture is absorbed and contract when moisture is desorbed. In stress-laminated bridges dimension instability can strongly affect bridge performance.

The noteworthy advantage of glulam over sawn timber is the smaller loss in bar force (force in high-strength steel bars that compress the deck) due to changes of moisture content. Because the glulam is dry, when installed, the laminations slowly absorb moisture and the elements swells slightly as it moves towards equilibrium moisture content. As a result, this swelling offsets force loss due to the stress relaxation in the wood.

Based on field evaluation (Ritter et al. 1994), the best bridge performance has been observed when the moisture content of the wood laminations at the time of

construction averages 10 to 16 percent. Acceptable performance has been observed when the moisture content is from 16 to 20 percent. When the moisture content is exceeding 20 percent, unfavourable performance becomes more pronounced and the moisture content of the bridge is increased.

Because of the above problems to maintain the minimum stress level, the following stress sequence is used (Ritter 1992):

- Firstly the deck is initially assembled and stressed to the design level required for the structure,
- Approximately after one week after initial prestressing the deck is restressed to the full level,
- Final stressing is completed four to six weeks after the second stressing.

When this sequence is followed not more than 50 till 60 percent of the stress will be lost over the life of the structure.

Based on monitoring results (Ritter et al.1995), it appears that above stressing sequence can be not enough in many cases, especially for bridges made from sawn timber. Many of these bridges after monitoring within the two year after construction need restressing. For bridges constructed with sawn timber, field observations indicate that the bar force should be checked at annual intervals for the first 2 years after construction and every 2 years thereafter. After bar force stabilizes, this period may be extended to 2- to 5-year intervals. For bridges constructed of glued laminated timber, field observations indicate that bar force should be checked every 2 years for the first 4 years after construction and every 5 years thereafter.

The bar force can also decrease when the temperature drops. The magnitude of this decrease depends on the temperature change, duration of cold temperature, the wood species and the moisture content. The temperature effect is most pronounced when the wood moisture content is at or above fibre saturation point. Short-term temperature declines over the period of 24 hours or less have little effect on bar force due to the fact that wood has low thermal conductivity. According to USA monitoring programme the cold temperature appears to be fully recoverable, and the bars force returns to the original level when the temperature is increased. However Nordic Timber Bridge Project (Pousette 2001) showed that there was a certain risk that the prestressing force would be too low the first winter unless restressing was carried out after about six months. Consequently it is vital to check prestress during the first year and in cold winters.

3 Bridge Construction

3.1 General description

A number of methods have been used to construct stress-laminated timber bridges. Methods can involve assembly on a site or manufacture in a factory.

When assembling on the bridge site, two options are possible. First one considers continuous laminations (no butt joints). They can be individually placed on abutments, bars can be inserted and the bridge stressed in place. Second option is to assemble the bridge at a staging area adjacent to the crossing, and then to lift the entire deck into place.

However in many applications the preferable method of assembly involves prefabrication of elements in the factory. The panels can be prefabricated, shipped to the bridge side, lift into a place and stressed together to form a continuous deck.

Depending on the transportation restrictions, there is also a possibility of construction of a whole bridge in the factory, see Figure 3.1. Firstly it is assembled and prestressed, next step is transportation and lifting into the place, see Figure 3.2. This method is economical and requires a minimum time for erection. Another advantage is that the restressing sequence can be completed in the fabric and no restressing on the bridge site is required.



Figure 3.1 Assembling the whole bridge in the factory. (Moelven Töreboda)



Figure 3.2 Transporting the prefabricated bridge into the site. (Moelven Töreboda)

3.2 Stressing methods

For acceptable bridge performance, all bars must be uniformly stressed to the full level during each of the three required stressings (see Chapter 2, Section 2.2.2). The laminations are stressed together with a hydraulic jack that applies tension to the prestressing rod by pulling the rod away from steel anchorage plates, see Figure 3.3. After the tension is applied, the nut is tightened against the anchorage plate and the tension remains in the rod when jack pressure is released.

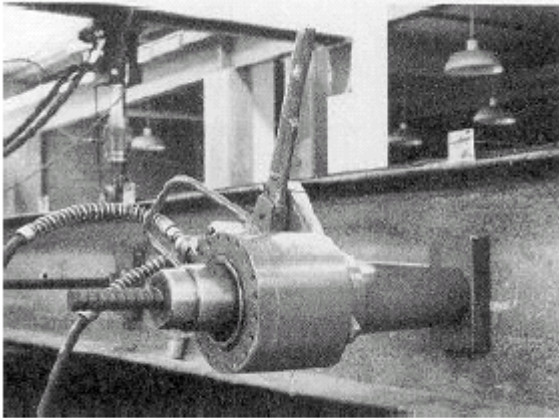


Figure 3.3 Hydraulic jack used to prestress stress-laminated bridges. (Ritter 1992)

The number of used jacks influences the loss of the prestressing force in time. When using the single-jack method, jacking starts at the first rod on one end of the bridge and is continued to the last rod on the opposite end. Field observations indicate that, when a single jack is used, stressing one bar compresses the deck at that location and reduces the force in adjacent bars. In bridges where each bar was stressed only one time, substantial variations in bar force were noted. To prevent these variations, to keep the bridge edges parallel and straight, each bar must be stressed several times starting at a low prestress that is gradually increased until the prestress level is uniform for all bars. The most successful construction method for accomplishing this uniformity is to begin stressing at one bridge end and sequentially stresses each bar along the bridge length. The design level of prestressing force is achieved by making four passes along the deck.

Using a multiple-jack system is more convenient but the purchase or renting it is more expensive. When using this system the entire deck is stressed in one operation.

Attachments to the bridge including curbs and railings should not be made until the bridge has been fully stressed two times. (Ritter et al. 1995)

The typical spacing between stressed rods is showed on two design drawings below, Figure 3.4 and 3.5. As it can be observed the spacing is almost the same for both types of bridge and different span length.

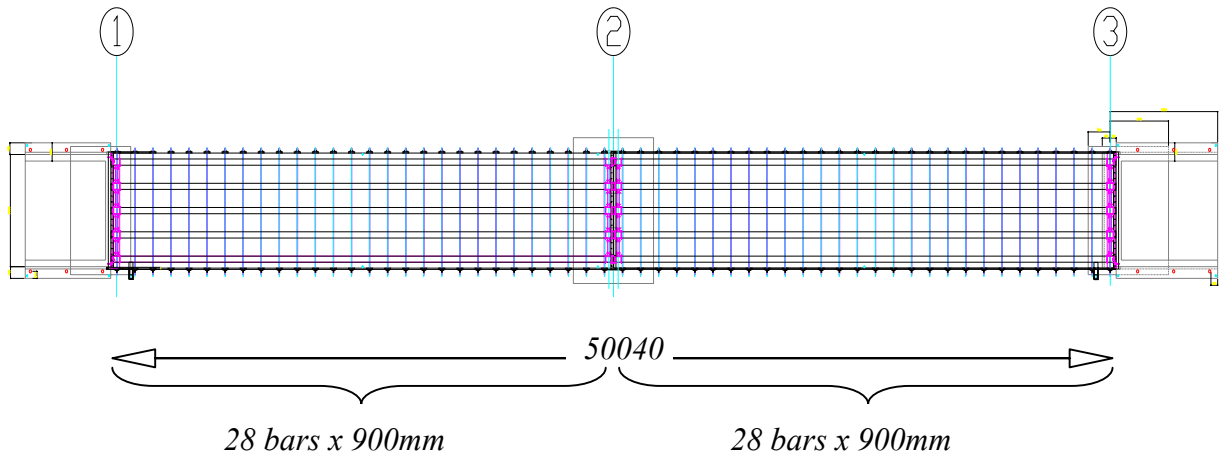


Figure 3.4 Distance between prestressed bars for a double span T-beam pedestrian bridge in Falun. (Moelven Töreboda)

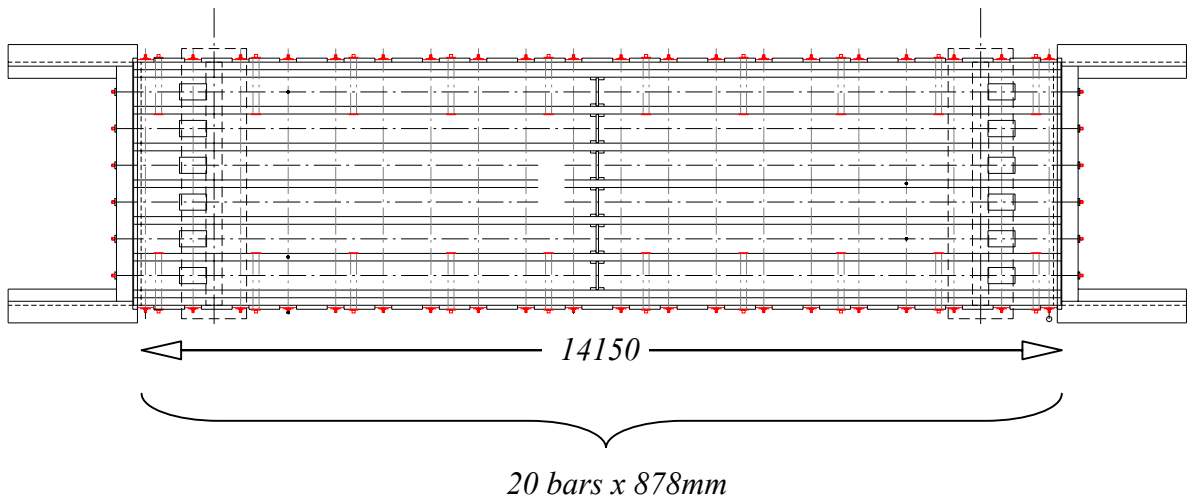


Figure 3.5 Distance between prestressed bars for a single span Box-beam bridge. (Moelven Töreboda)

3.3 Features of stress-laminated bridges

3.3.1 Advantages

1. For spans no longer than 20m the price of stress-laminated bridges compared to those using other bridge materials can be lowered by 20%. This is due to the fact that the components are lighter and do not need very large concrete supports and foundations. As well as they do not demand any highly skilled labour and specialized equipment for assembly.
2. Stress-laminated bridges can be very fast erected. The reason is that they can be completely prefabricated at the fabrication plant and shipped to the project site.
3. The design service life is assumed to be 80 years. (Crocetti 2005) It depends on the accuracy and quality of fabrication and construction. When proper and careful practices dominate, both the economics and long-term serviceability of the bridge will be not affected.
4. The elements of stress-laminated timber bridges can be constructed from sizes and lengths of timber commercially available.
5. Stress-laminated glulam deck bridges have no butt joints, they provide improved load distribution characteristic compared to stress sawn timber beam bridges with butt joints.
6. In the past, several wood deck systems employing nail-laminated timber have been associated with cracking or disintegration of asphalt wearing surfaces. Differential movements among individual laminations or vertical movement at joints caused the deterioration. Because stress-laminated decks act as a large wood plates and the applied prestress sufficiently prevents vertical movement of the individual laminations, asphalt cracking and deterioration were not observed on any of the stress-laminated decks. (Ritter et al.1995)
7. There is no fatigue problem in timber bridges like in steel and concrete bridges.

3.3.2 Disadvantages

1. The timber structures have relatively low stiffness in nature, so the design process is often determined by Serviceability Limit State rather than Ultimate Limit State. Stress-laminated timber bridges are more flexible than comparable decks built from either concrete or steel.
2. Current design regulation in Europe and USA do not include design guidelines for T-beam and box-beam stress-laminated bridges.
3. Durability of timber connections.

4 Material Description

Nowadays the most common materials for stress-laminated bridges are glulam beams.

Glued laminated timber is a highly engineered building material, providing many advantages over solid timber. It is made by aligning sheets (called lamellas) of wood in the direction of the grain and gluing them together. The fact that it is a manufactured product, glulam can be produced in a wide range of shapes to virtually any size limited only by the transportation. They can be formed into structural members for applications such as stringers (beams), longitudinal or transverse decks, garage door headers, floor beams, and arches. The glulam has significantly greater strength and slightly greater stiffness than a comparable sawn timber member of the same size. It is caused by the fact that the laminating process disperses strength-reducing characteristics throughout the member (for instance the knots are spread more evenly). As glulam is produced from dry timber, it provides better dimensional stability.

The manufacturing process of glulam consists of four main phases:

- (1) Drying and grading the timber;
- (2) End-jointing the timber into longer laminations; the most common end joint is a finger joint about 2.8 cm long. The finger joints are machined on both ends of the timber with special cutter heads;
- (3) Face gluing the laminations; the glue used is a weather-resistant type, which can be dark or light in colour depending on the customer's preference;
- (4) Finishing and fabrication.



Figure 4.1 Glulam beams.

4.1 Characteristic strength and stiffness parameters

For the beams that fulfil the requirements of the lay-up of timbers, (see Table 4.1) the design calculations may be carried out as for homogeneous cross-sections.

Table 4.1 Beam lay-ups (Anon. 1995)

Strength class		GL20	GL24	GL28	GL32	GL36
Homogeneous glulam	All laminations	C18	C22	C27	C35	C40
Combined glulam	Outer laminations	C22	C24	C30	C35	C40
	Inner laminations	C16	C18	C22	C27	C35

The properties for glulam are as in the Table 4.2:

Table 4.2 Characteristic values (MPa) for calculation of the resistance and stiffness of glued laminated timber and glued structural timber according to BKR.

	L40	L30	LK30	LK20
Glued laminated timber ¹				
Glued structural timber				
<i>Strength properties</i>				
Bending parallel to grain, f_{mk}	33 ³	26 ³	30	24
Tension parallel to grain, f_{tk}	23	17	20	16
Tension perpendicular to grain, f_{t90k}	0.5	0.5	0.5	0.5
Compression parallel to grain, f_{ck}	36	29	29	23
Compression perpendicular to grain, f_{c90k}	8	7	7	7
Longitudinal shear, f_{vk} ²	4 ⁴	3	3	3
<i>Stiffness properties for calculation of resistance</i>				
Modulus of elasticity E_{Rk}	10 400	8 700	8 700	6 900
Shear modulus, G_{Rk}	700	600	600	450
<i>Stiffness properties for calculation of deformations</i>				
Modulus of elasticity parallel to grain, E_k	13 000	12 000	12 000	10 500
Modulus of elasticity perpendicular to grain, E_{90k}	450	400	400	350
Shear modulus, G_k	850	800	800	700

Young's modulus in the direction of laminations is independent of the prestress level in the deck. However the effective longitudinal stiffness is reduced when butt joints are introduced into system. EC5 (2004) gives the requirements concerning the minimum distance between them. Transverse stiffness of the bridge is not affected by the butt joints.

The value $E_{0, \text{mean}}=E_k$ can be found in Swedish Design Regulation BKR (see Table 4.2). The other mechanical properties should be calculated according to the relations given in EC5 (2004) (see Table 4.3).

Table 4.3 System properties of laminated deck plate. EC5 (2004)

Type of deck plate	$E_{90, \text{mean}}/ E_{0, \text{mean}}$	$G_{0, \text{mean}}/ E_{0, \text{mean}}$	$G_{90, \text{mean}}/ G_{0, \text{mean}}$
Stress-laminated planed	0,02	0,04	0,10
Glued-laminated	0,03	0,06	0,15

As the web of a T-beam timber bridge is firstly glued and then prestressed transversely, values for glued-laminated timber are possible to use. Flanges require using values for stress-laminated timber.

The typical strength class of timber used in stress-laminated timber bridges in Sweden is L40, which corresponds to GL32 according to European standards.

The resultant values of modulus of elasticity, shear modulus and Poisson's ratio for L40 are in Table 4.4.

Table 4.4 Mechanical properties of L40.

Part of the bridge	Type of properties	$E_{0, \text{mean}}$ [MPa]	$E_{90, \text{mean}}$ [MPa]	$G_{0, \text{mean}}$ [MPa]	$G_{90, \text{mean}}$ [MPa]	ν_0	ν_{90}
Flange	Stress-laminated	13000	260	520	52	0,025	0,4
Web	Glued-laminated	13000	390	780	78	0,025	0,4

The density of timber can be assumed $\rho=600 \text{ kg/m}^3$. (Crocetti 2005)

4.2 Design values of material properties [EC5 (1993)]

4.2.1 Partial factor for material properties γ_M

For fundamental combinations, the recommended partial factor for material properties γ_M for glued laminated timber is **1.25**.

4.2.2 Service classes

Structure shall be assigned to one of the service classes. In the design example shown in Appendix A, the bridge is assumed to be protected from direct weathering, so the class 2 is assigned.

4.2.3 Load-duration classes

- (1) Variable actions due to passage of vehicular and pedestrian traffic should be regarded as **short-term** actions.
- (2) Initial pre-stressing forces perpendicular to the grain should be regarded as **short-term** actions.

If a load combination consists of actions belonging to different load-duration classes a value of k_{mod} should be chosen which corresponds to the action with the shortest duration.

Table 4.5 Values of k_{mod}

Glued laminated timber	Service class		
	1	2	3
Permanent	0,60	0,60	0,50
Long-term	0,70	0,70	0,55
Medium-term	0,80	0,80	0,65
Short-term	0,90	0,90	0,70
Instantaneous	1,10	1,10	0,90

4.2.4 Stiffness parameters in the serviceability limit state.

The final deformation, δ_{fin} , under an action should be calculated as:

$$\delta_{fin} = \delta_{inst} (1 + k_{def})$$

where k_{def} is a factor that takes into account the increase in deformation with time due to combined effect of creep and moisture. The values of k_{def} are given in a table below.

Table 4.6 Values of k_{def}

Glued-laminated timber	Service class		
	1	2	3
Permanent	0,60	0,80	2,00
Long-term	0,50	0,50	1,50
Medium-term	0,25	0,25	0,75
Short-term	0,00	0,00	0,30

According to the Eurocode, for the case of calculating the deflection for a glued-laminated timber due to traffic load, the k_{def} factor is 0 so creep and moisture does not influence the deformation.

5 Load analysis

5.1 Actions on the bridge

In order to design main elements of the bridge the load was assigned according to the Swedish code Bro 2004. The following loads were taken into account.

5.1.1 Permanent loads

5.1.1.1 Self-weight (g_{1k})

Due to the fact that the bridge is made from wood, the value of the self-weight is equal to 6kN/m^3 and is taken from Bro 2004 according to Table 5.1:

Table 5.1 Self-weight of materials. [Bro 2004]

Aluminium 27 kN/m^3
Normal concrete, reinforced 25 kN/m^3
Normal concrete, not reinforced 23 kN/m^3
Steel 77 kN/m^3
Timber 6 kN/m^3

5.1.1.2 Surfacing (g_{2k})

The surface of the bridge consists of three layers. Thickness, density and weight of every layer are shown in Table 5.2.

Table 5.2 Layers of the surface. (Crocetti 2005)

	Thickness [mm]	Density [kN/m^3]	Load [kN/m^2]
Asphalt over isolation carpet	18	17,2	0,31
HABT11	25	24	0,60
ABS>16	45	22,2	1,00
Σ	88		1,91

The height of the surfacing is assumed to be 88mm. Due to the fact that there was no sidewalk requested, surfacing load $g_2=1,91\text{kN/m}^2$ was distributed on the whole cross-section and length of the bridge.

5.1.2 Variable load

5.1.2.1 Traffic load (P_k, q_{1Bk})

To simulate traffic load acting on the bridge, a type of the vehicle due to Bro 2004 is analysed see Figure 5.1.

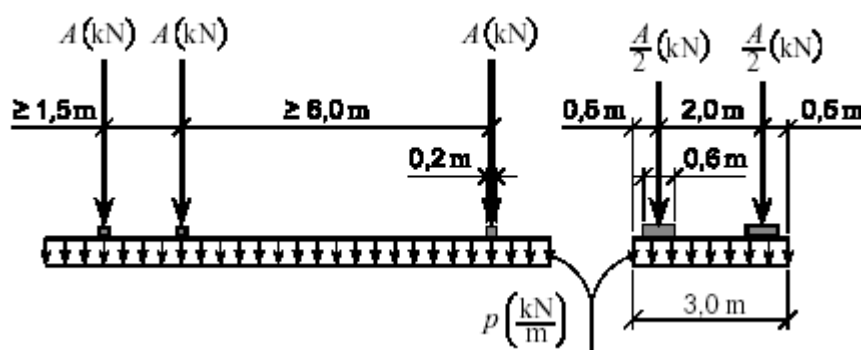


Figure 5.1 Equivalent load type 1. [Bro 2004]

As it is shown on the Figure 5.1 applied traffic load consists of three pairs of point load and uniformly-distributed load. The uniformly-distributed load $q_{1Bk}=p=12\text{kN/m}$ is summed up from the width of 3 m and acts on the total length of the bridge $L=15\text{m}$. The value of single point wheel force is $P_k=A/2=125\text{kN}$.

5.2 Load combinations

The elements of the bridge need to be verified according to Serviceability Limit State and Ultimate Limit State. Therefore the hand calculations were made according to Combination IV:A -ULS and V:C -SLS in Bro 2004, see Table 5.3.

Table 5.3 Respective load coefficient $\psi\gamma$. [Bro2004]

Laster	Lastkombination											
	I	II	III	IV:A	IV:B	V:A	V:B	V:C	VI	VII	VIII	IX
Permanent laster												
Egentyngd (21.11)	max	1,05		1	1,15	1,05						
	min	1	0,95	1	0,9 ^{b)}	0,95	1		1	1	1	1
Beläggning (21.121)	max			1	1,15	1,2						
	min			1	0,8	0,8	1		1	1	1	1
Variabla laster												
Ekv last 1 (21.2221)				0,7/1,5	0,7	1		0,8			0,3	1

5.2.1 Combination in Serviceability Limit State

The deflection of the bridge should be calculated in Serviceability Limit State according to Combination V:C in Bro 2004. Due to the Table 5.3 the value of the applied load should be reduced by respective factor $\psi\gamma$ see Table 5.4

Table 5.4 Value of the reduction factor used in SLS combination.

SLS combination	$\psi\gamma$
Traffic load	0,8

The reduced point wheel force is equal to: $P_{def} = \psi\gamma \cdot P_k = 100kN$

5.2.2 Combination in Ultimate Limit State

For the verification of elements according to the Ultimate Limit State the Combination IV:A should be used. Therefore, values of the load should be increased by the factor $\psi\gamma$, see Table 5.5.

Table 5.5 Partial safety factors.

ULS combination	$\psi\gamma$
Self-weight	1,0
Surfacing	1,0
Traffic load	1,5

The increased wheel point load is equal to:

$$P = \psi\gamma \cdot P_k = 187,5kN$$

The increased uniformly distributed traffic load is equal to:

$$q_{1B} = \psi\gamma \cdot q_{1Bk} = 18 \frac{kN}{m^2}$$

Different position of the vehicle load will be further analysed to obtain the greatest shear force and the greatest moment.

6 Development of Hand Calculation - WVU Design Method (Davalos and Salim 1993, Taylor et al. 2000)

Design procedure for stress-laminated T-system timber bridges, called WVU method is presented in this chapter. The method is based on the definition on a wheel load distribution factor derived from a macro-flexibility orthotropic solution of a plate stiffened by stringers (GangaRao and Raju 1992). The wheel load factor reduces the design of the superstructure to the design of a T-beam section. However, since the normal stress along the flanges of the multiple 'T' cross-section is not constant, mainly due to the phenomenon of shear lag, an approach that is used in design consists of defining an effective flange width over which the normal stress is assumed to be constant. This assumption enables to apply simple beam bending formulas to T-beam sections. Therefore, an effective flange width for stress-laminated T-beam timber bridges is used in the WVU design method. In addition to global analysis, local analysis must be also performed. Local effects consisting of maximum transverse deflection and stress caused by a wheel load applied to the deck between two adjacent webs should be investigated.

6.1 Determination of the effective flange width

The variables that have a major effect on the effective flange width are web spacing, bridge span, ratio of web depth to thickness and the ratio of the web's longitudinal elastic modulus to flange elastic modulus.

In 1993 Davalos and Salim developed equations for the determination of effective flange width. Because of the complexity of the derived equation, a simplified linear solution was performed. According to the analysis the effective width of the flange should be taken as the minimum value of the three following equations.

$$b_{ef} = \min \left\{ \begin{array}{l} b_{e1} = 2 \cdot b_m + t_w \\ b_{e2} = S \\ b_{e3} = \frac{L}{8} \end{array} \right\} \quad (6.1)$$

The effective over-hanging flange width b_m is determined by Eq. (6.2).

$$\frac{b_m}{B} = 0.4586 + \left(\frac{1}{B} \right) \cdot \left(\frac{D}{t_f} \right) \cdot \left(\frac{E_{Lw}}{E_{Lf}} \right) \quad (6.2)$$

where:

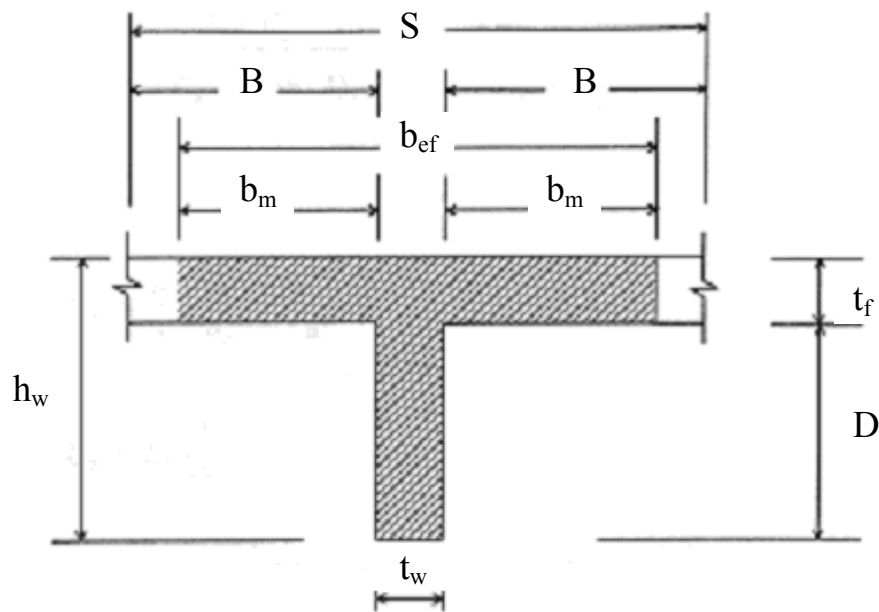


Figure 6.1 Isolated T-beam and the corresponding effective flange width.

- t_f Thickness of the flange
- t_w Width of the web
- S Spacing of webs
- L Length of the bridge span
- B One-half clear distance between the webs
- D Depth of portion of web that is outside the deck
- E_{Lw} Longitudinal modulus of elasticity of the web
- E_{Lf} Longitudinal modulus of elasticity of the deck

Further studies at the West Virginia University Constructed Facilities Centre resulted in slightly different design procedures for T-beam bridges, especially for determining the effective flange width (Taylor 2000). The effective flange width should be taken as a maximum value of the following two equations.

$$b_{ef} = \max \left\{ \begin{array}{l} b_{ef1} = 2 \cdot b_m + t_w \\ b_{ef2} = \frac{S_c}{2} + t_w \end{array} \right\} \quad (6.3)$$

For the box-beam bridge the formula for effective flange width is shown in Eq. (6.4).

$$b_{ef} = \max \left\{ \begin{array}{l} b_{ef1} = 2 \cdot b_m + t_w \\ b_{ef2} = \frac{2 \cdot S_c}{3} + t_w \end{array} \right\} \quad (6.4)$$

Effective overhangs of T-beam and box-beam b_m should be computed from Eq. (6.5).

$$b_m = \frac{S_c}{2} + \left[\frac{1 + \nu_{xz} \cdot \left(\frac{S_c}{L} \right)^2}{1 + \frac{E_{Lw}}{G_{xz}} \cdot \left(\frac{S_c}{L} \right)^2} \right] \quad (6.5)$$

where:

- S_c Clear distance between the webs $S_c = 2 \cdot B$
- L Length of the bridge span
- ν_{xy} Poisson's ratio
- E_{Lw} Longitudinal modulus of elasticity of the web
- G_{xz} Shear modulus (z is the longitudinal direction)

6.2 Determination of wheel load distribution factors (W_f)

Traffic load distribute through the flanges into the webs of a T-beam or box-beam bridge system. These result in one or more of the webs receiving more loads than others. Wheel factor indicates how much load the most used web takes. When the total lane load moment is multiplied by wheel distribution factor, stresses in the most loaded section can be determined and the cross-section can be designed.

The degree of distribution depends on the transverse stiffness of the flange, the number of lanes, and to lesser extent the truck configuration.

In 1993 Davalos and Salim proposed Eq. (6.6) for computation the maximum wheel load distribution factor for symmetric load case for T-beam bridge. Expected values for W_f should be not higher than 0.6 in case of multi-web cross-section.

$$W_f = \frac{1 + C_o}{n \cdot C_o + \frac{2}{\pi} \cdot (n - 1)} \quad [-] \quad (6.6)$$

where:

$$C_o = \frac{b}{\pi} \cdot \frac{D_T}{B_e} \cdot \frac{8 \cdot \alpha^2 + 1}{\alpha^4} \quad [-] \quad (6.7)$$

$$D_T = E_{T_w} \cdot \frac{t_f^3}{12} \quad [Nm] \quad (6.8)$$

$$B_e = E_{L_w} \cdot I_{ex} \quad [Nm^2] \quad (6.9)$$

n Number of webs across the bridge width

b Centre to centre distance between exterior webs

L Length of the bridge span

α Aspect ratio b / L

E_{L_w} Longitudinal modulus of elasticity of the web

I_{ex} Composite moment of inertia of the edge beam plus the overhanging flange width b_m

For single-lane bridges the edge deflection under asymmetric load controls the design. Therefore, the symmetric load distribution factor W_f should be multiplied by 1.6 (empirical constant).

Evaluation of Eq. (6.6) based one Finite Element Method and a Macro Approach resulted in Eq. (6.10) and (6.11) for distribution factor W_f .

Equation for T-beam bridge:

$$W_f = \frac{2 \cdot N_L}{1.64 \cdot n - 0.64} \quad [-] \quad (6.10)$$

Equation for box-beam bridge:

$$W_f = \frac{3 \cdot N_L}{2.64 \cdot n - 0.64} \quad [-] \quad (6.11)$$

where:

N_L Number of traffic lanes

n Number of webs across the bridge width

6.3 Design the deck for the local effects

6.3.1 Maximum local deflection

The variables that effect the most transverse deflection are web spacing and depth of the deck. The maximum local deflection is computed from Eq (6.12). The basis of this equation is the displacement method that is used to calculate the response to loads and/or imposed deformations of statically indeterminate structures. In this case it is a continuous beam with one span loaded with concentrated load P_{def} . This formula will be further compared with a solution obtained from FEM analysis in Section 7.5.1.

$$\delta_{local} = \frac{P_{def} \cdot S^3}{4 \cdot K_{\delta} \cdot \frac{E_{Tf}}{1 + k_{def}} \cdot t_f^4} \quad [m] \quad (6.12)$$

$$K_{\delta} = -10.9 + 7.8 \cdot \left(\frac{S}{t_f} \right) + 0.27 \cdot \left(\frac{E_{Lf}}{E_{Tf}} \right) \quad [-] \quad (6.13)$$

where:

P_{def} Wheel point force reduced by factor $\psi\gamma=0.8$, see Section 6.2.1

S Spacing of webs

E_{Lf} Longitudinal modulus of elasticity of the deck

E_{Tf} Transverse modulus of elasticity of the deck

k_{def} Factor taking into account the increase in deformation with time, see Section 2.2.4.

Suggested limit for the local deflection is 0.1 to 0.2 inches (2.54mm - 5.08mm). (GangaRao and Raju 1992)

According to Eurocode 5 (2004) local deflection is limited by value $S/400$, where S is the spacing between the webs. The spacing of models analysed in this thesis is in between 935mm and 1520mm so the limit deflection is from 2.34mm to 3.8mm.

6.3.2 The maximum local transverse stress

The maximum local transverse stress is calculated according to Eq. (6.14). This equation will be further compared with solution obtained from FEM analysis in Section 7.5.1.

$$\sigma_{\max} = \frac{3 \cdot P \cdot S}{2 \cdot K_{\sigma} \cdot t_f^3} \quad [Pa] \quad (6.14)$$

$$K_{\sigma} = 3 + 3.1 \cdot \left(\frac{S}{t_f} \right) + 0.15 \cdot \left(\frac{E_{Lf}}{E_{Tf}} \right) \quad [-] \quad (6.15)$$

where:

P Wheel point force increased by factor $\psi\gamma=1.5$, see Section 5.2.2

The maximum transverse stress must be limited by the design value of compression perpendicular to the grain.

6.4 Global analysis

6.4.1 Bending stresses

The maximum stresses are determined by live load and dead load bending moment. The check of the stresses should be made at the top of the web and at the top of the deck. The Eq. (6.16) for the maximum stress is based on beam theory.

$$\sigma = \frac{M_l + M_g}{I} \cdot y \quad [Pa] \quad (6.16)$$

$$M_l = M \cdot W_f \quad [Nm] \quad (6.17)$$

$$M = M_t + \frac{q_{1B} \cdot L^2}{8} \quad [Nm] \quad (6.18)$$

$$M_g = \frac{(g_1 \cdot A + g_2 \cdot S) \cdot L^2}{8} \quad [Nm] \quad (6.19)$$

where:

M Live load bending moment (vehicle load acting on the bridge),

M_l Live load bending moment, with corresponding to the most loaded web

M_t The greatest moment obtained due to three couples of wheel point forces

M_g Dead load bending moment

I Composite moment of inertia of isolated T-beam

Y Distance from T-beam neutral axis to the top or bottom fibres

g_l Self-weight load in $[N/m^3]$

A Area of one 'T' cross-section $[m^2]$

- g_2 Surface load in $[N/m^2]$
- S Length of surface load distributed into one web in $[m]$, for interior webs is equal to spacing between them

The applied bending stresses must not exceed the design value of bending strength of the web and compression strength of the deck. In the design, if the applied stresses exceed the design values, the area of the web should be increased.

6.4.2 Maximum shear stresses

Shear stress in the elements is determined by standard linear elastic theory. Maximum horizontal shear stress in the web is calculated at a distance x equal to one thickness of the deck from the support (EC5 1993). The total value of shear force V in the most utilized web is the result of dead load V_g and live load V_t see Eq. (6.20).

$$V = V_g + V_t \quad [N] \quad (6.20)$$

The maximum shear force due to live load V_t is computed from Eq. (6.21). This equation assumes that interaction between webs in transmitting shear is not as effective as in transmitting bending. That is why to obtain shear due to traffic load in the most utilized web only half of the total shear force is multiplied with the wheel factor and the other half is multiplied by the factor 0.6 which is always higher than the wheel factor in case of multi-web cross-section.

$$V_t = 0.5 \cdot (0.6 \cdot V_{LU} + V_{LD}) \quad [N] \quad (6.21)$$

where:

V_{LU} Maximum shear force at a distance x caused by design value of: concentrated 3 pairs of wheel load and uniformly distributed traffic load, without load distribution, see Figure 5.1.

V_{LD} Maximum shear force at a distance x caused by design value of: concentrated 3 pairs of wheel load and uniformly-distributed traffic load, multiplied by load wheel distribution factor W_f , see Eq. (6.22)

$$V_{LD} = N_L \cdot W_f \cdot V_{LU} \quad [N] \quad (6.22)$$

N_L Number of lanes

In a conservative approach the web carries the maximum vertical shear stress alone. Therefore, the Eq. (6.23) can be used.

$$\tau = \frac{1.5 \cdot V}{t_w \cdot h_w} \quad [Pa] \quad (6.23)$$

where:

t_w Width of the web

h_w Depth of the web

Maximum shear stress cannot exceed design value of longitudinal shear stress given in codes.

6.4.3 Maximum punching shear stress

The deck between the webs should be designed for punching shear. The punching shear, known also as the local shear, is the force, which causes one deck lamina to slip relative to an adjacent lamina. Studied shear force is caused by the influence of the wheel load situated in the middle of two interior webs. Wheel load is acting on the effective area according to Figure 6.2. (GangaRao and Raju 1992)

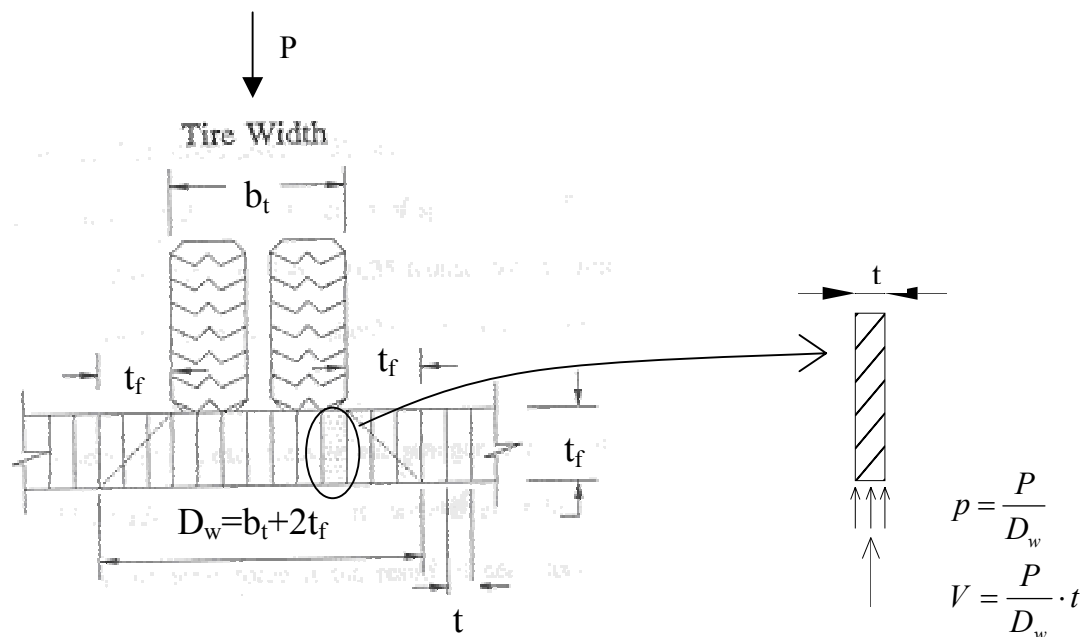


Figure 6.2 Punching shear.

However, according to EC5 (2004) the angle of dispersion in the direction perpendicular to the grain is not 45° but 15° and the reference plane should be in the middle of the deck therefore:

$$D_w = b_t + 2 \cdot \frac{t_f}{2} \tan 15^\circ \quad [m] \quad (6.24)$$

To calculate punching shear, the concentrated force P is divided by the number of laminations (see Figure 6.2) in order to get the shear force in between the lamellas. Therefore the applied shear force is computed from Eq. (6.25):

$$V = \frac{P}{D_w} \cdot t \quad [N] \quad (6.25)$$

where:

- P Applied wheel load in [N]
 b_t Width of the contact area in the transverse direction
 t_f Thickness of the deck
 t Width of a lamina

To avoid vertical inter-laminar slip the applied shear force V should not exceed the resisting frictional force V_{res} equal to a pre-stress over the area of the longitudinal length of the tire and the thickness of the deck. The resisting frictional force is calculated from Eq. (6.26).

$$V_{res} = f_p \cdot b_l \cdot t_f \cdot \mu_s \quad [N] \quad (6.26)$$

where:

- f_p Final pre-stress level,
 b_l Tire contact length in the direction of span
 μ_s Coefficient of static friction, can be assumed as 0.35

6.4.4 Maximum shear in the surface between web and flange

Shear stress at the interface between the web and the flange is determined by maximum shear force V caused by dead and live loads, see Section 6.4.2. It should be calculated from Eq. (6.27).

$$\tau_v = \frac{V \cdot Q}{I \cdot t_w} \quad [Pa] \quad (6.27)$$

where:

$$Q = b_m \cdot t_f \cdot e \quad [m^3] \quad (6.28)$$

- b_m Overhanging flange width
 e Distance from flange mid-surface to transformed section neutral axis
 t_f Thickness of the flange
 t_w Thickness of the web
 I Moment of inertia of the transformed section

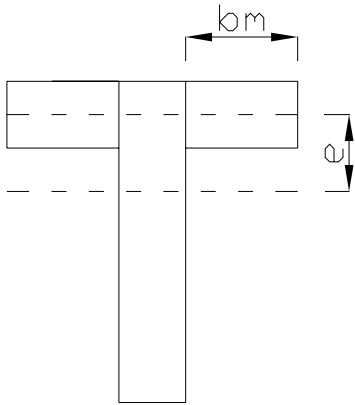


Figure 6.3 Transformed section.

The value τ_v should be less than the resistance value $f_{vd} = 2.88\text{MPa}$, see Appendix A, Section 4.0.

6.5 Check of the deflection

Elements of the bridge should be verified respecting the Serviceability Limit State. The longitudinal displacement caused by live load and dead load must be checked.

6.5.1 Live load deflection

To calculate the vertical displacement in an approximate way, traffic load need to be transformed into equivalent concentrated load P_e , which is acting at the centre of the T-beam and produces a maximum moment, see Figure 6.4. An equivalent concentrated load P_e is defined by Eq. (6.29).

$$P_e = M \cdot \frac{4}{L} \quad (6.29)$$

where:

M Live load bending moment (vehicle load acting on the bridge),

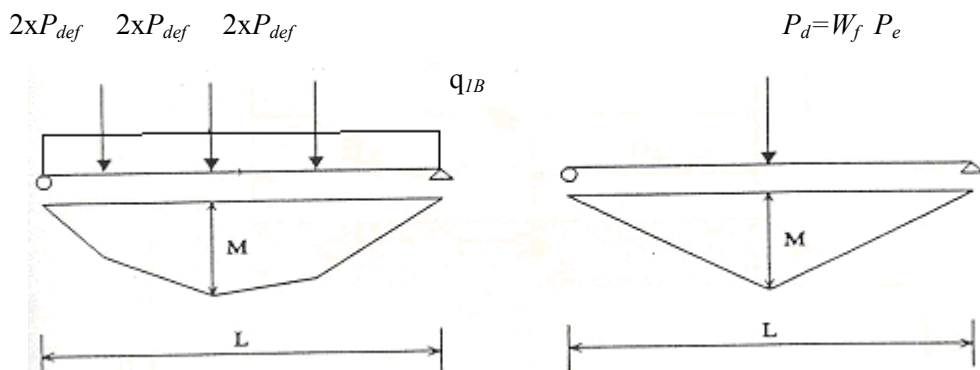


Figure 6.4 Definition of equivalent concentrated design load.

This load P_e is then modified for wheel load distribution and number of lanes to produce the design concentrated load P_d see Eq. (6.30).

$$P_d = W_f \cdot P_e \quad (6.30)$$

For single-lane bridges, the edge deflection under asymmetric loading controls the design so for the reason of calculating the deflection, the wheel factor W_f should be multiplied by 1.6 (empirical constant).

The maximum live load deflection is computed from Eq. (6.31). Variable actions due to passage of traffic should be regarded according to EC5 (1993) as short-term actions. The value of $k_{def} = 0$ should be assumed, see Section 4.2.4.

$$\delta_{\max} = \frac{P_d \cdot L^3}{48 \cdot E_{Lw} \cdot I} \cdot (1 + k_{def}) \quad [m] \quad (6.31)$$

where:

P_d Design concentrated load, see Eq. (6.30)

L Length of the bridge span

E_{Lw} Longitudinal modulus of elasticity of the web

I Composite moment of inertia of isolated T-beam

The range of limiting values for deflections due to the traffic load only for beams, plates and trusses with span l is given in EC5 (2004) and is shown in Table 6.1.

Table 6.1 Limiting values for deflection for beams, plates and trusses. [EC5 (2004)]

Action	Range of limiting values
Characteristic traffic load	$l/400$ to $l/500$
Pedestrian load and low traffic load	$l/200$ to $l/400$

As the length of the investigated bridge L is 15m the maximum longitudinal deflection is according to Table 6.1:

$$\delta_{\lim} = \frac{L}{400} = 37.5mm \quad (6.32)$$

6.5.2 Dead-load deflection (Initial stage)

The dead-load deflection should be computed from Eq. (6.33).

$$\delta_d = \frac{5 \cdot (g_1 \cdot A + g_2 \cdot S) \cdot L^4}{384 \cdot E_{Lw} \cdot I} \quad [m] \quad (6.33)$$

where:

g_1 Self-weight load in [kN/m³]

A Area of distribution of the self-weight in [m²]

g_2 Surfacing load in [kN/m²]

S Distance of distribution of the surfacing load in [m], for interior webs is equal to spacing between them

L Length of the bridge span

E_{Lw} Longitudinal modulus of elasticity of the web

I Composite moment of inertia of isolated T-beam

6.5.3 Long-term deflection

The long-term deflection is the dead load deflection multiplied by factor 1.5 (Davalos and Salim 1992), see Eq. (6.34).

$$\delta_{final} = 1.5 \cdot \delta_d \quad [m] \quad (6.34)$$

However, according to EC5 (1993) the long-term deflection should be calculated as follows:

$$\delta_{final} = \delta_d \cdot (1 + k_{def}) \quad [m] \quad (6.35)$$

where:

k_{def} Creep and moisture factor (according to Table 4.6 for dead load and service class 2, k_{def} is equal to 0.8)

$$\delta_{final} = 1.8 \cdot \delta_d \quad [m] \quad (6.36)$$

The camber that needs to be provided in the bridge should be equal to:

$$\text{Camber} \geq 2 \text{ or } 3 \text{ times } \delta_{final}$$

6.6 Check of Vibrations according to BRO 2004

The vertical acceleration should be checked for bridges, which are both for vehicle and pedestrian traffic, according to Eq. (6.37):

$$a_{RMS} = \frac{4 \cdot F \cdot v}{\pi \cdot \sqrt{2 \cdot m \cdot E_{Lw} \cdot I_{tot}}} \quad \left[\frac{m}{s^2} \right] \quad (6.37)$$

where,

F Point load, can be assumed as $F = 240000N$

v Velocity of the vehicle, can be assumed as 15 m/s

m Total mass of the bridge in [kg/m]

I_{tot} Composite moment of inertia of the whole section of the bridge

E_{Lw} Longitudinal modulus of elasticity of the web

The limiting value for a road bridge with pedestrian traffic is given in Bro 2004:

$$a_{RMS} \leq 0.5 \frac{m}{s^2}$$

Natural frequency for the vertical deformation should be calculated for the pedestrian bridges according to Eq.(6.38):

$$f_n = \frac{3.14}{2 \cdot L^2} \cdot \sqrt{\frac{E_{Lw} \cdot I_{tot}}{m}} \quad [Hz] \quad (6.38)$$

where:

L Length of the bridge span

The limiting value for a pedestrian bridge is given in Bro 2004:

$$f_n \geq 3.5Hz$$

There is no need to check the natural frequency of road bridges without any pedestrian traffic.

7 Finite Element Analysis

Analysis of the bridge was performed with I-DEAS, a commercially available software package.

Two models were analysed. Model 1 was used in all further analysis except from the analysis of the dispersion angle of a concentrated load (Section 7.5.2) where Model 2 was used.

The models assumed linear elastic theory and complete composite action (Taylor et al. 2000). The prestressing was taken into account by using suitable transverse modulus of elasticity and shear modulus. The prestressing bars were not modelled separately.

7.1 Description of Model 1

7.1.1 Mesh

A three dimensional Model 1 was created by use of shell and beam elements. Beam elements were 0.25m long. Shell elements had 0.25m in longitudinal direction Z and 52.2mm or 72mm in the transverse direction X depending on the geometric configuration, see Figure 7.1. Different geometric configurations with the reasons for the choice of such configurations are presented in Section 7.3.

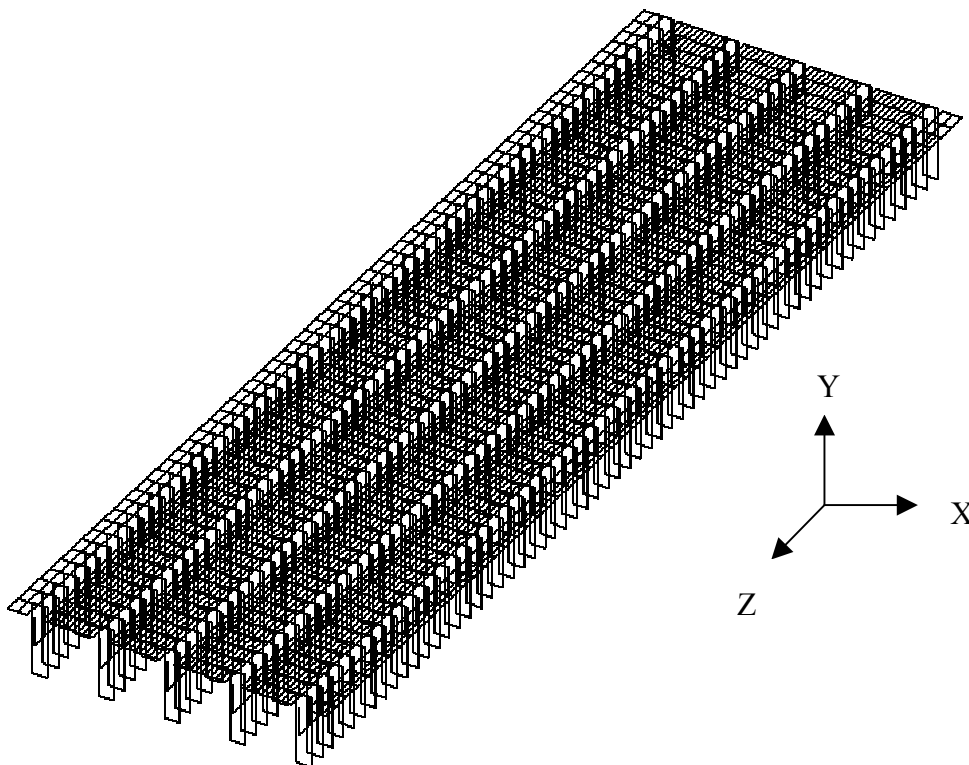


Figure 7.1 Mesh of Model 1.

Nodes in the web were connected by the use of rigid element. The connection between nodes of the beam and shell elements was made by coupling degrees of freedom (X, Y, Z translation and rotation active), see Figure 7.2.

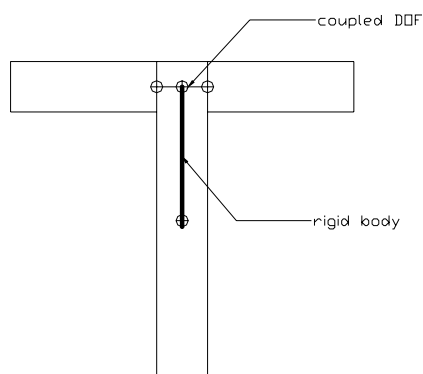


Figure 7.2 The connection between beam and shell elements.

7.1.2 Boundary conditions

Boundary conditions were attached to the nodes of the beam elements. To eliminate vertical displacement all nodes were fastened in Y direction. Furthermore only one side of a bridge had nodes held in Z direction. This simulated a simply-supported condition with a bridge end free to move in the longitudinal direction Z. Also two opposite nodes in the corners had been locked in X direction to provide the needed restraint to the model in the transverse direction, see Figure 7.3.

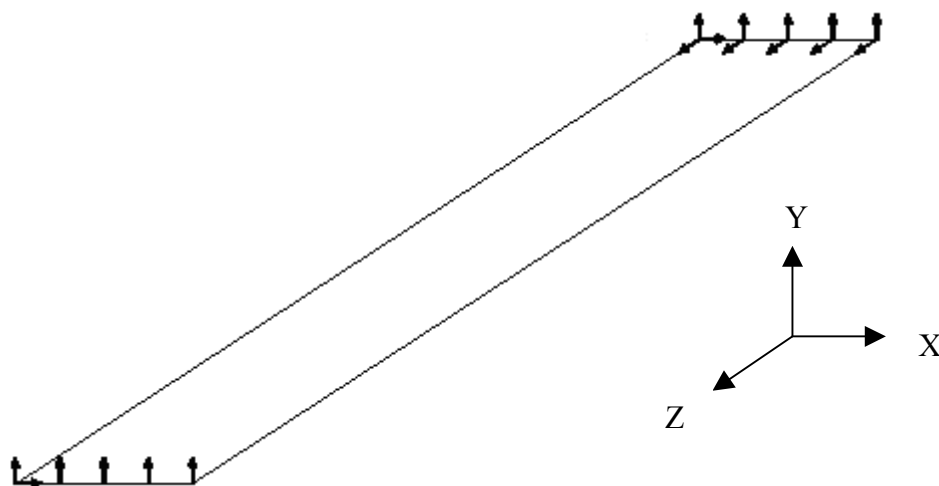


Figure 7.3 Boundary conditions of the 5-web bridge model.

7.1.3 Material properties

Material properties were defined for the quality of timber L40, see Chapter 4. Bridge deck (modelled with shell elements) was assumed to be orthotropic with material properties described in X, Y and Z direction in the following way:

$$E_0 = E_z$$

$$E_{90} = E_x = E_y$$

$$G_0 = G_{zx} = G_{zy}$$

$$G_{90} = G_{xy}$$

$$\nu_0 = \nu_{zx} = \nu_{zy}$$

Webs as they were modelled with beam elements were assumed to be made from isotropic material. The following values were used: $E = 13000\text{MPa}$, $\nu = 0.4$, shear modulus was calculated from equation: $G = E/2(1 + \nu)$.

7.2 Description of Model 2

7.2.1 Mesh

A three dimensional Model 2 using only solid elements was created. To obtain accurate results, the mesh of the middle flange where concentrated load was induced was very dense and had an element size of $15 \times 20\text{mm}$.

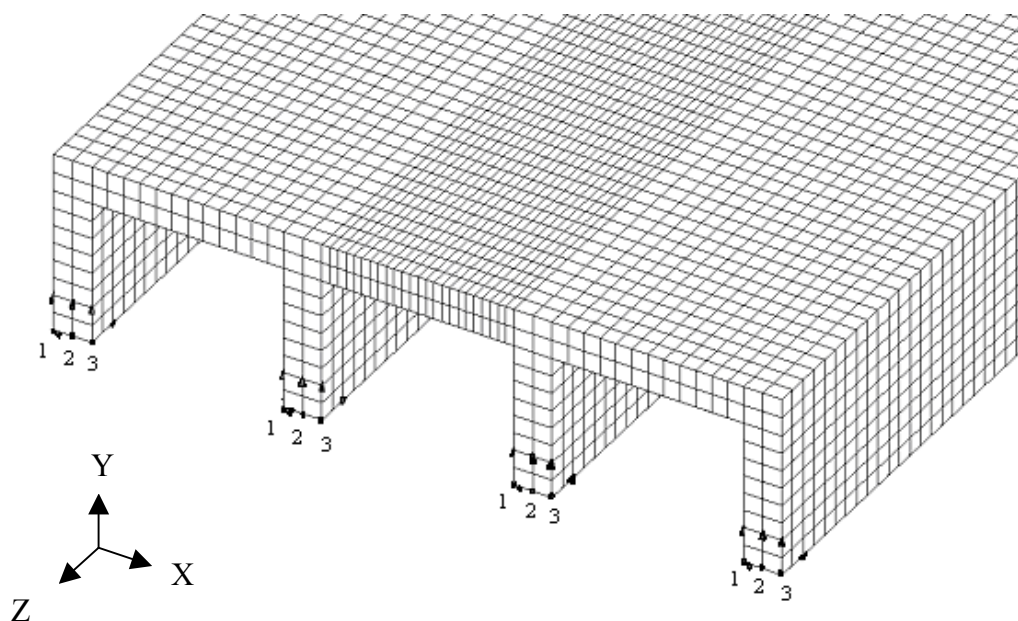


Figure 7.4 Boundary conditions of Model 2.

7.2.2 Boundary conditions

The numbers 1, 2, 3, see Figure 7.4, are the node numbers for the nodes at the bottom of each web at the beginning of the bridge. All of these nodes were held in the Z direction and the Y direction to simulate a pinned condition. The corresponding nodes on the opposite end of the bridge were held in the Y direction and were allowed to move in the Z direction. The nodes marked with number 3 as well as the corresponding nodes on the opposite end of the bridge were additionally held in X direction.

7.2.3 Material properties

Material properties were defined for the quality of timber L40, see Chapter 4. As the web of a T-beam timber bridge is firstly glued and then prestressed transversely, values for glued-laminated timber should be used. Flanges require using values for stress-laminated timber. The whole bridge was assumed to be orthotropic with material properties described in X, Y and Z direction in the following way:

$$E_0 = E_z$$

$$E_{90} = E_x = E_y$$

$$G_0 = G_{zx} = G_{zy}$$

$$G_{90} = G_{xy}$$

$$\nu_0 = \nu_{zx} = \nu_{zy}$$

7.3 Determination of effective flange width

The effective flange width is a fictitious width over which the normal stress in the centre of the flange resulting from elementary beam theory equals the maximum stress according to the correct theory, taking into account the shear deformations in the flanges. In reality the stresses are greatest where the web connects to the flange and smaller at the unsupported area. This effect is due to the so called ‘‘shear lag’’.

Maintaining a constant flange thickness, the contribution of the flanges to the bending stiffness and bending capacity of the cross-section consequently decreases with increasing distance between webs. The extension of the stress decreases mainly on the ratio S/l and E_0/G_0 , where S is the web spacing, l is the span length, E_0 is longitudinal modulus of elasticity of the flange and G_0 its longitudinal shear modulus. The effective width decreases with increasing ratios S/l and E_0/G_0 .

Another reason that determines the effective length is that flanges loaded in compression are prone to buckling. If a detailed investigation is not made, the clear flange width between the webs should not be greater than twice the effective width to avoid plate buckling. This issue will not be discussed in this thesis as for the models analysed below the effective flange width, as it will be presented, is more than 80% of the web spacing, see Table 7.3.

As the effective width depends on the spacing of the webs, three various web spacing of the Model 1 described in Chapter 7.1 were analysed with the thickness of 215mm (Configuration 1, 2A, 3A). Moreover to investigate influence of the thickness, two additional configurations (Configuration 2B, 3B) were performed with the thickness of the deck 280 mm (Crocetti 2005), see Figure 7.5, 7.6, 7.7. Additionally to calculate the effective flange of the box-beam bridge, Configuration 4 was investigated, see Figure 7.8.

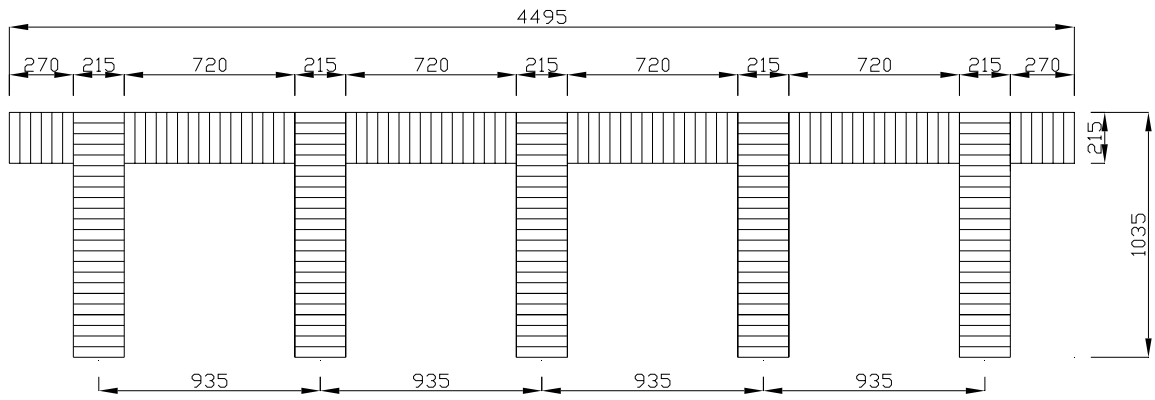


Figure 7.5 Configuration 1: T-beam model with 5 webs.

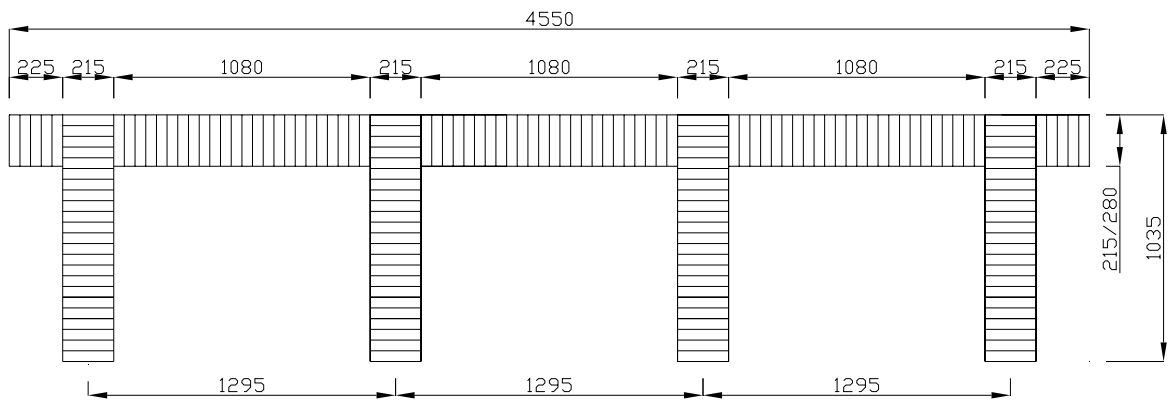


Figure 7.6 Configuration 2A/2B: T-beam model with 4 webs.

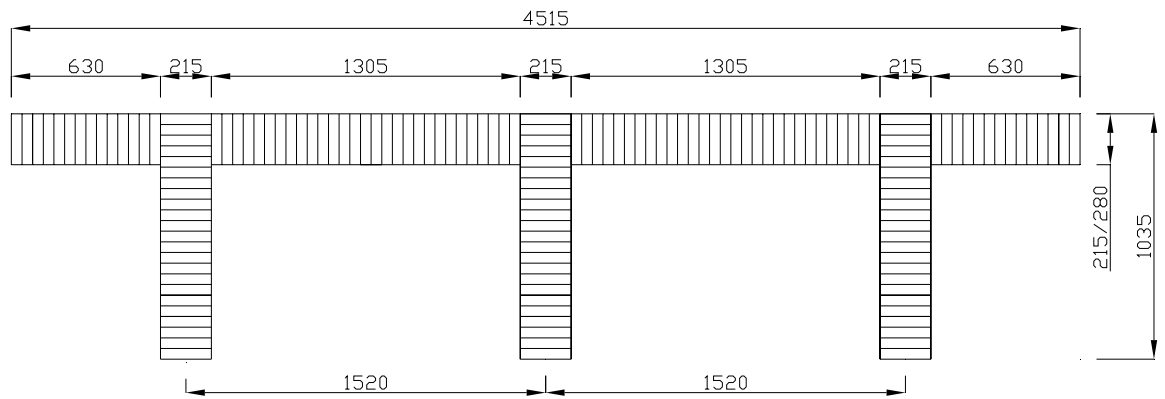


Figure 7.7 Configuration 3A/3B: T-beam model with 3 webs.

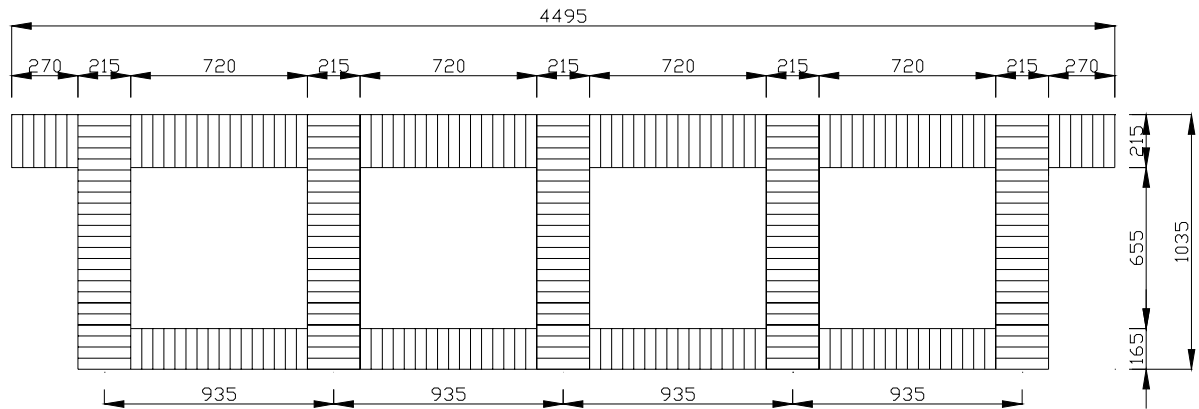


Figure 7.8 Configuration 4: Box-beam model with 5 webs.

7.3.1 Acting load

To calculate the effective flange width, the whole surface of the bridge had to be loaded with a uniformly-distributed load. To achieve that, shell elements (flanges) were loaded with uniformly-distributed surface load $q = 1.91 \text{ kN/m}^2$ (see Section 5.1.1.2.) and beam elements (webs) were loaded with the respected linear beam load $q \times 0.215 \text{ m} = 0.41 \text{ kN/m}$. To check if the effective flange is independent of the value of the load, the same analysis was performed for a three times higher load.

7.3.2 Method

The effective flange width is calculated in the middle of the span of the bridge due to the fact that it influences bending stress in the hand calculation. The shear stress in hand calculation is determined considering the area of the web alone (conservative), so the effective flange does not influence the shear stress calculations.

Firstly the area between the point in the web with maximum value of bending stress and the points in flanges with minimum value of bending stress is calculated. The bending stress considered, is the one in the longitudinal direction Z according to the Figure 7.9.

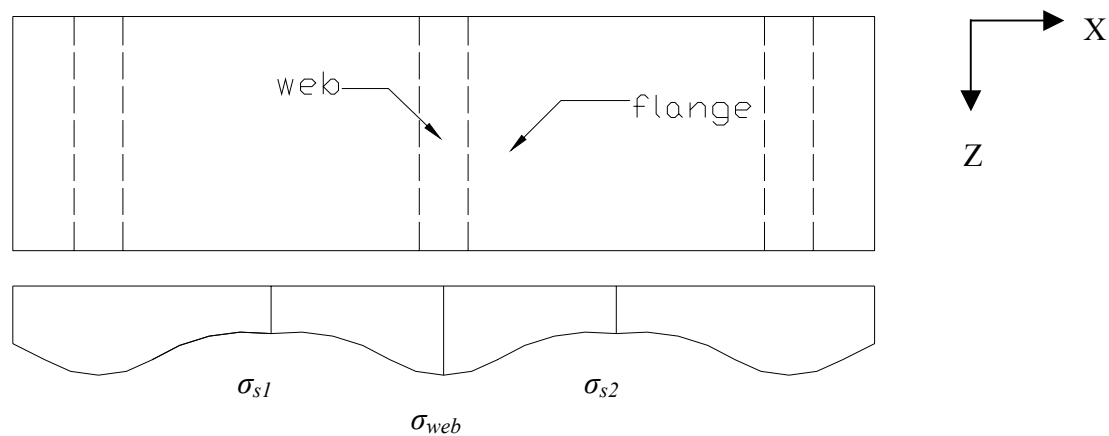


Figure 7.9 Bending stress distribution in the longitudinal direction of the bridge.

Secondly the calculated area (for example by means of AutoCAD) is transformed into a rectangular area with a constant stress and the effective width according to the Eq. (7.1).

$$\sigma_{\max} \cdot b_{\text{eff}} = \int \sigma \cdot dx \quad (7.1)$$

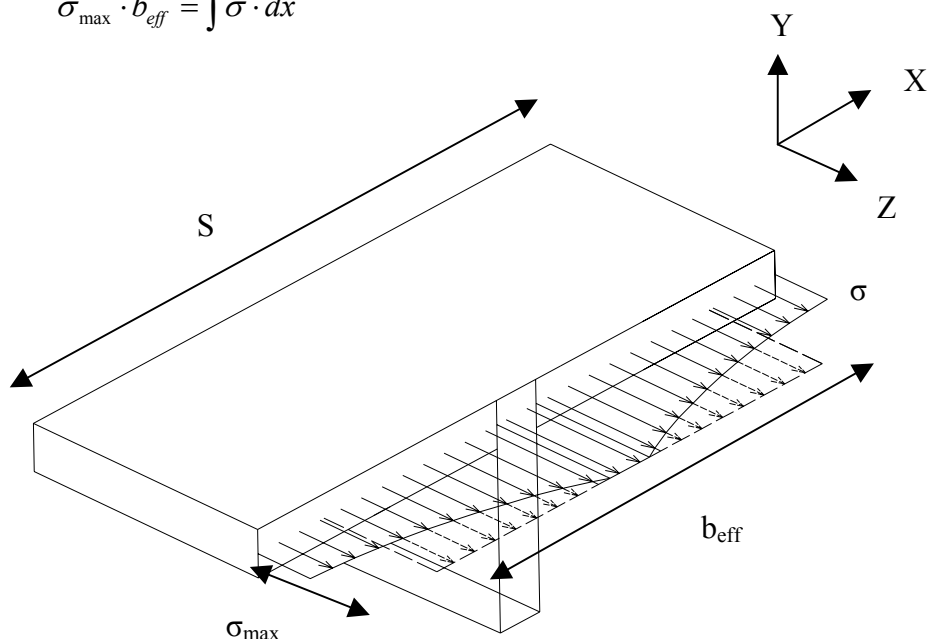


Figure 7.10 Determination of the effective flange width.

7.3.3 Results

Figures below present the variation of stress in the longitudinal direction (σ_z) due to the constant moment across the bridge for three different values of web spacing, two different deck thickness and two types of deck cross-section. The plots show the stress in the middle plain of the deck.

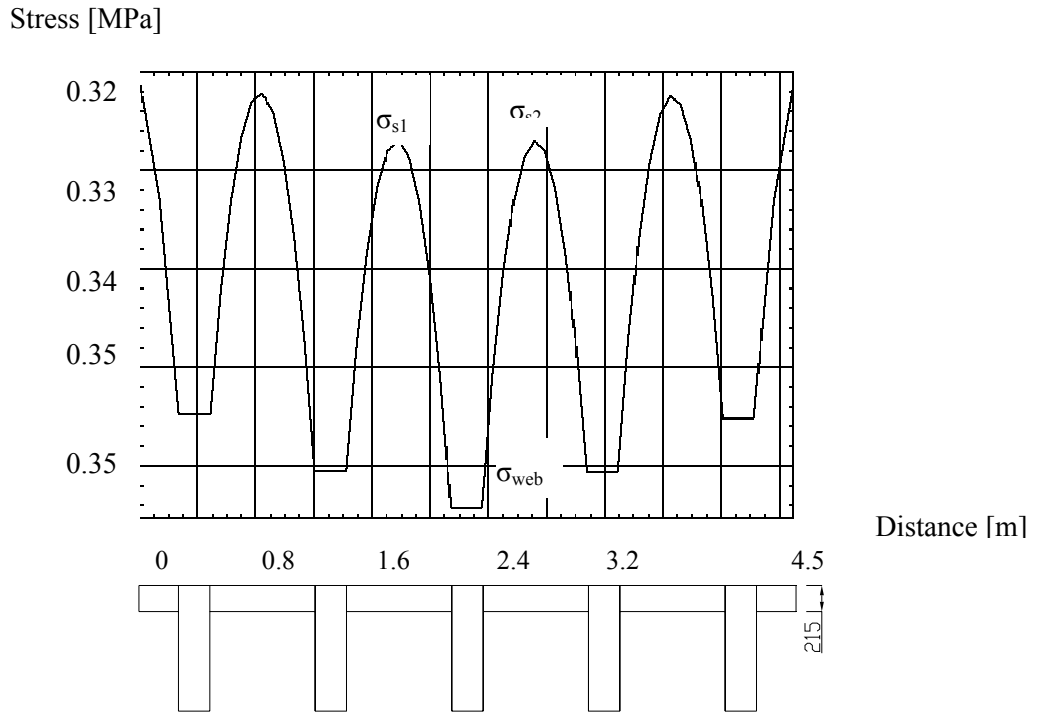


Figure 7.11 Stress σ_z in Configuration 1 (5 webs, deck 215mm).

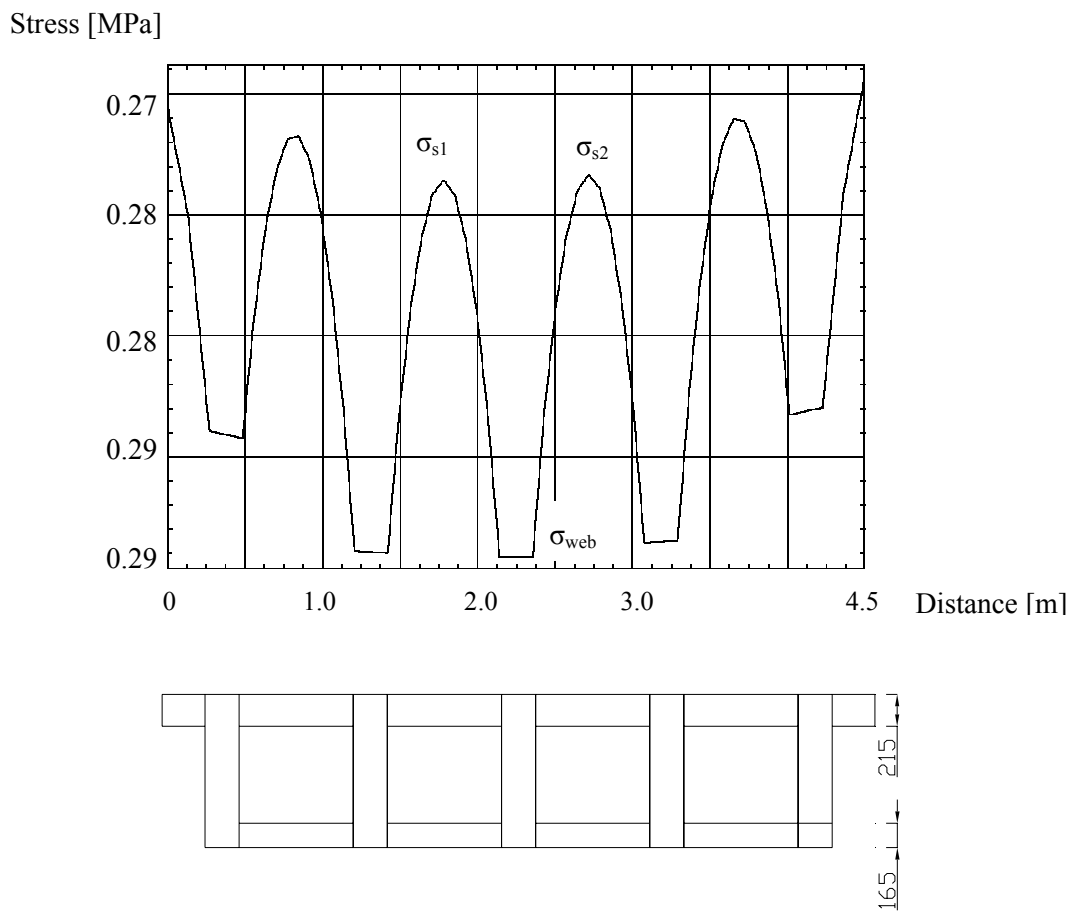


Figure 7.12 Stress σ_z in Configuration 4 (5 webs, deck 215/165mm).

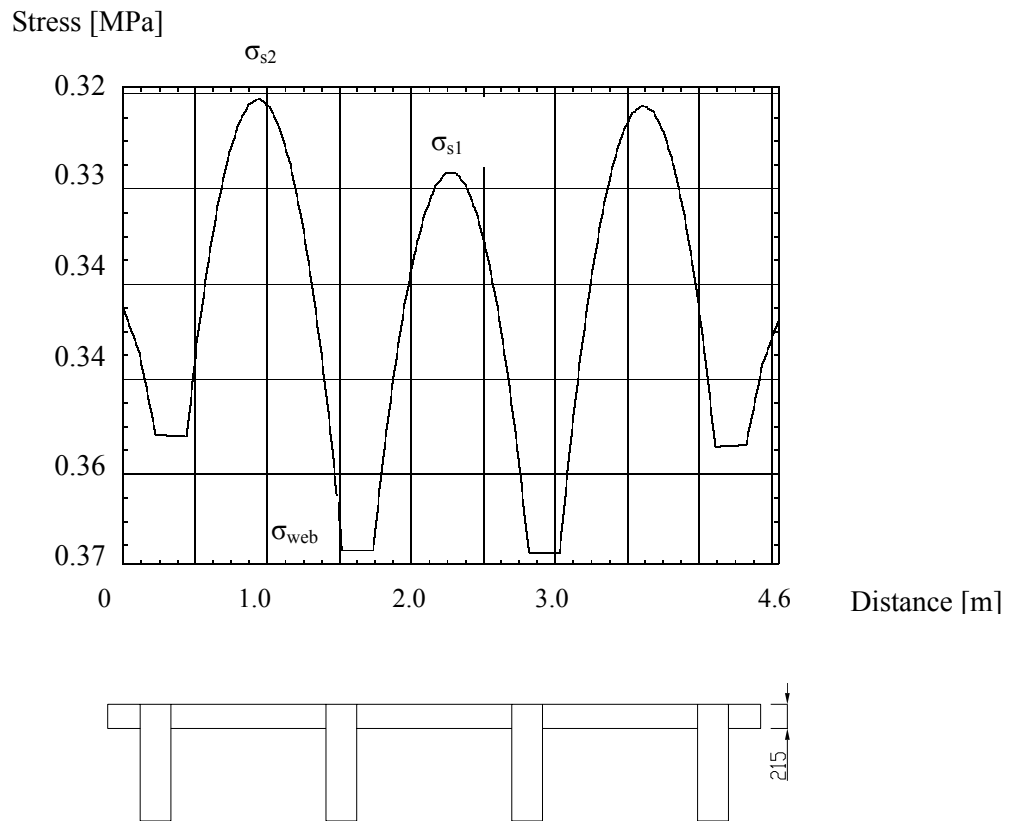


Figure 7.13 Stress σ_z in Configuration 2A (4 webs, deck 215mm).

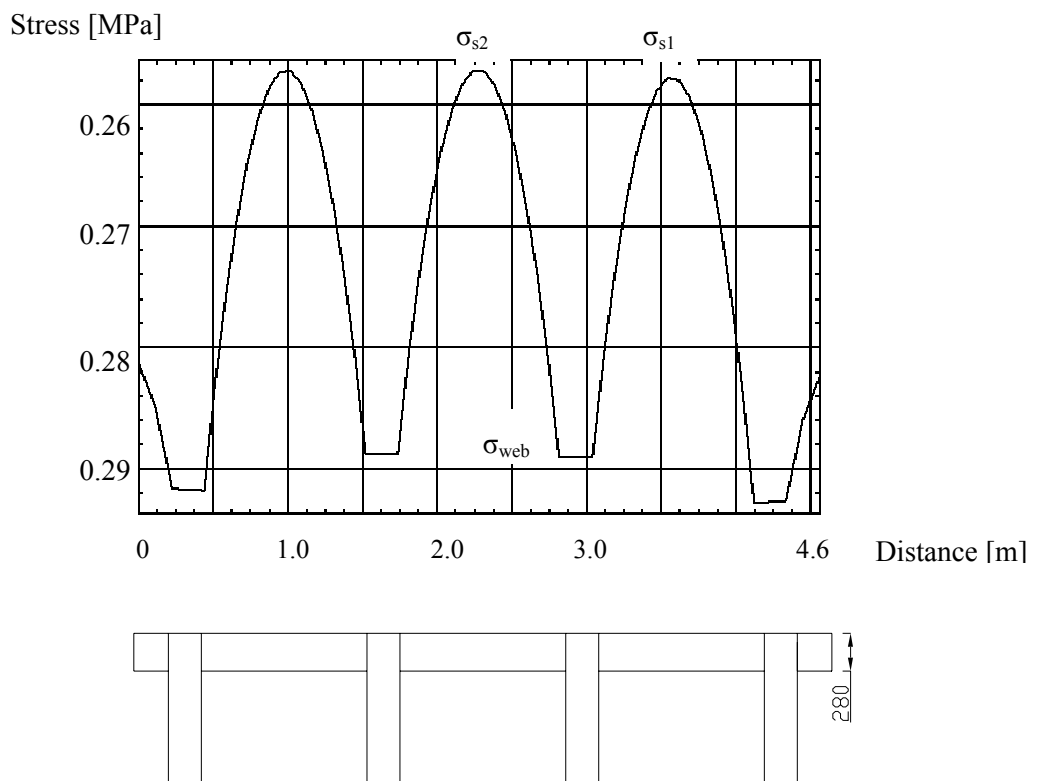


Figure 7.14 Stress σ_z in Configuration 2B (4 webs, deck 280mm).

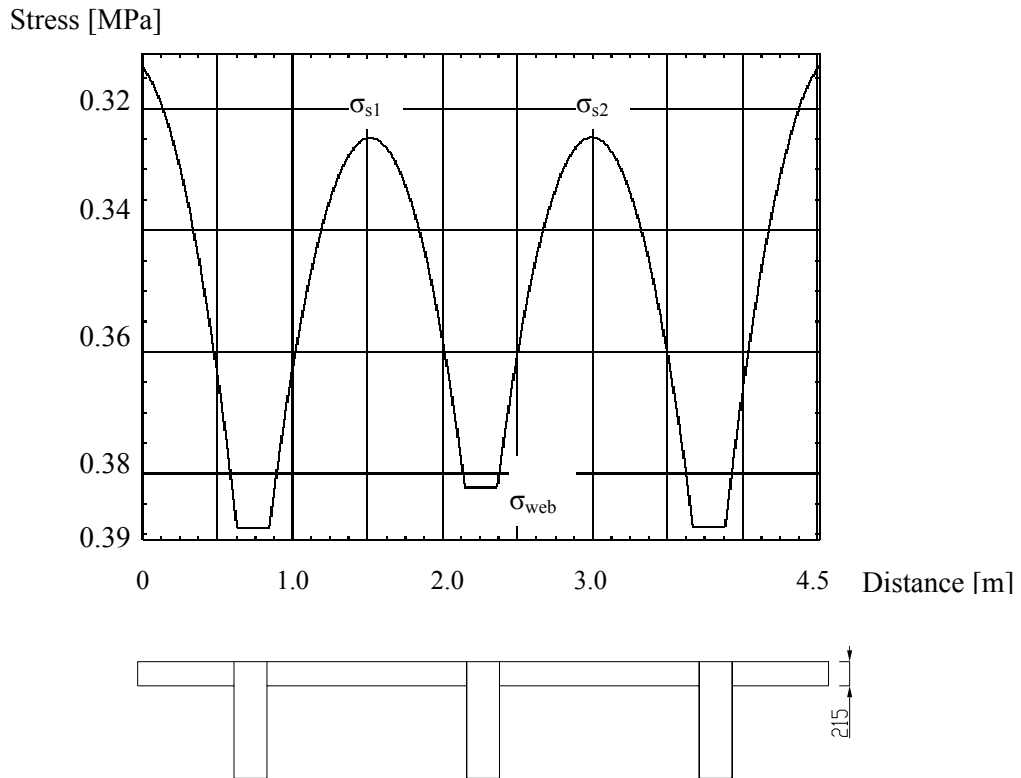


Figure 7.15 Stress σ_z in Configuration 3A (3 webs, deck 215mm).

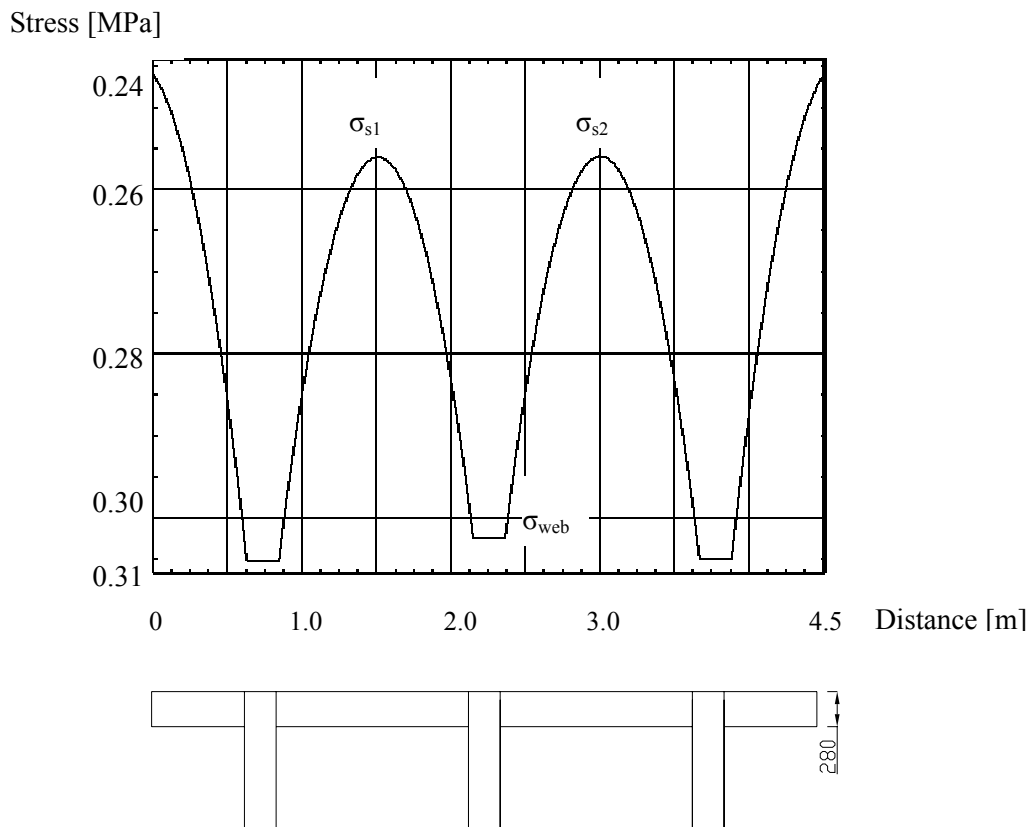


Figure 7.16 Stress σ_z in Configuration 3B (3 webs, deck 280mm).

The results from the figures above are summarized in the Table 7.1 and according to the method described above the effective flange width is determined.

Table 7.1 Comparison between web spacing (S) and the effective flange width (b_{eff}) in FEM.

Config. no.	Deck width [mm]	Number of webs	Stress in the middle layer of the deck [MPa]			Δ_1 [%]	S [mm]	b_{eff} [mm]	Δ_2 [%]
			At the web σ_{web}	Between webs					
				σ_{s1}	σ_{s2}				
1	215	5	-0,347	-0,328	-0,328	5,5	935	910	2,7
2A	215	4	-0,367	-0,328	-0,322	10,6	1295	1222	5,6
2B	280		-0,289	-0,259	-0,255	11,1	1295	1215	6,2
3A	215	3	-0,382	-0,325	-0,325	14,9	1520	1390	8,6
3B	280		-0,302	-0,256	-0,256	15,2	1520	1380	9,2
4	215	5	-0,294	-0,278	-0,278	5,4	935	912	2,5

Where:

$$\Delta_1 = \frac{\sigma_{web} - \sigma_s}{\sigma_{web}} \cdot 100\% \quad \sigma_s = \frac{\sigma_{s1} + \sigma_{s2}}{2}$$

$$\Delta_2 = \frac{S - b_{eff}}{S} \cdot 100\%$$

The effective flange width was also determined for the three times higher load of a value $5,73 \text{ kN/m}^2$ to check if the effective flange width is independent on the value of the load. The study of the T-beam Configuration 3B with increased load showed that the effective width was the same as for the first load and was equal to 1381 mm. These studies prove the hypothesis that the model behaves in an elastic manner.

7.3.4 Comparison of finite element method and hand calculation

The results from Table 7.1 are compared below (see Table 7.2) to the effective flange width determined by the equations given by West Virginia University. For T-beam bridges there are two formulas to calculate the effective flange width: WVU1 from year 1992 (Eq. 6.1) and a newer method WVU2 from the year 2000 (Eq. 6.3). For the box-beam bridge only formula WVU2 (Eq. 6.4) is considered.

Table 7.2 Comparison of the effective flange width for a T-beam bridge.

Config. no.	Deck thickness [mm]	Number of webs	Web spacing [mm]	Effective flange width [mm]		
				FEM	WVU1	WVU2
1	215	5	935	910	935	896
2A	215	4	1295	1222	1288	1171
2B	280		1295	1215	1119	1171
3A	215	3	1520	1390	1391	1313
3B	280		1520	1380	1222	1313

Table 7.3 Comparison of the effective flange width for a box-beam bridge.

Config. no.	Deck thickness [mm]	Number of webs	Web spacing [mm]	Position	Effective flange width [mm]	
					FEM	WVU2
4	215	5	935	Top flange	912	896
				Bottom flange	916	-----

The results in the Table 7.2 and 7.3 indicate that for all analysed cases the effective width is almost the same as web spacing. Even when the web spacing is increased up to 1520 mm the effective flange width is 91% of the spacing.

For all cases the effective widths computed by WVU2 formula are slightly lower than the ones from FEM. The highest difference between the WVU2 and FEM calculations appears for a T-beam Configuration 3A (three webs and the deck 215 mm) and is about 6%. This formula does not take into account the thickness of the flange. It can be observed that in FEM calculation the effective flange width for configurations that differ only with a thickness of the deck is very similar. Therefore the assumption about not considering the thickness of the flange in the hand calculation WVU2 Eq. (6.3) appears to be correct.

The WVU 1 method also seems to be in close agreement with the results obtained by FE analysis. The highest difference between this approach and FEM is for Configuration 3B and is equal to 12%. This difference comes from the fact that this formula is dependent on the deck thickness.

For the box-beam bridge the results obtained by FEM and WVU2 differ only 2%.

It can be said that both methods are in good agreement with the stress distribution obtained by FEM for T-beam and box-beam bridges and can be used in further hand calculations.

Factor λ (see Eq. 7.2) was also discussed as another way of determining the effective flange width. Since the distribution of stress predicted by FEM shows that the more decisive value is the distance between the webs than the thickness of the deck, the effective length in this case cannot be expressed by the ratio λ .

$$\lambda = \frac{S}{t_f} \quad (7.2)$$

where:

S Spacing of webs

t_f Thickness of the flange

7.4 Transversal load distribution

7.4.1 Description of the analysis

The aim here is to study how the transverse distribution of the load is affected by different geometrical configurations of Model 1. To investigate what part of the load a particular web takes, finite element analysis for three configurations was performed.

Firstly, the T-beam bridge was studied. For this type of bridge the influence of the web spacing was analysed. Therefore, two configurations (Configuration 1 and 3B) with different web spacing were used, see Figure 7.17 and 7.18.

The second case concerned comparison of the box-beam bridge (Configuration 4) and the T-beam bridge (Configuration 1). The studies were made in order to check the difference between the web interaction with and without additional flange in the bottom.

All configurations were loaded with asymmetric uniformly-distributed vehicle load 4kN/m^2 acting on the area $3\text{m} \times 15\text{m}$. Over the shell elements the load was induced as an uniformly-distributed load, while over the beam elements it had to be converted into the distributed beam load equal to $4\text{kN/m}^2 \times 0,215\text{m}$.

The cross-section of the modelled bridges and the applied load are showed in Figures 7.17, 7.18 and 7.19.

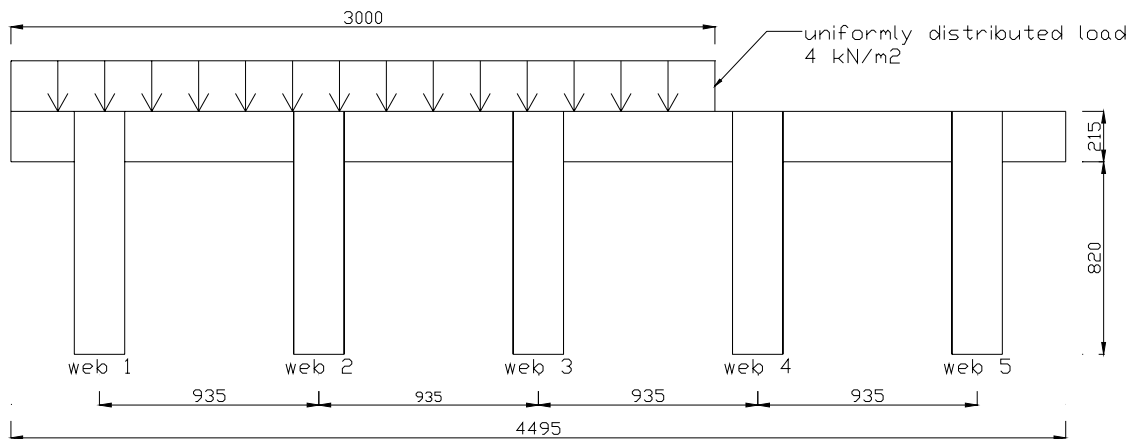


Figure 7.17 T-beam bridge: Configuration 1 with 5 webs.

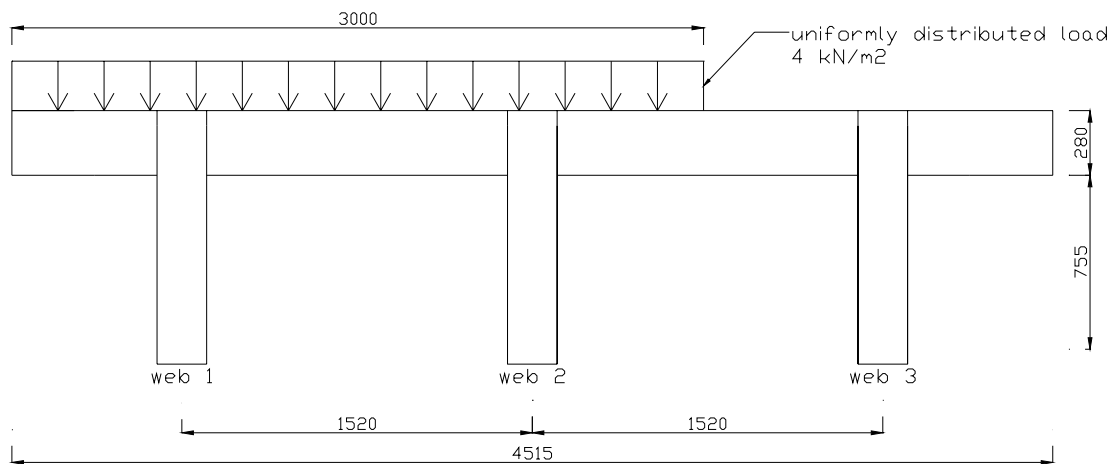


Figure 7.18 T-beam bridge: Configuration 3B with 3 webs.

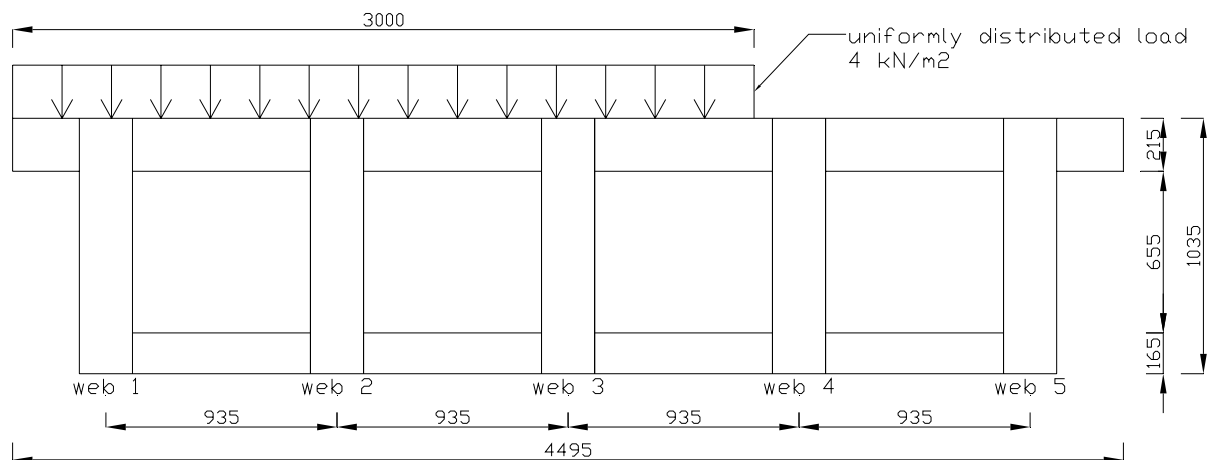


Figure 7.19 Box-beam bridge: Configuration 4 with 5 webs.

7.4.2 Comparison of the results and conclusions

7.4.2.1 Influence of the web spacing and number of webs: T-beam bridge

To see how the load distribution looks for different geometric configurations of the T-beam bridge, the graphs showing distribution of the shear force and bending moment are presented here. For the percentage of the total force acting on each single web the Eq. (7.3) was used.

$$r = \frac{R_i}{\sum_{i=1}^n R_i} \quad (7.3)$$

where:

R_i Shear force in the i -web at the support location

n number of webs

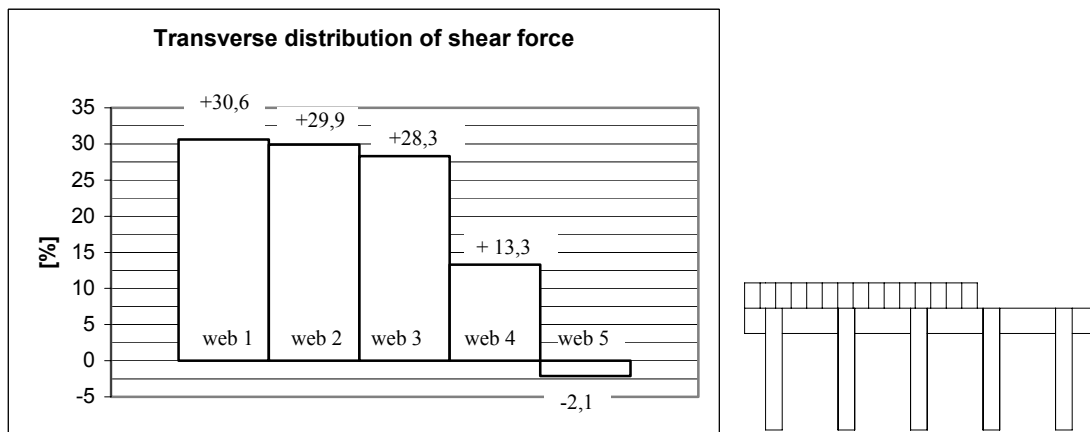


Figure 7.20 Distribution of the shear force in Configuration 1 (T-beam bridge).

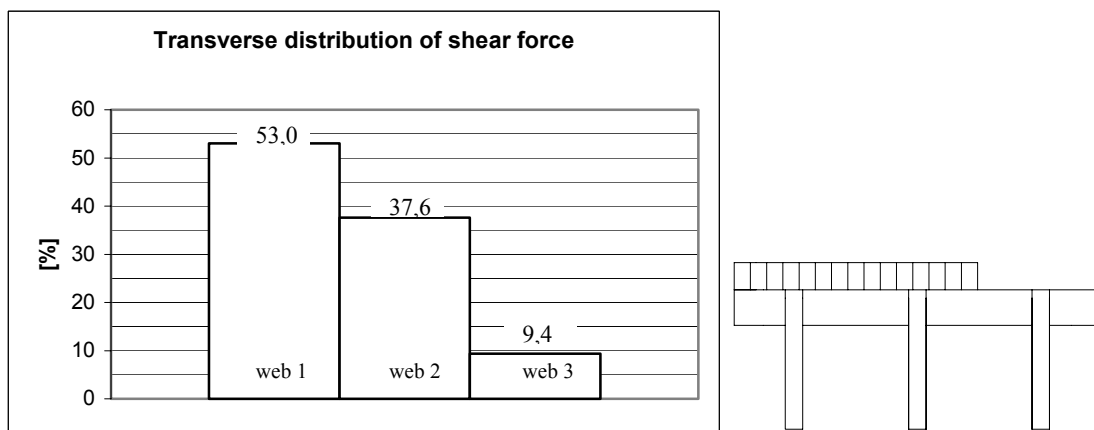


Figure 7.21 Distribution of the shear force in Configuration 3B (T-beam bridge).

Figures 7.20 and 7.21 show that the smaller the spacing is, the more uniformly-distributed load is. The most loaded web for the configuration with five webs takes

30% of the shear force, while the configuration with three webs takes up to 53%. It can be explained by the fact that the Configuration 1 with five webs has a greater transverse stiffness than Configuration 3B with 3 webs. In Configuration 1 in the unloaded web no. 5 the uplifting force appeared. Therefore this configuration needs to be checked further for possible appearing of the uplifting force in the most unfavourable load case, see Section 7.4.3.

The figures above indicate that webs that are not loaded directly also take part in the load distribution. In Configuration 1, unloaded webs no. 4 and no. 5 together take about 11% of applied load. While in Configuration 3, unloaded web no. 3 takes 9% of the load.

The distribution of bending moment was calculated in similar way. The bending moment in every web was divided by the total bending moment in the middle of the bridge span. The results are shown in Figures 7.22 and 7.23.

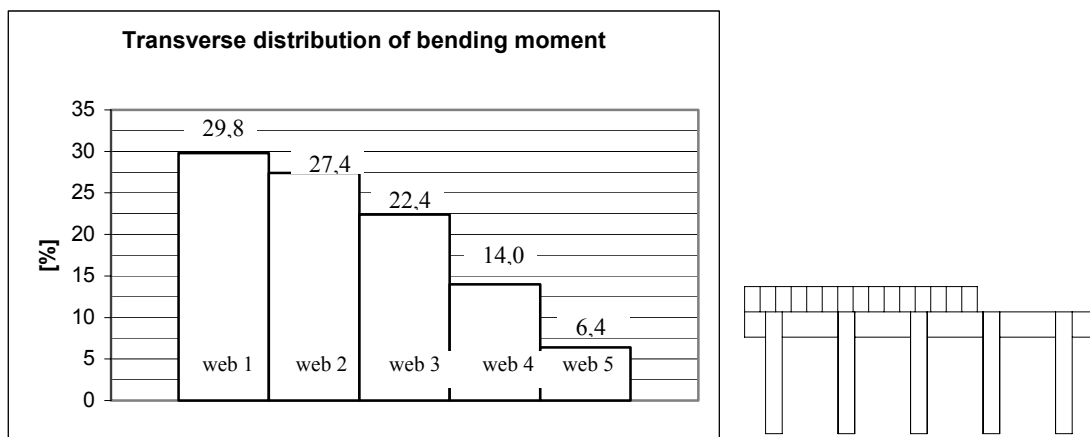


Figure 7.22 Distribution of bending moment in Configuration 1 (T-beam bridge).

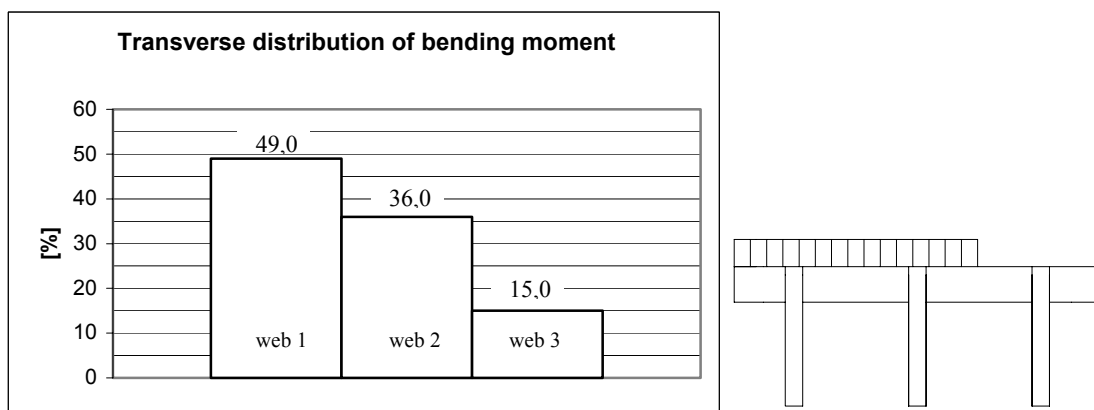


Figure 7.23 Distribution of the bending moment in Configuration 3B (T-beam bridge).

The Figures 7.22 and 7.23 show that the most loaded web in both configurations takes almost the same amount of bending moment as of shear force. However the unloaded webs take greater amount of bending moment than of the shear force.

The studies indicate that Configuration 1 with five webs works better because the load is distributed more evenly and the webs are utilized in a better manner. An increase in number of webs used in design is nearly proportional to an increase in bridge stiffness.

7.4.2.2 Influence of the type of the bridge: T-beam and box-beam bridge

Firstly, the distribution of the shear force was analysed in a T-beam and box-beam bridge and is presented in Figures 7.24, 7.25.

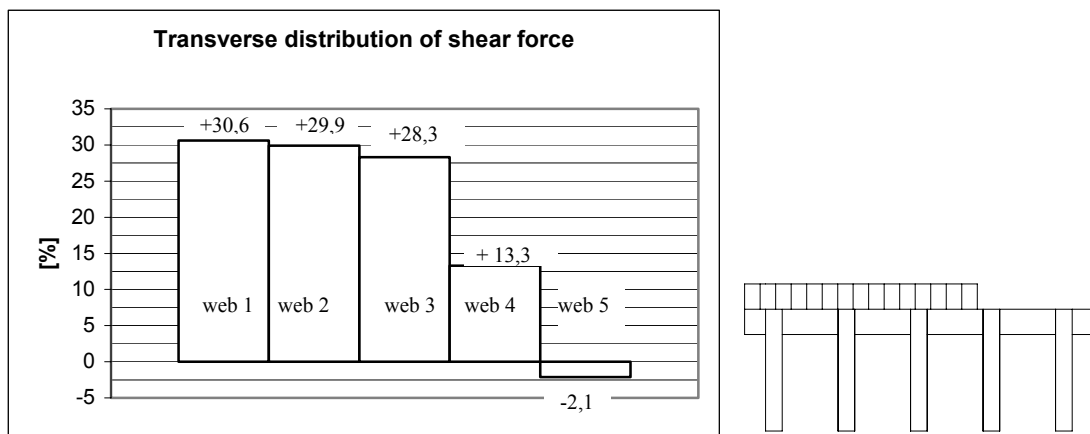


Figure 7.24 Distribution of the shear force in Configuration 1 (T-beam bridge).

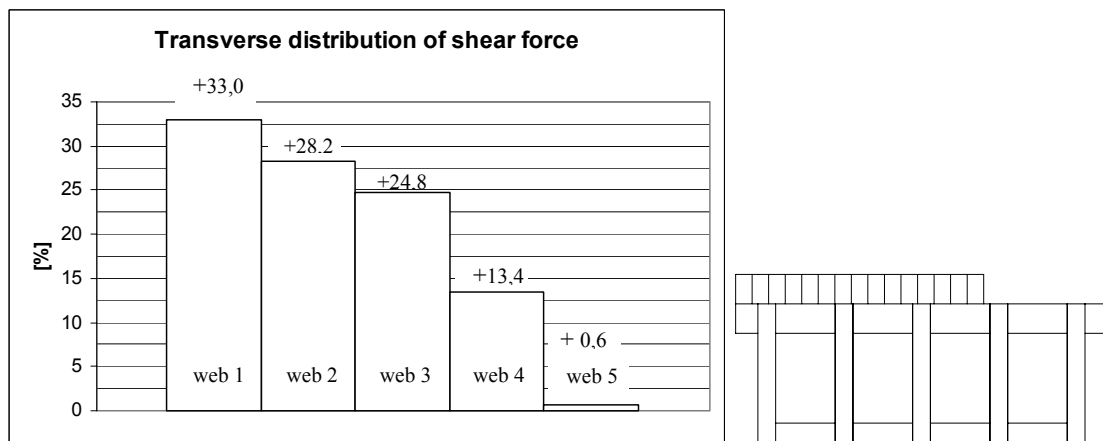


Figure 7.25 Distribution of the shear force in Configuration 4 (box-beam bridge).

It can be observed that for a box-beam bridge the first web takes almost the same amount of the load that for the corresponding T-beam bridge configuration. However, for the box-beam configuration the uplifting force does not appear.

Check of values of the shear stress was performed. From elastic beam theory it might be recalled that the shear force at any point of the cross-section of a beam can be written as:

$$\tau_{vx} = \frac{V \cdot S_x}{I_x \cdot t_w} \quad (7.4)$$

where:

V Shear force

S_x The first moment of area of the shear plane at the level of consideration

I The second moment of the area about the neutral axis

t_w The width of the shear plane

The shear stress was calculated from the reaction forces obtained by FEM analysis according to Eq. (7.4), for calculation see Appendix D.

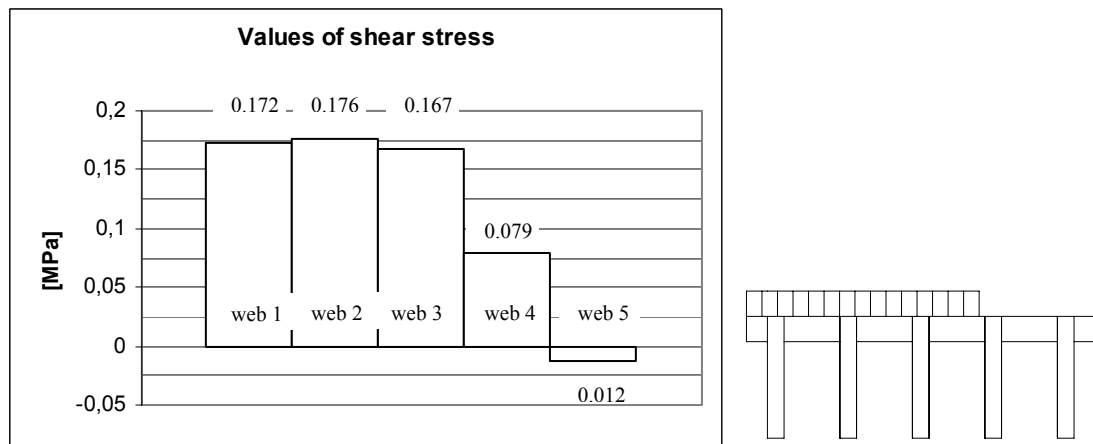


Figure 7.26 Values of the shear stress in Configuration 1 (T-beam bridge).

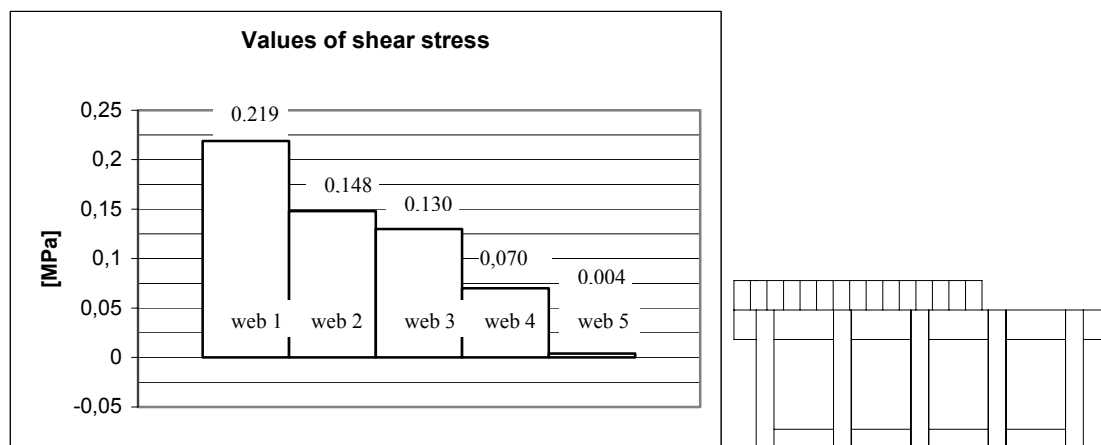


Figure 7.27 Values of the shear stress in Configuration 4 (box-beam bridge).

Figures 7.26 and 7.27 show that the values of shear stress in the interior webs are lower in the box-beam bridge. However, in most loaded exterior web the value is

greater. It can be caused by the fact that the exterior beam has a different cross-section (only bottom flange on one side).

The values of the bending moment and the bending stress were taken from the FEM analysis in the middle of the bridge.

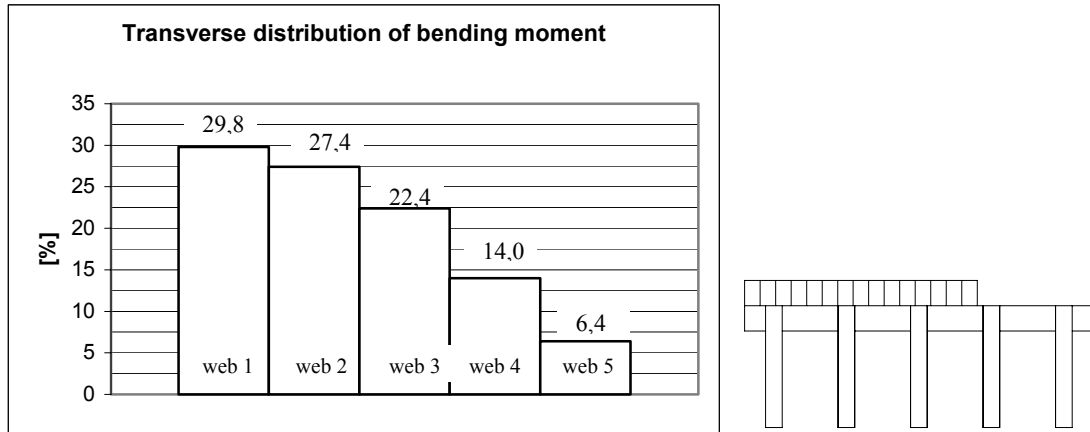


Figure 7.28 Distribution of bending moment for Configuration 1 (T-beam bridge).

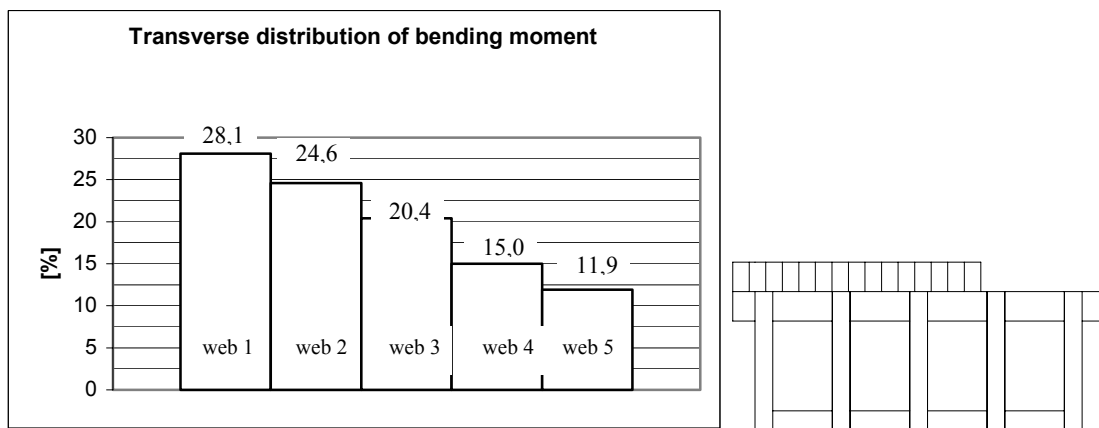


Figure 7.29 Distribution of bending moment for Configuration 4 (box-beam bridge).

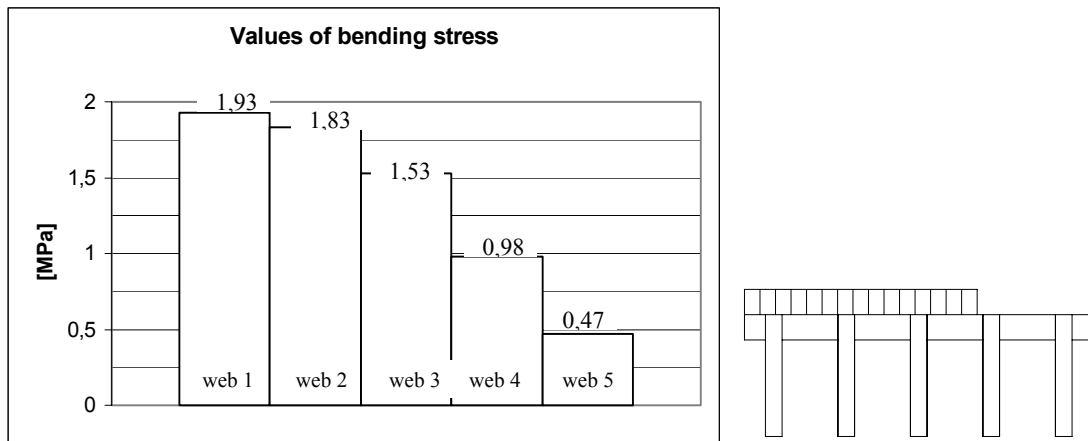


Figure 7.30 Distribution of bending stress for Configuration 1 (T-beam bridge).

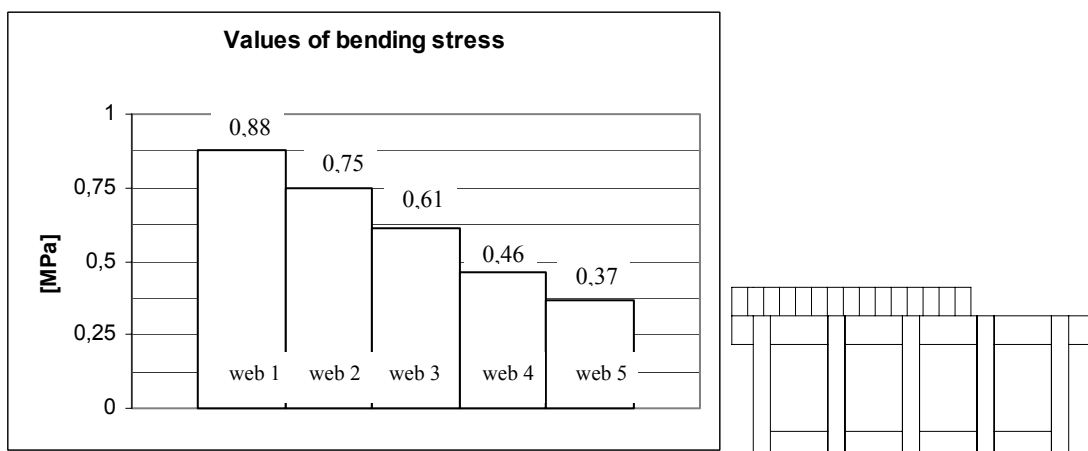


Figure 7.31 Distribution of bending stress for Configuration 4 (box-beam bridge).

Figures above indicate that the box-beam bridge distributes the bending moment more efficiently comparing to T-beam bridge. The unloaded exterior web in a box-beam configuration takes almost two times more of the bending moment comparing to T-beam, see Figures 7.30 and 7.31. The values of bending stress are much lower for a box-beam bridge. The highest value of the bending stress is 0.88 MPa for a box-beam configuration, while for a T-beam is 1.93MPa.

The directly not loaded webs in the case of bending moment distribution as well as shear force distribution carry generally around 20% of the applied load. Therefore the assumption of the interaction between webs in the design of these types of bridge has to be considered.

7.4.2.3 Wheel distribution factor

Wheel distribution factor can be calculated by knowing the deflection of each web, or by knowing a particular stress or other load effect. In this analysis, distribution factor was calculated according to the deflection and the maximum bending stress in the bottom fibre of the web. To determine the factor Eq. (7.5) was used:

$$W_f = \frac{\delta_{\max}}{\sum_{i=1}^n \delta_i} \quad [-] \quad (7.5)$$

where:

δ_{\max} Maximum midspan deflection of most loaded web

δ_i Midspan deflection of the i-web

n Number of webs across the bridge width

When the deflection was substituted by the value of stress, the wheel distribution factor based on bending stress was obtained.

Table 7.4 Wheel distribution factor based on the midspan deflection.

Model 1		δ_{\max} [mm]					W_f
		Web1	Web2	Web3	Web4	Web5	
T-beam bridge	Config. 1	5,32	4,92	4,05	2,48	0,99	0,300
	Config. 3B	7,59	5,46	2,18	---	---	0,498
Box-beam bridge	Config. 4	3,01	2,59	2,12	1,54	1,09	0,291

Table 7.5 Wheel distribution factor based on the bending stress.

Model 1		σ_{\max} [MPa]					W_f
		Web1	Web2	Web3	Web4	Web5	
T-beam bridge	Config. 1	1,93	1,83	1,53	0,98	0,47	0,287
	Config. 3B	3,01	2,21	0,984	---	---	0,485
Box-beam bridge	Config. 4	0,88	0,75	0,61	0,46	0,37	0,286

The Tables 7.4 and 7.5 show that the distribution factors based on deflection and stress are almost the same.

The results from tables above are summarized below and compared to the distribution factors determined by the equations given by West Virginia University. For T-beam bridges, the same as for determining the effective flange width, there are two formulas

to calculate the distribution factor: WVU1 from year 1992 (Eq. (6.6)) and a newer method WVU2 from the year 2000 (Eq. (6.10)). For the box-beam bridge only equation WVU2 (Eq. (6.11)) is considered. Comparison of maximum wheel load distribution factors obtained by different methods is presented in the Table 7.6.

Table 7.6 Comparison of the maximum wheel distribution factor obtained by different methods.

Model 1		FEM analysis		WVU1	WVU2
		$W_f^{\text{deflection}}$	W_f^{bending}		
T-beam bridges	Config.1 (5 webs, deck 215mm)	0,300	0,287	0,334	0,265
	Config. 3B (3 webs, deck 280mm)	0,498	0,485	0,505	0,467
Box-beam bridge	Config. 4 (5 webs)	0,291	0,286	---	0,239

The studies above show that the wheel distribution is influenced by number of webs, spacing between them and bridge cross-section type (T or Box).

The results indicate that the manner in which the wheel factor is calculated by FEM for T-beam bridges gives values in between both design methods (WVU1 and WVU2). The WVU1 gives the results higher than obtained by FEM. This design method can be considered as a conservative one. While the newer approach WVU2 gives lower distribution factors for all the configurations.

For the T-beam Configuration 1 the value obtained by FEM is almost 11% higher than the one from WVU2 approach. In the box-beam configuration the difference in the results between FEM and hand calculation is the highest. The wheel factor for the most loaded web is 28% higher than the one proposed by WVU2. It can be said that this design method of the calculation of the distribution factor is not conservative and should be evaluated.

7.4.2.4 Wheel distributed factor calculated by means of influence lines

To check the results of wheel distribution factor due to uniformly-distributed load from the section before, wheel distribution factor was calculated by means of influence lines. Additionally W_f was estimated separately for concentrated wheel loads what has not been done in previous section, see Figure 7.32.

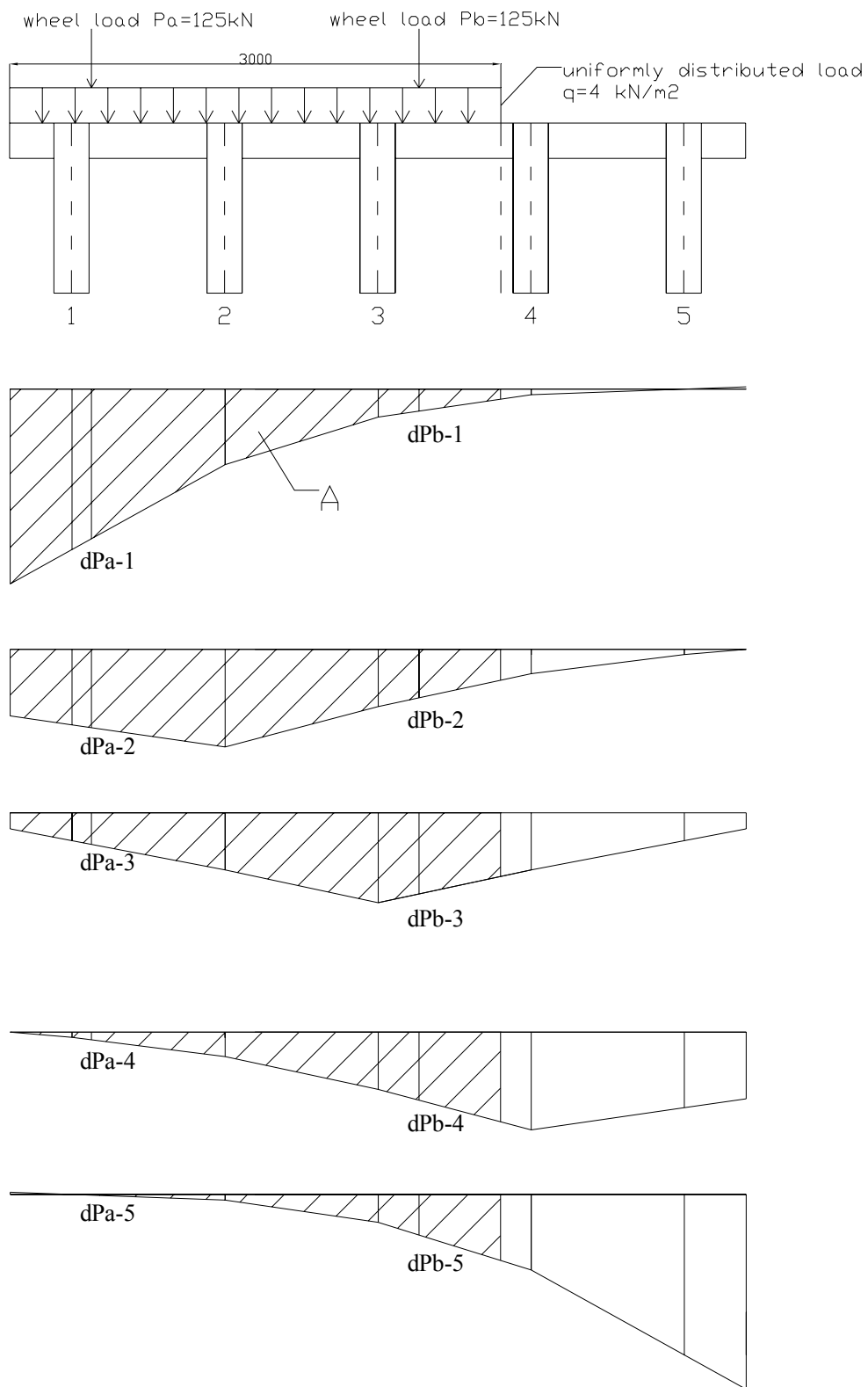


Figure 7.32 Influence lines of deflection (d) for web 1 to 5.

After having drawn the influence lines, the deflection in every web was calculated due to concentrated load (see Eq. 7.6) and due to distributed load (see Eq. 7.7).

$$\delta_{P-i} = P_a \cdot dP_{a-i} + P_b \cdot dP_{b-i} \quad (7.6)$$

$$\delta_{Q-i} = A_i \cdot q \quad (7.7)$$

where:

δ_{P-i} Midspan deflection of the i-web due to concentrated load

δ_{Q-i} Midspan deflection of the i-web due to uniformly-distributed load

Then using Eq. (7.5) the wheel distribution factor was determined, see Table 7.7 and Table 7.8.

Table 7.7 Wheel distribution factor based on the midspan deflection due to distributed load.

Model 1		δ_{\max} [mm]					W_f
		Web1	Web2	Web3	Web4	Web5	
T-beam bridge	Config. 1	5,80	5,19	4,25	2,63	1,33	0,29
Box-beam bridge	Config. 4	3,27	2,78	2,30	1,65	1,16	0,29

Table 7.8 Wheel distribution factor based on the midspan deflection due to concentrated wheel load.

Model 1		δ_{\max} [mm]					W_f
		Web1	Web2	Web3	Web4	Web5	
T-beam bridge	Config. 1	13,06	9,66	8,58	5,77	3,15	0,32
Box-beam bridge	Config. 4	7,08	5,40	4,84	3,56	2,41	0,30

The difference of the wheel distribution factor based on deflection due to distributed load and due to concentrated load is only slightly different.

The same procedure was followed to obtain W_f on the base of bending stress, see Table 7.9 and 7.10.

Table 7.9 Wheel distribution factor based on the bending stress due to distributed load.

Model 1		σ_{\max} [MPa]					W_f
		Web1	Web2	Web3	Web4	Web5	
T-beam bridge	Config. 1	2,79	2,48	2,02	1,31	0,59	0,30
Box-beam bridge	Config. 4	1,34	1,14	1,01	0,62	0,39	0,30

Table 7.10 Wheel distribution factor based on the bending stress due to concentrated wheel load.

Model 1		σ_{\max} [MPa]					W_f
		Web1	Web2	Web3	Web4	Web5	
T-beam bridge	Config. 1	6,46	3,99	4,44	2,85	0,11	0,35
Box-beam bridge	Config. 4	3,09	1,87	2,22	1,41	0,85	0,33

Based on tables above it can be concluded that wheel distribution factor based on bending stress due to distributed load is a bit lower than due to concentrated load. Using the wheel factor calculated due to distributed load, for the whole traffic load consisting of the concentrated wheel loads as well, is not on the safe side.

Table 7.11 Comparison of wheel distribution factor based on the procedures described in Section 7.4.2.3 and 7.4.2.4.

Model 1		$W_f^{\text{deflection}}$ calculated in Section 7.4.2.3	$W_f^{\text{deflection}}$ calculated in Section 7.4.2.4
T-beam bridge	Config. 1	0,30	0,29
Box-beam bridge	Config. 4	0,29	0,29

Table 7.12 Comparison of wheel distribution factor based on the procedures described in Section 7.4.2.3 and 7.4.2.4.

Model 1		W_f^{bending} calculated in Section 7.4.2.3	W_f^{bending} calculated in Section 7.4.2.4
T-beam bridge	Config. 1	0,29	0,30
Box-beam bridge	Config. 4	0,29	0,30

The two procedures described in Section 7.4.2.3 and Section 7.4.2.3 give almost the same results for wheel distribution factor for uniformly-distributed load based on deflection as well as based on bending stress, see Table 7.11 and 7.12. Both procedures are appropriate to determine wheel distribution factor.

7.4.3 Check of the uplifting force for T-beam bridge

The Section 7.4.2 showed that the uplifting force could appear in a T-beam bridge with five webs (Configuration 1) when it was loaded with the unsymmetrical vehicle load only. As this configuration will be studied further, the check of the uplifting force needs to be made.

In reality this load case with traffic load only is impossible, because the self-weight of the bridge has to be taken into account. To check if the uplifting force can really appear, the FEM analysis of the Configuration 1 with five webs loaded with a variable load increased by the safety factor $\gamma=1,5$ and self-weight (see Section 5.2.2).

The studies showed that the lowest value of the reaction force (shear force in the web at the support location) was equal to $R=9,88\text{kN}$ and it was in the fifth beam, see Figure 7.33.

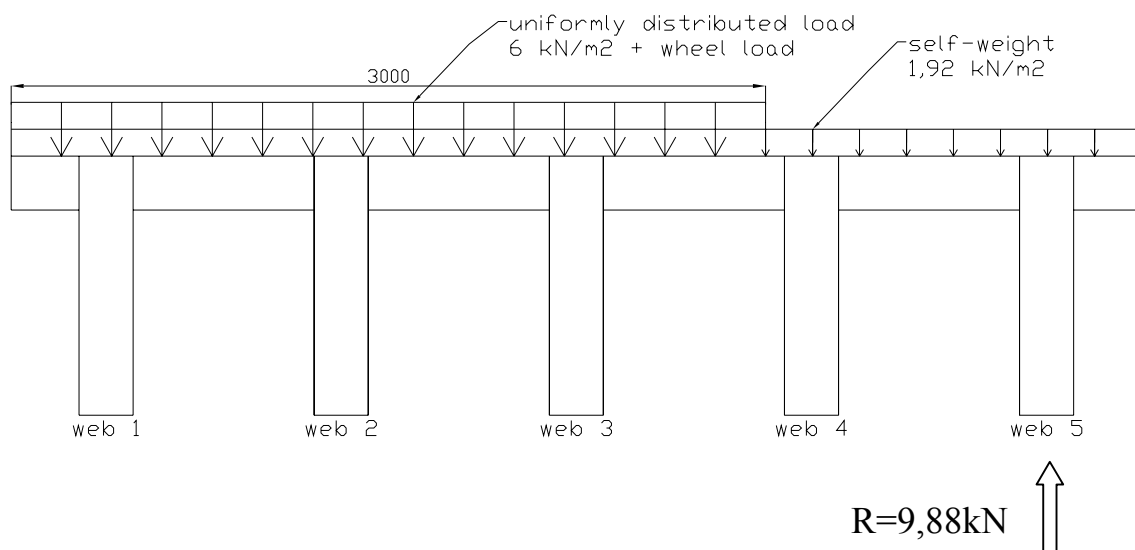


Figure 7.33 Value of the reaction force in the last web.

It can be observed that for the most unfavourable load case the uplifting force cannot appear. In the check above the surface load was not taken into account, but it would give the favourable effect and increase the reaction force. As a result, there is no danger of uplift during the lifetime of the bridge.

7.5 Local effect of the wheel load

According to Eurocode 5 (2004) loads should be considered at a reference plane in the middle of the deck. An effective contact area of the wheel should be calculated according to the Figure 7.34 and Table 7.13.

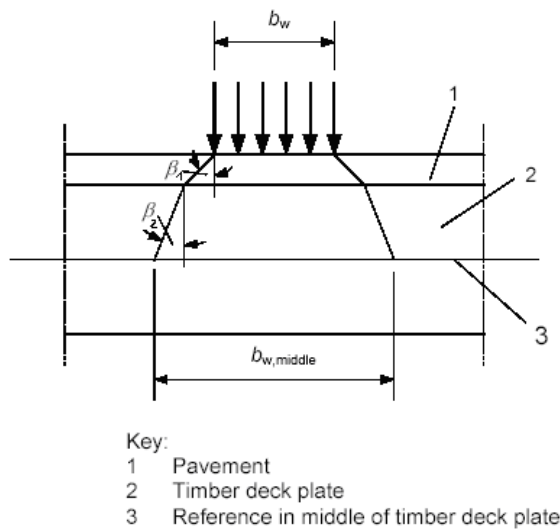


Figure 7.34 Dispersion of concentrated loads from contact area width b_w for plate decks. [EC5 (2004)]

Table 7.13 Dispersion angle β of concentrated loads for various materials. [EC5 (2004)]

Pavement (in accordance with EN 1991-2 clause 4.3.6)	45°
Boards and planks	45°
Laminated timber deck plates:	
– in the direction of the grain	45°
– perpendicular to the grain	15°
Plywood and cross-laminated deck plates	45°

7.5.1 Wheel load between the webs

7.5.1.1 Description of the analysis

The deck between webs should be designed for local effect of the wheel load. The web spacing and depth of the deck should be selected in such a way that conditions concerning maximum transverse deflection and stress are fulfilled. The maximum local transverse deflection is 2.54mm (GangaRao and Raju 1992).

In the finite element program, the local analysis of T-beam bridge (Model 1) with 5 webs and the 215mm deck thickness (Configuration 1) was performed. Since the deck was modelled with shell elements, it was loaded with concentrated wheel load acting on an effective contact area with respect to the middle plane of the deck (case 'a') based on EC5 (2004), see Figure 7.35.

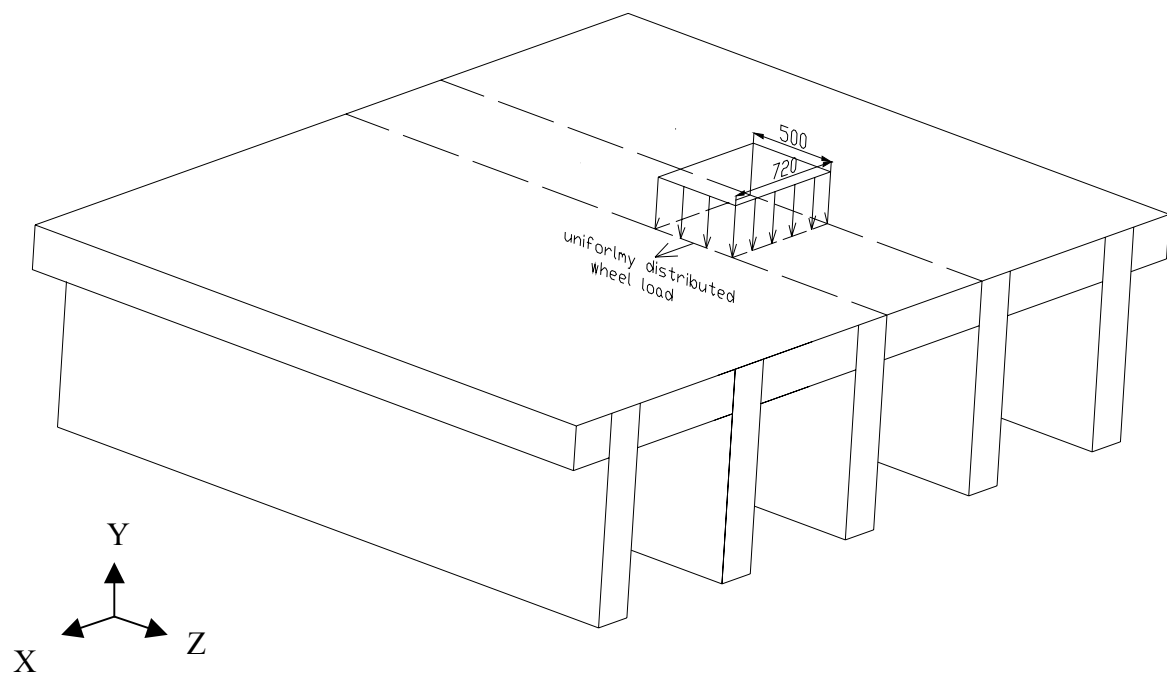


Figure 7.35 Contact area of the wheel load in FEM model, case 'a'.

Although the calculated effective area was 776mm x 591mm, (see Table 7.14) for the finite element method analysis slightly different area was assumed. This approximation was caused by the choice of the dimensions of shell elements. The deck was modelled with 72mm x 250mm shell elements so the reference wheel load

was distributed on the area of 720mm x 500mm. Therefore the concentrated load of 125kN (Bro 2004) was transformed into pressure of 347,22kN/m².

Table 7.14 Contact area of the wheel load.

Through laminated timber deck plates	s ₁ [mm]	s ₂ [mm]	β ₁ [°]	β ₂ [°]	b _w [mm]	Calculated b _{w,middle} [mm]	FEM b _{w,app} [mm]
Perpendicular to the lamination	88	215	45	15	600	776	720
In the direction of the lamination	88	215	45	45	200	591	500

β₁, β₂ see Figure 7.34

b_w Width of the load area on the contact surface of the deck plate. According to Bro 2004 b_w = 0.6m in the transversal direction and 0.2 in the direction of the traffic.

b_{w,middle} Width of the load area referred to the middle lane of the deck plate.

s₁ Wearing layer thickness

s₂ Deck thickness

To compare the results, a second analysis with point force equal to 125kN was performed (case 'b'), see Figure 7.36.

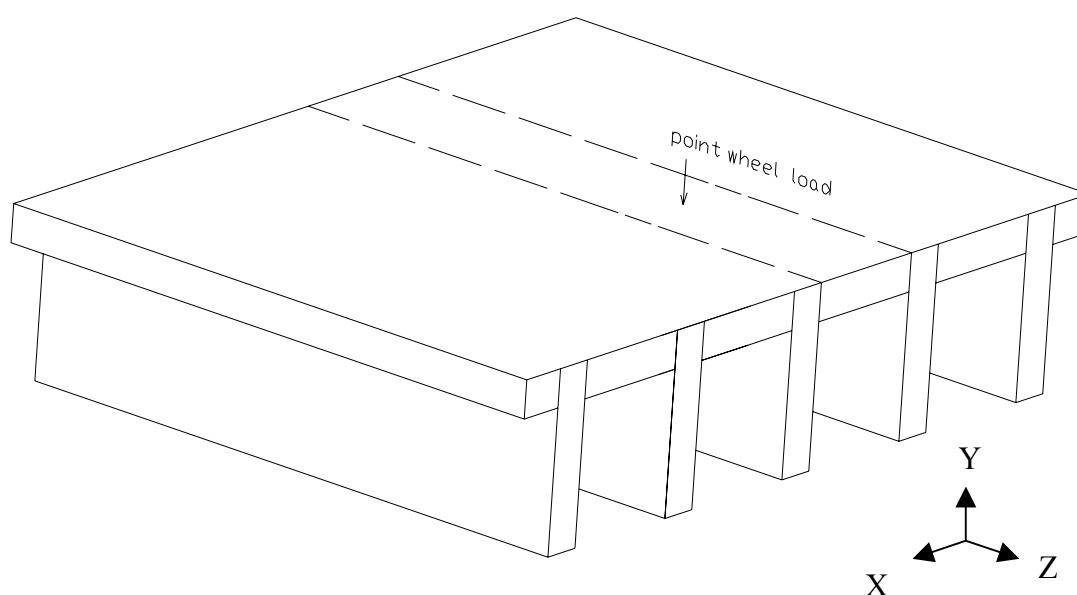


Figure 7.36 Point wheel load in FEM model, case 'b'.

7.5.1.2 Results

Based on the FEM results it can be determined if the bridge fulfils the local conditions according to GangaRao (1992).

To calculate relative local transverse deflection, from the displacement of the plate δ_m obtained by FEM, the mean displacement of the adjacent web was subtracted, see Eq. (7.8).

$$\Delta = \delta_m - \left(\frac{\delta_2 + \delta_1}{2} \right) \quad (7.8)$$

Transverse deflection for case 'a' (distributed load) was equal to **1.55mm** < **2.54mm** (limit value- GangaRao 1992).

Figure 7.37 indicates values of the displacement in the most deformed cross-section of the bridge. It can be observed that the highest displacement occurs in the middle of the two adjacent webs, between which wheel load was applied.

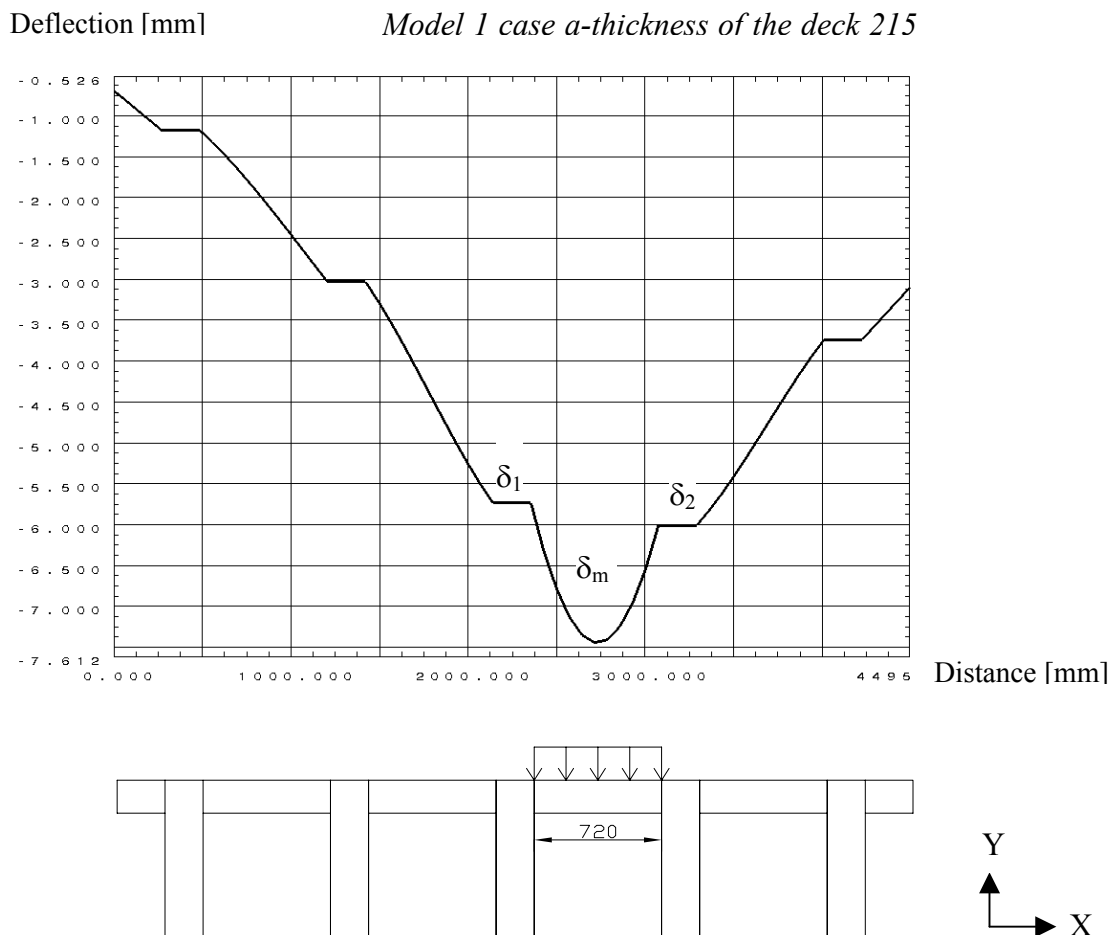


Figure 7.37 Deflection of the deck in the most deformed cross-section.

Maximum local transverse stress obtained from FEM $\sigma_{xx} = 0,48\text{MPa}$ (distributed load). To compare this stress with the design value of maximum compression perpendicular to the grain, it is necessary to add the value of prestress f_p .

$$0.48\text{MPa} + f_p \leq f_{c90d} = f_{ck} \cdot \frac{k_{\text{mod}}}{\gamma_m} = 5.76\text{MPa}$$

It can be assumed that the value of prestress is less than 1MPa so the condition about local compression stress is fulfilled.

Table 7.15 shows the values of the transverse stress and deflection for FEM Model 1 and hand calculation.

Table 7.15 Comparison of the transverse stress and deflection obtained by FEM and hand calculation.

Type of analysis		Local transverse stress [MPa]	Transverse deflection [mm]
FEM	Distributed load, case a	0,48	1,55
	Point load, case b	1,41	4,02
WVU1		Eq. (6.14) 0,74	Eq. (6.12) 1,26

Different ways of applying wheel load in FEM analysis give significantly different results. When the wheel load is applied as point load the results are overestimated. In real model the load is distributed over the tire width. Thus, the second FEM analysis with distributed wheel load shows more accurate values. Eq. (6.12) and Eq. (6.14) recommended by WVU are not in agreement with FEM analysis case 'b'. Even though the formulas are developed due to concentrated load, they are comparable with the case 'a'. They give results that are conservative for the case 'a' but not at all on the safe side for case 'b'.

The investigation of shear force was necessary in order to check the probability of slippage between lamellas. This phenomenon is most likely due to the transverse shear τ_{xz} caused by the transverse shear force V_x as depicted in the Figures 7.38 and 7.39 (the Y direction is the direction of the traffic while X is the transverse direction).

This vertical shear must be carried by the frictional force between the laminations which is induced by the stressing rods.

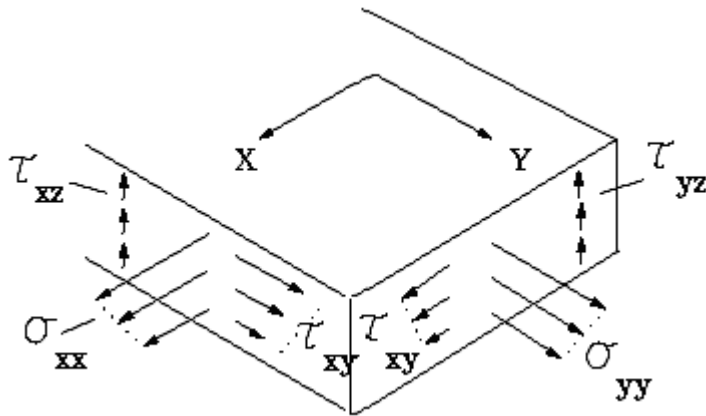


Figure 7.38 Shell stresses. (I-DEAS help)

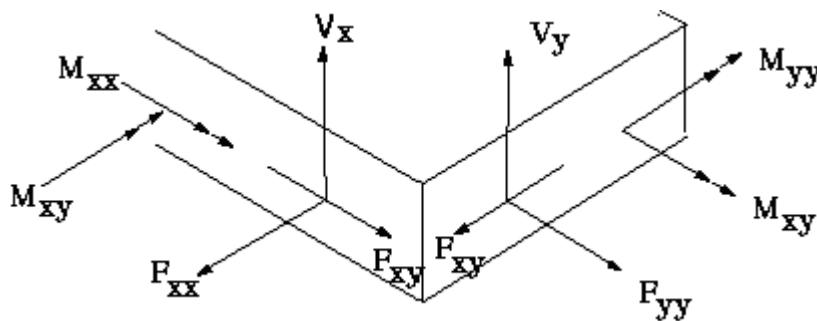


Figure 7.39 Shell forces. (I-DEAS help)

$$\begin{pmatrix} F_{xx} \\ F_{yy} \\ F_{xy} \end{pmatrix} = \int \begin{pmatrix} \sigma_{xx} \\ \sigma_{yy} \\ \tau_{xy} \end{pmatrix} dz = \text{membrane stress resultants (element forces)}$$

$$\begin{pmatrix} M_{xx} \\ M_{yy} \\ M_{xy} \end{pmatrix} = \int \begin{pmatrix} \sigma_{xx} \\ \sigma_{yy} \\ \tau_{xy} \end{pmatrix} z dz = \text{bending stress resultants (element forces)}$$

$$\begin{pmatrix} V_x \\ V_y \end{pmatrix} = \int \begin{pmatrix} \tau_{xz} \\ \tau_{yz} \end{pmatrix} dz = \text{transverse shear stress resultants (element forces)}$$

According to FEM analysis the greatest shear force appeared under the wheel load near the web and was equal to 13.5kN. Based on this force the required prestress level was calculated using the following Eq. (7.9) from EC5 (2004):

$$F_{v,Ed} \leq \mu_d \cdot \sigma_{p,\min} \cdot h \quad (7.9)$$

where:

$F_{v,Ed}$ The design shear force per unit length

μ_d The design value of coefficient of friction,

$\sigma_{p,\min}$	The minimum long-term residual compressive stress due to prestressing
h	The thickness of the plate

In the case of analysed bridge:

$$F_{v.Ed} = \frac{13.5kN}{element_length}$$

$\mu_d = 0.35$ The moisture content is assumed in between 12% and 16%

$$h = 0.215m$$

$$\sigma_{p,\min} \geq \frac{F_{v.Ed}}{h \cdot \mu_d} = 0.718MPa$$

The initial prestress should be two times higher than the long-term prestressing and according to EC5 (2004) at least 1MPa. In this case it would be about $2 \times 0.718MPa = 1.436MPa$ which is about 1.5MPa.

7.5.2 Dispersion of a concentrated load

The aim of this section is to check if the values of the dispersion angles of concentrated loads given in EC5 (2004) for plate deck bridges can be adopted for T-beam bridges.

Two cross-section configurations of Model 2 were created in FEM program. The first configuration consisted only of a deck plate; the second was the T-beam bridge model with web spacing 935mm (Model 2, see Section 6.2). Stress-laminated plate deck was modelled in the same way as Model 2 of T-beam bridge. The area on which the wheel was acting was equal to 360mm x 400mm. The point force of one wheel 125kN was divided into 525 concentrated forces (238N) and applied in every node of 480 elements over the area 360mm x 400mm.

The distribution of load in the transverse direction of the bridge can be observed from vertical stresses σ_y plotted along the paths according to the Figure 7.40. Path 1 is in the top surface of the deck and the path 2 is in the middle surface.

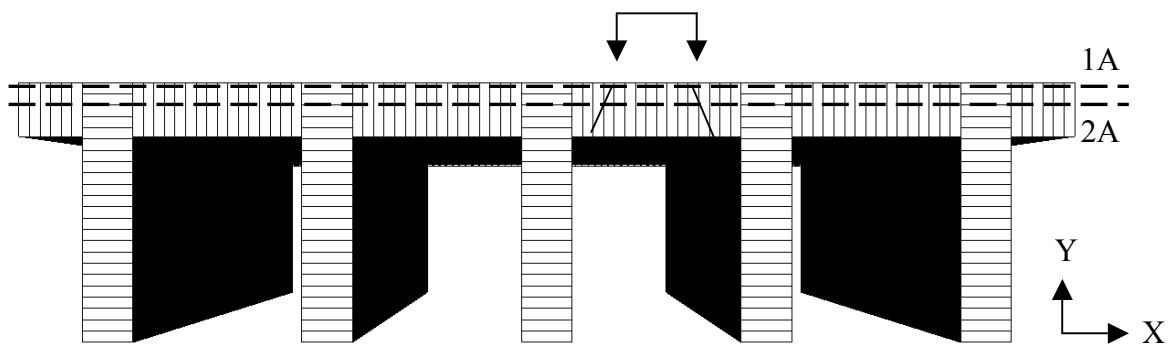
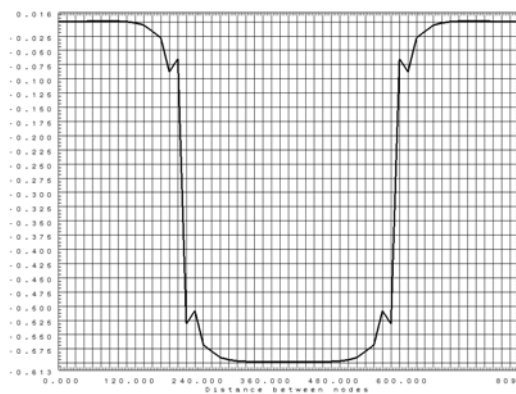


Figure 7.40 Paths in the direction perpendicular to the grain of lamination.

Plate deck- path 1A-Top layer



T-beam bridge- path 1A-Top layer

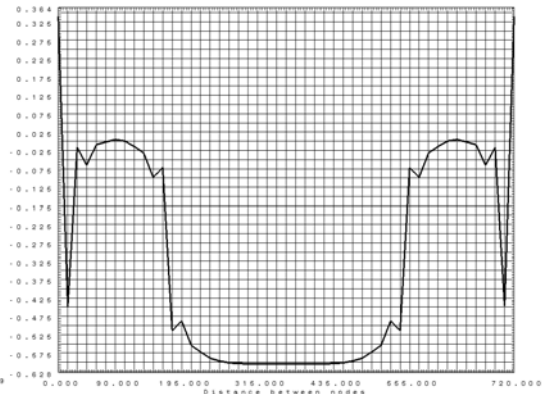
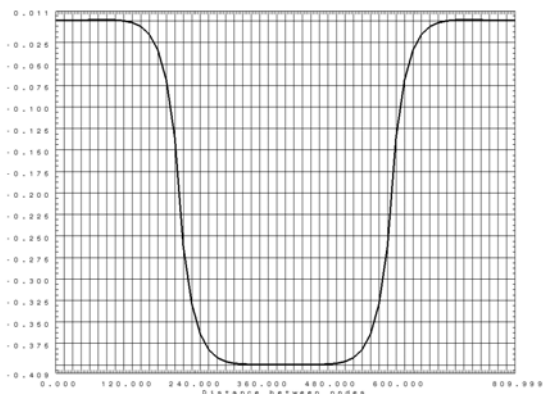


Plate deck- path 2A-Middle layer



T-beam bridge- path 2A-Middle layer

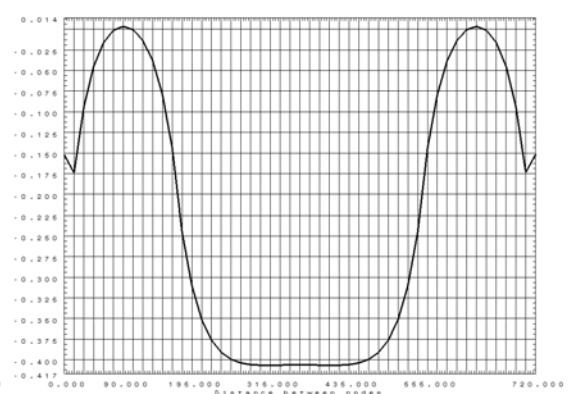


Figure 7.41 Plot of the stress σ_y in the transverse direction.

Due to the mesh size the width of the loaded area at the reference plane in the middle of the stress laminated deck is 420mm. The corresponding width in the T-beam deck is 400mm. The calculated dispersion factors are summarized in the table below.

Table 7.16 Contact width of the wheel load perpendicular to the grain.

Type of the bridge	s_2 [mm]	b_w [mm]	EC5		FEM $b_{w,F}$ [mm]	
			β [°]	$b_{w,middle}$ [mm]	β [°]	$b_{w,F}$ [mm]
Plate deck	215	360	15	418	16	420
T-beam bridge					11	400

Table 7.16 indicates that for the T-beam model effective contact length is only 5% lower than for the stress-laminated deck. Therefore the influence of webs is negligible and the dispersion factor in the direction perpendicular to the grain from EC5 (2004) can be used.

The distribution of load in the longitudinal direction of the bridge can be observed from vertical stresses σ_y , plotted along the paths according to the Figure 7.42

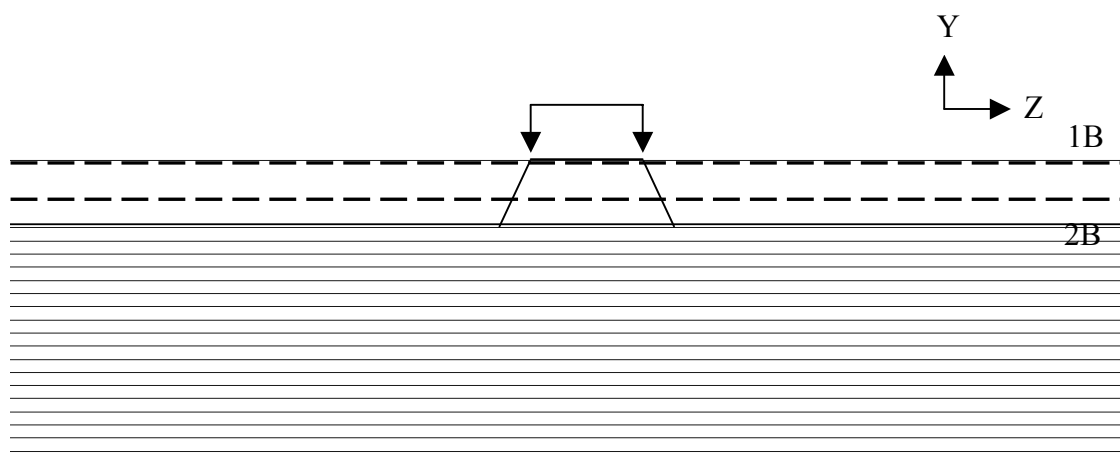
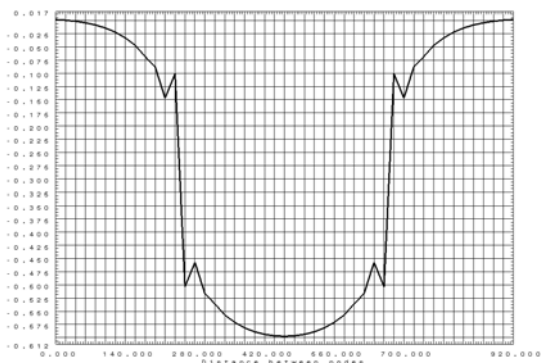


Figure 7.42 Paths in the direction parallel to the grain of lamination.

Plate deck- path 1b-Top layer



T-beam bridge- path 1b-Top layer

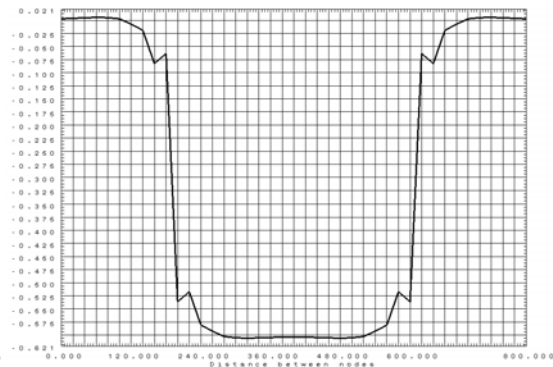
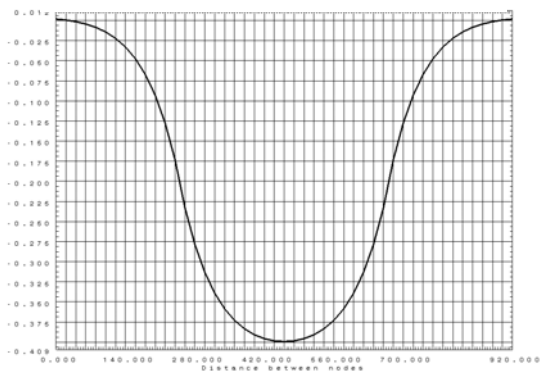


Plate deck- path 2b-Middle layer



T-beam bridge- path 2b-Middle layer

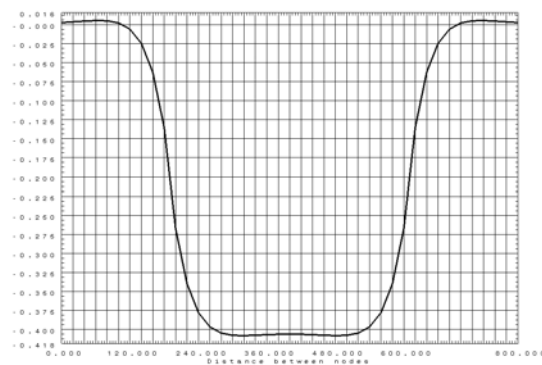


Figure 7.43 Plot of the stress σ_y in the longitudinal direction.

On the contrary the effective lengths in direction of the grain differ significantly.

For the plate deck, this length from FEM it is exactly the same as the one according to EC5 (2004). However the effective length in the case of T-beam bridge is 500mm, see Table 7.17.

Table 7.17 Contact area of the wheel load in the direction of the grain.

Type of the bridge	s_2 [mm]	b_w [mm]	EC5		FEM $b_{w,F}$ [mm]	
			β [°]	$b_{w,middle}$ [mm]	β [°]	$b_{w,F}$ [mm]
Plate deck	215	400	45	615	45	615
T-beam bridge					25	500

As it can be observed in the table, for the T-beam model the contact length is 23% shorter than for the plate deck. It can be explained by the influence of the webs that make the bridge stiffness higher. Therefore the dispersion angle is smaller.

7.6 Global analysis of the bridge performed by FEM

7.6.1 General description

The global analysis was studied to check the agreement between the hand calculations and the finite element method analysis.

The three types of bridges were modelled in FEM program (Model 1): Config. 1, Config. 2A and Config. 3B. Details concerning geometry of the models can be found in Table 7.18.

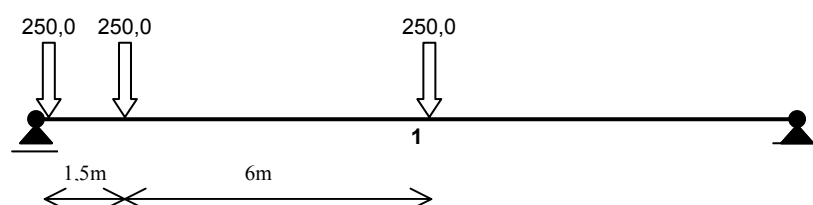
Table 7.18 Geometry of the analysed models of the bridge.

Model no.	Thickness of the deck [mm]	Number of webs	Web spacing [mm]	Height of the webs [mm]	Thickness of the webs [mm]
1	215	5	935	1035	215
2a	215	4	1295	1035	215
3b	280	3	1520	1035	215

7.6.2 Load combinations

There were two unfavourable load cases of traffic load that were investigated. First case produced maximum shear in the longitudinal direction and second case produced maximum moment in the longitudinal direction.

- Vehicle load case 1 – The highest value of the shear force occurs when the first couple of wheel load forces is placed one element from the edge. The distance between the other forces is 1,5m and 6m in the longitudinal direction and 2m in the transverse direction, see Figure 7.44 and 7.45.



1 - midspan

Figure 7.44 Longitudinal position of wheels to produce maximum shear. (Bro 2004)

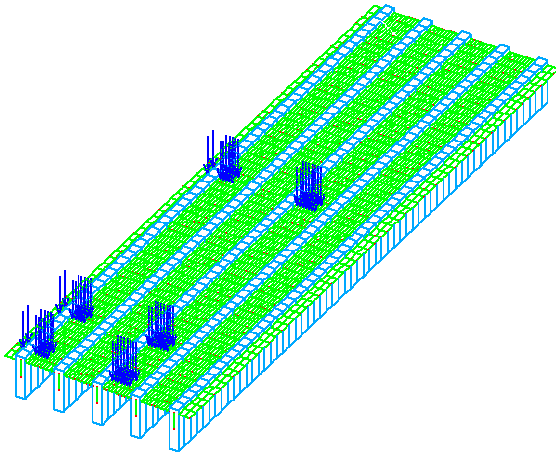
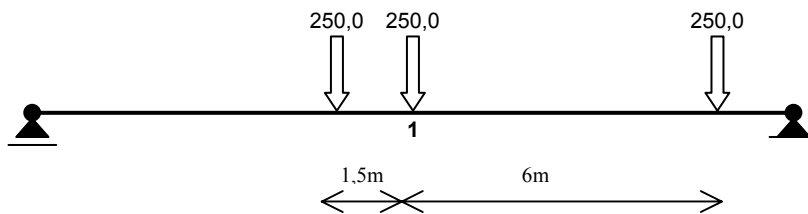


Figure 7.45 Longitudinal position of wheels (acting on contact area) to produce maximum shear. (Bro 2004)

- Vehicle load case 2 – The highest value of the bending moment occurs when the first couple of wheel load forces are placed 1,5m from the edge. The second and third couple of forces are placed in longitudinal distance 6m and 1,5m respectively, see Figure 7.46 and 7.47.



1 - midspan

Figure 7.46 Longitudinal position of wheels to produce maximum moment.

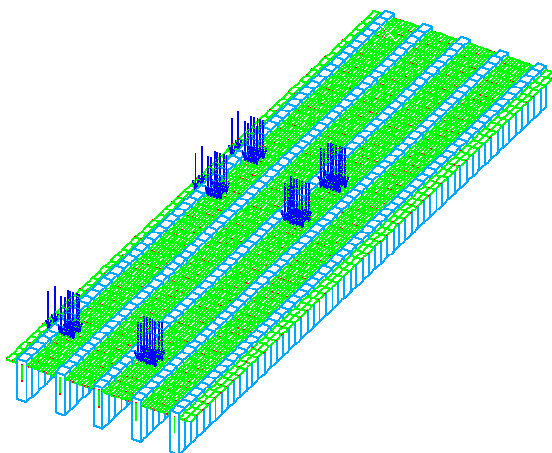


Figure 7.47 Longitudinal position of wheels (acting on contact area) to produce maximum moment.

Additionally in both cases the uniformly-distributed traffic load acted on the area of 3m x 15m and was placed in the transverse position, just from the edge of the bridge, in order to obtain the highest values of stresses and deformation in the transverse direction.

The analysed load combinations consisted also of the self-weight load and surfacing load, see Table 7.19.

Table 7.19 Load combinations.

Load combination 1	Self-weight	Surfacing	Vehicle load case 1
Load combination 2	Self-weight	Surfacing	Vehicle load case 2

7.6.3 Comparison of the results from FEM and hand calculation

All the results below are due to the characteristic loads. The comparisons are made in that way because they show only the difference between the different methods and not design checks if the stresses are within the allowable level. These checks are made only for a selected model in the next chapter.

The results for the single beam are due to the loads acting only on its cross-section in the case when one of the axes of the traffic load is placed over it. This method assumes no interaction between the webs.

The results from other methods take into consideration the whole load acting on the bridge decreased by the corresponding wheel factor W_f that describes the part of the whole load taken by the most loaded web.

The Table 7.20 presents the results for the Model 1, Configuration 1. Results for Config. 2A and Config. 3B are in the Appendix C.

Table 7.20 Comparison of maximum values of stress and deflection of the bridge Config. 1 (5 webs, deck 215mm), beff calculated according to WVU1.

		FEM max results	Single beam		WVU conservative		WVU new approach	
			Hand calc.	Δ_1 [%]	Hand calc.	Δ_2 [%]	Hand calc.	Δ_3 [%]
Surface + self- weight + vehicle	Bending stress in the beam [MPa]	15,82	22,23	+40	16,46	+4	13,46	-15
	Shear force in the beam [kN]	286,01	353,56	+24	344,68	+21	321,08	+13
	Shear stress in the beam [MPa]	2,06	2,38	+16	2,32	+13	2,16	+5
	Compressive stress in the deck-Top [MPa]	-9,59	-11,98	+25	-8,87	-8	-7,25	-24
Vehicle	Deflection [mm]	33,8	43,12	+28	49,40	+46	39,11	+16

The difference Δ is calculated in the following way:

$$\Delta_i = \frac{FEM_{result} - Hand.calc.}{FEM_{result}} \cdot 100\%$$

Calculating the beam as single is not recommended. The values of the shear force and bending moment for such a beam are higher than in the ‘real’ model for a beam interacting with the rest of the beams. It is caused by the fact that the beam is not taking the entire load directly above it, but other webs contribute to the load transmitting. The smaller the spacing between the webs the worse is the method.

The FEM model predicts that the highest compression stresses occur in the flange, usually beneath the wheel load. For the case when the wheel loads are between the webs, the FEM produces stresses in the flange slightly higher than those determined by hand calculation.

7.6.4 Analysis of the T-beam and box-beam bridge in the ULS

7.6.4.1 Description of the models

To check the difference in stress between the two types of the bridge following analysis had been performed. Two models that were investigated are shown in Figure 7.48 and 7.49.

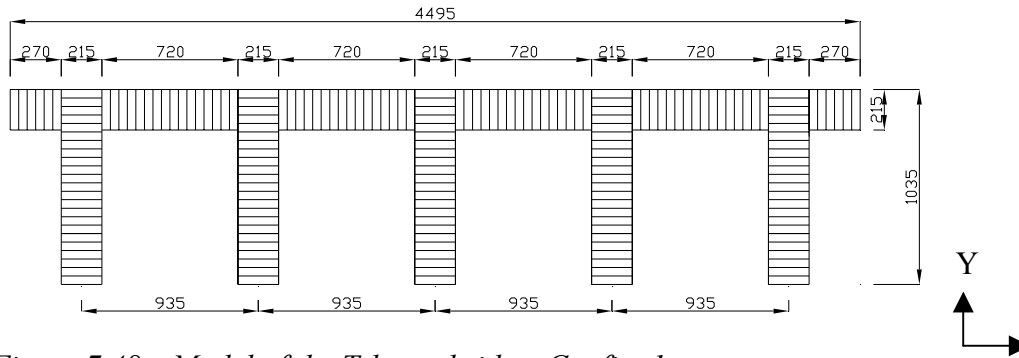


Figure 7.48 Model of the T-beam bridge, Config. 1.

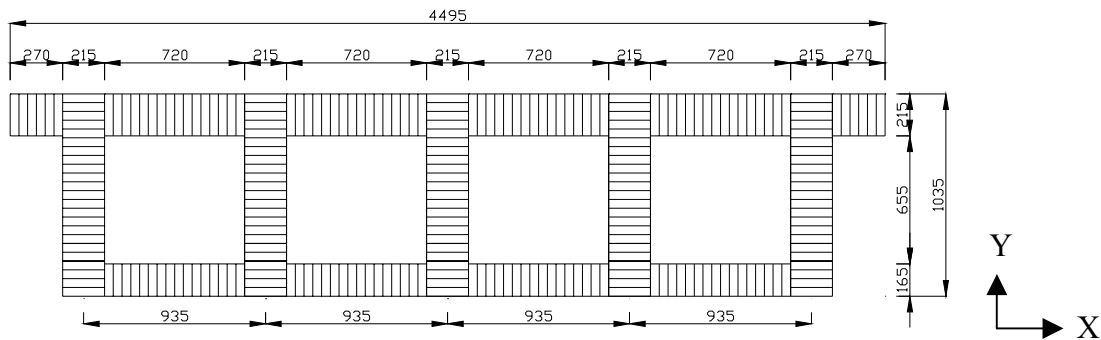


Figure 7.49 Model of the box-beam bridge, Config. 4.

The elements of the bridge were verified respecting the Ultimate Limit State.

$$ULS_combination = 1,0 \cdot self - weight + 1,0 \cdot surfacing + 1,5 \cdot traffic_load$$

To determine the maximum shear stress, the first axle of the vehicle was placed one element from the support, vehicle load case 1. To obtain the greatest bending the different position was analysed, vehicle load case 2.

The deflection of the bridge was verified respecting the Serviceability Limit State, and it was calculated from live load case 2.

$$SLS_combination = 0,8 \cdot traffic_load$$

7.6.4.2 Comparison of the results

The way the results in the Table 7.21 were obtained, can be found in Appendix A for the T-beam bridge (WVU1) and in Appendix B for the box-beam bridge.

Table 7.21 Comparison of maximum values of stress and deflection of the bridges.

		T-beam bridge			Box-beam bridge		
		FEM Model 1 Config.1	WVU1	Δ [%]	FEM Model 1 Config.4	WVU2	Δ [%]
ULS comb.	Bending stress in the beam [MPa]		23,05				
		19,22		-17			
	Shear force in the beam [kN]	414,65	504,5	+21	419,00	461,29	+10
			467,32	+13			
	Shear stress in the beam [MPa]	3,00	3,40	+13	3,22	3,11	-3
			3,15	+5			
	Compressive stress in the deck-Top [MPa]	-13,7	-12,94	-6	-10,00	-8,11	-19
			-10,49	-23			
SLS comb.	Deflection [mm]	27,48	39,82	+45	15,63	19,08	+22
			31,55	+15			

The results from hand calculations above are from the case where the effective flange was calculated according to the WVU2. The first method WVU1 took into account the width of the deck and it came out from the FEM analysis that the width of the deck does not have such an influence on the effective width as the method WVU1 predicts. In the table the first value of results for T-beam bridge corresponds to the wheel factor calculated according to WVU1 and the second value is corresponding to the wheel factor according to WVU2.

The biggest difference is between the value of deflection in FEM and the one calculated according to the guidelines WVU1. It seems that the recommendation to multiply the value of the deflection by the factor 1.6 (see Section 6.5.1) may be too conservative.

Table 7.22 Verification of the elements - results from FEM.

		Limiting values	T-beam bridge	Utilization	Box-beam bridge	Exploitation
ULS comb.	Bending stress in the beam [MPa]	$f_{md} = 23.76$	23,05	97%	7,79	33%
	Shear stress in the beam [MPa]	$f_{vd} = 2.88$	3,00	104%	3,22	112%
	Compressive stress in the deck-Top [MPa]	$f_{cd} = 25.92$	13,7	53%	10,00	39%
SLS comb.	Deflection [mm]	$\delta = 37.5$	27,48	73%	15,63	42%

Table 7.23 Verification of the elements - results from hand calculation.

		Limiting values	T-beam bridge	Utilization	Box-beam bridge	Exploitation
ULS comb.	Bending stress in the beam [MPa]	$f_{md} = 23.76$	23,72	100%	10,25	43%
			19,22	83%		
	Shear stress in the beam [MPa]	$f_{vd} = 2.88$	3,39	118%	3,11	108%
			3,15	109%		
	Compressive stress in the deck-Top [MPa]	$f_{cd} = 25.92$	12,94	50%	8,11	31%
			10,49	40%		
SLS comb.	Deflection [mm]	$\delta = 37.5$	39,82	106%	19,08	51%
			31,55	84%		

where:

f_{md} Design value of the bending stress parallel to the grain

f_{vd} Design value of the longitudinal shear stress

f_{cd} Design value of the compression stress perpendicular to the grain

The Table 7.22 shows that there is almost no difference between shear stress between analysed models. However it can be observed that the bending stress and deflection of the box-beam bridge are much lower than for the T-beam bridge. The webs in the box-beam bridge interact better with distribution of the bending moment. Therefore the utilisation of the compressive and bending stresses is much lower than for the T-beam bridge. The deflection of the box-beam bridge is more than two times lower than for a T-beam bridge.

Due to the high shear stress the area of the web should be increased in both type of the bridges.

7.7 Dynamic analysis

Dynamic effects can be significant in short-span timber bridges. Therefore road bridges with pedestrian or bicycle traffic must be designed for the dynamic loads imposed by passing vehicles.

In Bro 2004 there are specific limitations of vertical acceleration for road bridges with pedestrian and bicycle traffic.

For road bridges without any pedestrian traffic there is no need to check vertical acceleration and natural frequency. However, just to show the difference of natural frequency between the T-beam bridge and the box-beam bridge FEM analysis and hand calculation (according to Eq. (6.38)) were performed.

In dynamics analysis performed in I-DEAS it is only possible to predict the undamped natural frequencies and natural modes of vibration of a structure. The software solves for the modes and frequencies of the finite element model.

Mode shapes and natural frequencies are used for identification of structural resonance, which may produce an undesirably large structural response to dynamic inputs. Further, the response of most structures to dynamic inputs can often be assumed to be a combination of the mode shapes corresponding to each mode. This lets mode shapes construct a numerically efficient representation of the structure (called a modal representation) for use in further analyses.

The analysis was studied for a T-beam bridge Model 1 Configuration 1 and for a box-beam bridge, loaded by a vehicle load.

Table 7.24 Comparison of the results of the Dynamic Analysis

Type of the bridge	1 st natural frequency obtained by FEM [Hz]	1 st natural frequency obtained by hand calculation [Hz]
T-beam bridge	5,77	7,46
Box-beam bridge	10,78	9,78

In hand calculation despite the recommendations in Bro2004, the influence of railings on the global dynamic behaviour was ignored. (Crocetti 2005)

8 Final remarks

8.1 Discussion

Stress-laminated timber T-beam and box-beam bridges showed good experience Australia, Canada, United States and Nordic countries. Generally in the rest of Europe those types of the structures are not commonly used. Good example of increase of the competitiveness of timber bridges compared with other materials like steel and concrete was the Nordic Timber Program that started in 1994. The major goal of the program was to show that timber bridges are durable and environmentally friendly and to develop solutions to increase the use of timber bridges. The program resulted in building more than 200 timber bridges in Sweden. Many of these bridges are pedestrian bridges but the number of new bridges for heavy traffic is increasing.

In Nordic countries T-beam and box-beam bridges have particular interest for application, as they utilise material, which is readily available from the timber industry and has reasonable quality and reliability.

It is anticipated that the results of testing and studies made in USA, Australia and Nordic countries permit soon the development of rational design procedures for T-beam and box-beam stress-laminated bridges.

8.2 Conclusions from the studies

Three T-beam bridges and one box-beam bridge were analysed by FEM. The models assumed complete composite action between the web and the flange. Results of the finite element model were compared to the results of the proposed design method to determine areas where future research may be required. The studies concentrated on effective flange width, wheel load distribution factor, effective contact area of the tire and the design check. Based on the review of the literature, FEM and hand calculation following statements have been made.

- There is fair agreement between the hand calculation formulas suggested by West Virginia University and performed FEM analysis concerning the effective flange width of the bridge. The studies showed that the decisive value for the effective flange is web spacing and the thickness of the deck is not a significant factor. It can be said that according to performed analysis of the transverse load distribution and literature an increase in number of webs in design is nearly proportional to an increase in bridge stiffness.
- Wheel distribution factor determined by proposed hand calculation formulas gave reasonable results compared with FEM calculation for T-beam bridges. However for the box-beam bridge there was a significant difference in the distribution factors predicted by two methods. For this type of bridges WVU design method resulted in factors that were more liberal than those of the FEM. Generally a conclusion can be drawn that the greater number of webs, the cooperation between the webs is more efficient and thus wheel distribution factor is lower.

- Analysis of the effective contact area of the wheel and corresponding dispersion angles indicate that for T-beam bridges the load in the direction of the grain is distributed on shorter length than for plate decks. However contact width of the wheel load perpendicular to the grain seems to be in good agreement with values from EC5 (2004) for plate decks. The studies show that further investigations concerning built-up decks may be warranted in this area.
- When comparing corresponding T-beam and box-beam models it can be observed that for the box-beam model the values of the deflection and bending stresses in the web and flange are definitely lower. This is mainly due to the fact that box-beam bridge provides good serviceability stiffness that allows to minimise the deflection and bending stress. However the values of the shear stress are almost the same for the two types of bridge. The reason of that can be caused by the some simplification made in the FEM analysis.
- The design check made to determine if the stresses and deflection are within the limiting values show that for proposed final models of the T-beam and box-beam the depth of the webs should be slightly increased. This is caused by high shear stress occurring in the webs.
- The level of prestress has more significant effect on the stiffness of the deck in plate stress-laminated decks than in built-up section. It is mainly due to the higher stiffness caused by webs.

8.3 General recommendations after literature study

In order to adequate friction for composite action, it is recommended that the thickness of the deck should be at least 190 mm for built-up sections.

There are also a number of limitations that must be satisfied in design of a post-tension system:

- In order to maximise bar elongation and minimise stress loss, the diameter of the stressing bars or strands need to be selected in such a way that a force in the bars is between 90% and 95% of the characteristic strength.
- The design prestress force should not exceed the short-term characteristic strength (compression perpendicular to face grain) of timber.
- The spacing of bars must be such that the full prestress is developed uniformly in the deck. (Crews 2000)

To ensure that the assumption concerning composite action will be valid during the lifetime of the bridge following construction procedures should be fulfilled:

- When a bridge is stressed with a single jack, three to six passes should be made along the bridge length to ensure uniform prestress at the required level. The stress should be gradually increased over the first several passes to minimize deck distortion. (Ritter et al. 1995)

- Stressing the bridge three separate times over a period of six to eight weeks is recommended. However, field monitoring of built up bridges indicates that the prestressing sequence is not enough in some cases. In order to meet the SLS and ULS performance requirements, the bridge should be checked every two years for the first four years after construction and every five years thereafter. If the prestress level falls below the limiting value, the restressing must be carried out.
- In general creep of timber is not a problem in stress-laminated bridges. However, to offset the effect of the creep of timber, stress-laminated bridges can be cambered.
- Bar force loss because of the stress relaxation increases as the bridge width increases (the volume of wood between the bar anchorages increases). It is also proportional to the increase of the moisture content of wood. Thus, based on the assumption that 50 to 60 percent of the stress will be lost over lifetime of the bridge due to the relaxation and change of moisture content, the initial prestressing should be two times higher than minimum prestress level. (Davalos and Salim 1992)

9 References:

- Aasheim E. (2000): *Development of timber bridges in the Nordic countries*. World Conference on Timber Engineering, British Columbia, Canada, July 31-August 3, 2000.
- Anon. (1991): *Guide specifications for the design of stress-laminated wood decks*. American Association of State and Highway Transportation Officials, Washington, DC.
- Anon. (1993): *Eurocode 5 – Design of timber structures – Part 1-1: General rules and rules for buildings*. European Committee for Standardization, Brussels.
- Anon. (2004): *Eurocode 5 – Design of timber structures – Part 2: Bridges*. European Committee for Standardization, Brussels.
- Anon. (2004): *Bro 2004* (Swedish Building Code. In Swedish).
- Anon. (2000) *Design regulations BKR*. Boverket, BFS 1998:39.
- Anon. (1995): *Timber Engineering STEP 1*. Centrum Hout, Almere.
- Cesaro G. and Piva F. (2003): *Timber Bridges – Design and durability*. Master's Thesis, Department of Structural Engineering, Chalmers University of Technology, Göteborg, Sweden, 2003.
- Crews K, Bakoss S. (1996): *Fundamental Structural Behaviour of "Built-up" Stress Laminated Timber Bridge Decks*. National Conference on Wood Transportation Structures, Madison, USA, October 1996, pp. 39-48.
- Crews K. (2000): *Development of limit states design methods for stress-laminated timber "cellular" bridge decks*. World Conference on Timber Engineering, British Columbia, Canada, July 31-August 3, 2000.
- Crocetti R. (2005): *Personal communication*.
- Davalos, J. and H. Salim. (1992): *Design of Stress-Laminated T-system Timber Bridges*. T.B.I.R.C.: USDA. Forest Service, Northeastern Area.
- Duwadi S. R., Ritter M. A. (1997): *Timber bridges in the United States*. Vol. 60, No. 3, 1997.
- GangaRao H. V. S. and Raju P. R. (1992): *Transverse Wheel Load Distribution for Deck-Stringer Bridges*. Proc. Third NSF Workshop on Bridge Engineering Research in Progress, Univ. of CA, La Jolla, CA, November 1992, pp.109-112.
- Pousette A., Jacobson P., Gustafsson M., Horttanainen J., Dahl K (2001): *Stress Laminated Bridge Decks - Part II*, Nordic Timber Council – Träteck.
- Pousette A. (2001): *Design Values*. Nordic Timber Council – Träteck.

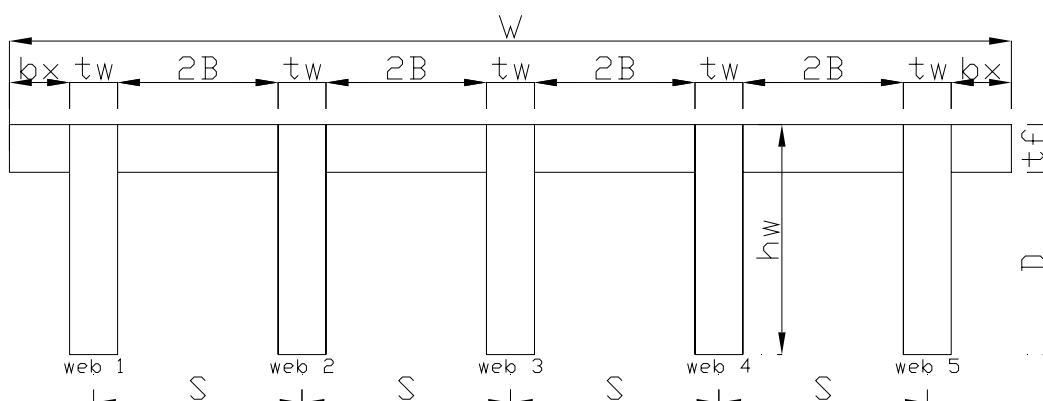
- Ritter M. A. (1992): *Timber Bridges: Design, Construction, Inspection, and Maintenance*. USDA Forest Service.
- Ritter M. A., Wacker J. P., Duwadi S. R. (1995): *Field Performance of Stress-Laminated Timber Bridges on Low-Volume Roads*. 6th International conference on low-volume roads, Vol. 2, Minneapolis, June 25-29, 1995, pp. 347-356.
- Ritter M. A., Williamson T. G., Moody R. C. (1994): *Innovations in Glulam Timber Bridge Design*. American Society of Civil Engineers, Vol. 2, Atlanta, April 24-28, 1994, pp. 1298-1303.
- Taylor S. E., Triche M. H., Morgan P.A., Bryant J., Hislop L.E. (2000): *Evaluation of Stress-Laminated Wood T-Beam and Box-Beam Bridge Superstructures* Project 96-RJVA-2821.
- Taylor S. E., Triche M. H., Hislop L.E., Morgan P.A. (2002): *Field investigations of Stress-Laminated T-Beam and Box-Beam Timber Bridges*. USDA Forest Service.

Appendix A – MathCAD file to perform an analysis of a T-beam bridge deck

1. Define Material Properties

$E_{LW} := 13000\text{MPa}$		mean value of longitudinal modulus of elasticity of the beams
$E_{Lf} := 13000\text{MPa}$		mean value of longitudinal modulus of elasticity of the deck
$E_{TW} := 0.03 \cdot E_{LW}$	$E_{TW} = 390\text{MPa}$	mean value of transverse modulus of elasticity of the beams
$E_{Tf} := 0.02 \cdot E_{Lf}$	$E_{Tf} := 260\text{MPa}$	mean value of transverse modulus of elasticity of the deck
$G_{0f} := 0.04 \cdot E_{Lf}$	$G_{0f} = 520\text{MPa}$	mean value of shear modulus
$\nu_0 := 0.025$		Poisson's ratio
Transverse modulus of elasticity and shear modulus calculated according to EC5		

2. Define Bridge Geometry

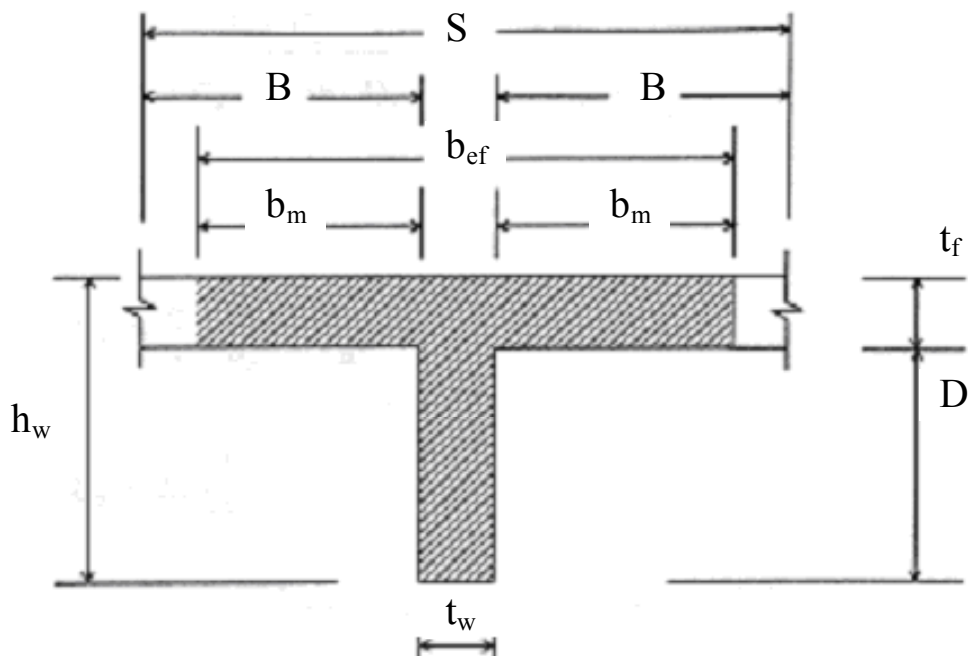


$L := 15\text{m}$	span of the bridge
$W := 4.495 \cdot \text{m}$	width of the bridge
$n_w := 5$	number of webs
$t_f := 215\text{mm}$	thickness of the flange
$t_w := 215\text{mm}$	width of the web
$S := 935\text{mm}$	spacing of the webs
$h_w := 1035\text{mm}$	height of the web
$N_L := 1$	number of lanes
$t := 45\text{mm}$	width of one lamella

$D := h_w - t_f$	$D = 0.82\text{m}$	depth of portion of web that is outside the deck
$B := \frac{(S - t_w)}{2}$	$B = 0.36\text{m}$	one half clear spacing of webs
$b := (n_w - 1) \cdot S$		center to center distance between exterior beams
$\alpha := \frac{b}{L}$		aspect ratio
$b_x := \frac{W - b - t_w}{2}$	$b_x = 0.27\text{m}$	width of exterior flange

2.1 Effective flange

2.1.1 Effective flange WVU1 - first possibility



The following formulas are according to J.F.Davalos and H.A. Salim

$$\frac{b_m}{B} = 0.4586 + \left(\frac{1}{198} \cdot \frac{L}{B} \cdot \frac{D}{t_f} \cdot \frac{E_{Lw}}{E_{Lf}} \right)$$

$$b_m := \left[0.4586 + \left(\frac{1}{198} \cdot \frac{L}{B} \cdot \frac{D}{t_f} \cdot \frac{E_{Lw}}{E_{Lf}} \right) \right] \cdot B$$

$$b_m = 0.454\text{m}$$

the effective over-hanging flange-width

$$b_{e1} := 2 \cdot b_m + t_w \quad b_{e1} = 1.123 \text{ m}$$

$$b_{e2} := S \quad b_{e2} = 0.935 \text{ m}$$

$$b_{e3} := \frac{L}{8} \quad b_{e3} = 1.875 \text{ m}$$

$$b_{ef} := \min(b_{e1}, b_{e2}, b_{e3}) \quad b_{ef} = 0.935 \text{ m}$$

2.1.2 Effective flange WVU2 - second possibility

The following formulas are according to Steven Taylor's report

$$b_m := \frac{2 \cdot B}{2} \cdot \left[\frac{1 + \nu_0 \cdot \left(\frac{2 \cdot B}{L} \right)^2}{1 + \frac{E_{LW}}{G_{of}} \cdot \left(\frac{2 \cdot B}{L} \right)^2} \right] \quad b_m = 0.34 \text{ m}$$

$$b_{ef1} := 2 \cdot b_m + t_w \quad b_{ef1} = 0.896 \text{ m}$$

$$b_{ef2} := \frac{2B}{2} + t_w \quad b_{ef2} = 0.575 \text{ m}$$

$$b_{ef} := \max(b_{ef1}, b_{ef2}) \quad b_{ef} = 0.896 \text{ m}$$

For further calculations the effective flange is determined according to WVU2

2.2 Moments of inertia

2.2.1. Moment of inertia of interior T-section

$$A := b_{ef} \cdot t_f + D \cdot t_w \quad A = 3689.0257 \text{ cm}^2$$

Location of the neutral axis

$$S_x := t_w \cdot \frac{D^2}{2} + b_{ef} \cdot t_f \cdot \left(h_w - \frac{t_f}{2} \right) \quad S_x = 2.509219 \times 10^5 \text{ cm}^3$$

$$y_c := \frac{S_x}{A} \quad y_c = 68.018 \text{ cm}$$

$$I := t_w \cdot \frac{D^3}{12} + t_w \cdot D \cdot \left(y_c - \frac{D}{2} \right)^2 + b_{ef} \cdot \frac{t_f^3}{12} + b_{ef} \cdot t_f \cdot \left(h_w - \frac{t_f}{2} - y_c \right)^2$$

$$I = 0.035 \text{ m}^4$$

2.2.2. Moment of inertia of exterior T-section

$$b_{ef.ex} := \min \left[b_{ef}, \frac{[W - [(n_w - 1) \cdot S + t_w]]}{2} + 0.5t_w + 0.5b_{ef} \right]$$

$$b_{ef.ex} = 0.825m$$

effective flange width of the exterior beam

$$A_{ex} := b_{ef.ex} \cdot t_f + D \cdot t_w$$

$$A_{ex} = 3537.6378cm^2$$

Location of the neutral axis

$$S_{x.ex} := t_w \cdot \frac{D^2}{2} + b_{ef.ex} \cdot t_f \cdot \left(h_w - \frac{t_f}{2} \right)$$

$$S_{x.ex} = 2.368807 \times 10^5 cm^3$$

$$y_{c.ex} := \frac{S_{x.ex}}{A_{ex}}$$

$$y_{c.ex} = 66.96cm$$

$$I_{ex} := t_w \cdot \frac{D^3}{12} + t_w \cdot D \cdot \left(y_{c.ex} - \frac{D}{2} \right)^2 + b_{ef.ex} \cdot \frac{t_f^3}{12} + b_{ef.ex} \cdot t_f \cdot \left(h_w - \frac{t_f}{2} - y_{c.ex} \right)^2$$

$$I_{ex} = 0.034m^4$$

3.0. Define Loading

All the loads according to BRO 2004

3.1. Loads

3.1.1. Permanent load

Self weight of the bridge $g_{1k} := 6 \cdot \frac{kN}{m^3}$

Surfacing:

			Width	Density	Load
			mm	kN/m ³	kN/m ²
Asfaltmastix på isolmatta			18	17,2	0,31
HABT11			25	24	0,60
ABS>16			45	22,2	1,00
			88		1,91

$$h_s := 88 \cdot mm$$

$$g_{2k} := 1.91 \cdot \frac{kN}{m^2}$$

3.1.2. Traffic load

Ekvivalentlast typ 1

3 equivalent axle loadings of 250 kN each

(one wheel load $P_k := 125\text{kN}$)

uniformly distributed load

$$q_{1Ak} := 3 \cdot 250 \cdot \text{kN}$$

$$q_{1Ak} = 750\text{kN}$$

$$q_{1Bk} := 12 \cdot \frac{\text{kN}}{\text{m}}$$

3.2 Load combinations

3.2.1 ULS

For calculating in ULS according to BRO 2004 the load combination IV:A is calculated as follows:

Self weight	$\psi\gamma_{g1} := 1.0$	$g_1 := \psi\gamma_{g1} \cdot g_{1k}$	$g_1 = 6 \frac{\text{kN}}{\text{m}^3}$
Surfacing	$\psi\gamma_{g2} := 1.0$	$g_2 := g_{2k} \cdot \psi\gamma_{g2}$	$g_2 = 1.91 \frac{\text{kN}}{\text{m}^2}$
Traffic load	$\psi\gamma_{q1} := 1.5$	$q_{1A} := q_{1Ak} \cdot \psi\gamma_{q1}$	$q_{1A} = 1.125 \times 10^3 \text{ kN}$
		$q_{1B} := q_{1Bk} \cdot \psi\gamma_{q1}$	$q_{1B} = 18 \frac{\text{kN}}{\text{m}}$
(one wheel load)		$P := P_k \cdot \psi\gamma_{q1}$	$P = 187.5\text{kN}$

3.2.2 SLS

one wheel load	$\psi\gamma_{\text{def}} := 0.8$	$P_{\text{def}} := \psi\gamma_{\text{def}} \cdot P_k$	$P_{\text{def}} = 100\text{kN}$
uniformly distributed traffic	$\psi\gamma_{\text{def}} := 0.8$	$q_{\text{def}} := q_{1Bk} \cdot \psi\gamma_{\text{def}}$	$q_{\text{def}} = 9.6 \frac{\text{kN}}{\text{m}}$

4.0 Design values

According to BKR2003

bending parallel to grain $f_{mk} := 33 \cdot \text{MPa}$

(In bending with the moment vector perpendicular to the plane of the glue joint the value of f_{mk} may be not more than 26 MPa)

tension parallel to grain $f_{tk} := 23\text{MPa}$

tension perpendicular to grain $f_{t90k} := 0.5\text{MPa}$

compression parallel to grain $f_{ck} := 36\text{MPa}$

compression perpendicular to grain $f_{c90k} := 8\text{MPa}$

longitudinal shear $f_{vk} := 4\text{MPa}$

According to EN 1995-2:2004 partial factor for material properties for glued laminated timber is:

$$\gamma_M := 1.25$$

For short term action for glued laminated timber $k_{mod} := 0.9$

$$f_{md} := f_{mk} \cdot \frac{k_{mod}}{\gamma_M} \quad f_{md} = 23.76 \text{MPa}$$

$$f_{td} := f_{tk} \cdot \frac{k_{mod}}{\gamma_M} \quad f_{td} = 16.56 \text{MPa}$$

$$f_{t90d} := f_{t90k} \cdot \frac{k_{mod}}{\gamma_M} \quad f_{t90d} = 0.36 \text{MPa}$$

$$f_{cd} := f_{ck} \cdot \frac{k_{mod}}{\gamma_M} \quad f_{cd} = 25.92 \text{MPa}$$

$$f_{c90d} := f_{c90k} \cdot \frac{k_{mod}}{\gamma_M} \quad f_{c90d} = 5.76 \text{MPa}$$

$$f_{vd} := f_{vk} \cdot \frac{k_{mod}}{\gamma_M} \quad f_{vd} = 2.88 \text{MPa}$$

5.0 Design the deck for local effects

5.1 The maximum local deflection

$$\delta_{max} = \frac{P_{def} \cdot S^3}{4 \cdot K_{\delta} \cdot \frac{E_{Tf}}{1 + k_{def}} \cdot t^4}$$

$$k_{def} := 0$$

for glue laminated timber for short term actions

$$P_{def} = 100 \text{kN}$$

one wheel load in combination V:C (Bro 2004)

$$K_{\delta} := -10.9 + 7.8 \left(\frac{S}{t_f} \right) + 0.27 \left(\frac{E_{Lf}}{E_{Tf}} \right) \quad K_{\delta} = 36.521$$

$$\delta_{max} := \frac{P_{def} \cdot S^3}{4 \cdot K_{\delta} \cdot E_{Tf} \cdot t_f^4} \quad \delta_{max} = 1.007 \text{mm}$$

$$\delta_{lim} := 2.54 \text{mm}$$

$$\delta_{max} = 1.007 \text{mm} < \delta_{lim} := 2.54 \text{mm} \quad \text{OK}$$

5.2 The maximum local transverse stress

$$\sigma_{\max} = \frac{3 \cdot P \cdot S}{2 \cdot K_{\sigma} \cdot t^3}$$

$$P = 187.5 \text{ kN}$$

one wheel load in combination IV:A (Bro 2004)

$$K_{\sigma} := 3 + 3.1 \cdot \left(\frac{S}{t_f} \right) + 0.15 \left(\frac{E_{Lf}}{E_{Tf}} \right)$$

$$K_{\sigma} = 23.981$$

$$\sigma_{\max} := \frac{3 \cdot P \cdot S}{2 \cdot K_{\sigma} \cdot t_f^3}$$

$$\sigma_{\max} = 1.103 \text{ MPa} <$$

$$f_{c90d} = 5.76 \text{ MPa} \quad \text{OK}$$

The value of σ_{\max} should be increased by the value of initial prestress

6.0 Maximum moment calculations

6.1 Maximum dead load moment

$$A_{\text{ex}} = 0.354 \text{ m}^2$$

$$A = 0.369 \text{ m}^2$$

$$S_{\text{ex}} := 0.5 \cdot S + 0.5 \cdot t_w + b_x$$

$$S_{\text{ex}} = 0.845 \text{ m}$$

$$S = 0.935 \text{ m}$$

$$M_g := \frac{(g_1 \cdot A + g_2 \cdot S) \cdot L^2}{8}$$

$$M_g = 112.479 \text{ kNm}$$

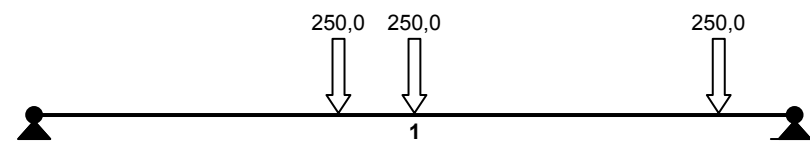
Maximum moment in the interior beam

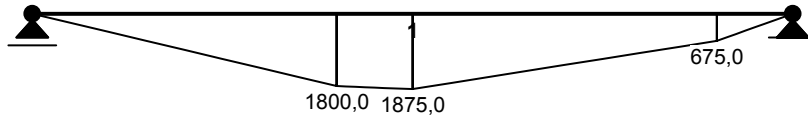
$$M_{g,\text{ex}} := \frac{(g_1 \cdot A_{\text{ex}} + g_2 \cdot S_{\text{ex}}) \cdot L^2}{8}$$

$$M_{g,\text{ex}} = 105.09 \text{ kNm}$$

Maximum moment in the exterior beam

6.2 Maximum live load moment





$$M_t := 1875 \text{ kNm}$$

maximum moment due to 3x250kN

$$\psi \gamma q_1 = 1.5$$

partial factor

$$M := M_t \cdot \psi \gamma q_1 + \frac{q_{1B} \cdot L^2}{8}$$

sum of the moment due to concentrated load and uniformly distributed

$$B_e := E_{LW} \cdot I_{ex}$$

stiffness of the composite edge web

$$B_e = 4.452 \times 10^5 \text{ kN} \cdot \text{m}^2$$

$$D_T := E_{Tf} \cdot \frac{t_f^3}{12}$$

$$D_T = 215.33 \text{ kN} \cdot \text{m}$$

$$W_f = \frac{1 + C_o}{n \cdot C_o + \frac{2}{3.14} \cdot (n - 1)}$$

wheel load distribution factor

$$C_o := \frac{b}{3.14} \cdot \frac{D_T}{B_e} \cdot \frac{8 \cdot \alpha^2 + 1}{\alpha^4}$$

$$C_o = 0.223$$

where

$$b := (n_w - 1) \cdot S$$

center to center distance between exterior beams

$$\alpha := \frac{b}{L}$$

aspect ratio

$$W_f := \frac{1 + C_o}{n_w \cdot C_o + \frac{2}{3.14} \cdot (n_w - 1)}$$

$$W_f = 0.334$$

$$M_I := W_f \cdot M$$

$$M_I = 1.108 \times 10^3 \text{ kNm}$$

7.0 Maximum bending stresses

7.1 Maximum tensile stress in the interior beam

$$\sigma_t := \frac{M_I + M_g}{I} \cdot y_c$$

$$\sigma_t = 23.537\text{MPa} < f_{md} = 23.76\text{MPa} \quad \text{OK}$$

7.2 Maximum tensile stress in the exterior beam

$$\sigma_{t.ex} := \frac{M_I + M_{g.ex}}{I_{ex}} \cdot y_{c.ex}$$

$$\sigma_{t.ex} = 23.719\text{MPa} < f_{md} = 23.76\text{MPa} \quad \text{OK}$$

7.3. Maximum compressive stress in the deck above interior beam

$$\sigma_c := \frac{M_I + M_g}{I} \cdot (h_w - y_c)$$

$$\sigma_c = 12.278\text{MPa} < f_{cd} = 25.92\text{MPa} \quad \text{OK}$$

7.4. Maximum compressive stress in the deck above exterior beam

$$\sigma_{c.ex} := \frac{M_I + M_{g.ex}}{I_{ex}} \cdot (h_w - y_{c.ex})$$

$$\sigma_{c.ex} = 12.943\text{MPa} < f_{cd} = 25.92\text{MPa} \quad \text{OK}$$

8.0 Maximum shear force calculation

8.1 Maximum shear force due to dead load

$$V_g := (g_1 \cdot A + g_2 \cdot S) \cdot \frac{L}{2} \quad V_g = 29.994\text{kN} \quad \text{maximum shear force in the interior beam}$$

$$V_{g.ex} := (g_1 \cdot A_{ex} + g_2 \cdot S_{ex}) \cdot \frac{L}{2} \quad V_{g.ex} = 28.024\text{kN} \quad \text{maximum shear force in the exterior beam}$$

8.2 Maximum shear force due to traffic load

$$V_{t1} := 587.3\text{kN} \quad \text{maximum shear force due to } 3 \times 250\text{kN}$$

$$V_{LU} := V_{t1} \cdot \Psi \gamma_{q1} + q_{1B} \cdot \frac{L}{2}$$

$$V_{LU} = 1.016 \times 10^3 \text{ kN} \quad \text{maximum shear force due to concentrated traffic load } 6 \times 187,5 \text{ kN} \\ \text{and uniformly distributed traffic load } 18\text{kN/m (design values),} \\ \text{without load distribution}$$

$$V_{LD} := N_L \cdot W_f \cdot V_{LU}$$

$$V_{LD} = 339.29\text{kN} \quad \text{maximum shear force due to concentrated traffic load } 6 \times 187,5 \text{ kN} \\ \text{and uniformly distributed traffic load } 18\text{kN/m,} \\ \text{with load distribution}$$

$$V_t := 0.5 \cdot (0.6 \cdot V_{LU} + V_{LD}) \quad V_t = 474.52\text{kN}$$

9.0 Maximum shear stress

9.1 Maximum shear stress in the interior beam

$$V := V_t + V_g \quad V = 504.515\text{kN}$$

$$\tau := \frac{1.5 \cdot V}{t_w \cdot h_w} \quad \tau = 3.401\text{MPa}$$

maximum shear stress carried by the beam alone (conservative)

$$\tau = 3.401\text{MPa} \quad > \quad f_{vd} = 2.88\text{MPa} \quad \text{NOT OK}$$

9.2 Maximum shear stress in the exterior beam

$$V := V_t + V_{g.ex} \quad V = 502.544\text{kN}$$

$$\tau := \frac{1.5 \cdot V}{t_w \cdot h_w} \quad \tau = 3.388\text{MPa}$$

maximum shear stress carried by the beam alone (conservative)

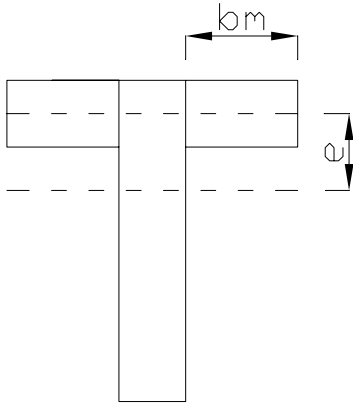
$$\tau = 3.388\text{MPa} \quad > \quad f_{vd} = 2.88\text{MPa} \quad \text{NOT OK}$$

The height of the web should be increased in order to take shear stress

9.3 Maximum shear stress at the interface between the web and the flange

$$V = 502.544\text{kN} \quad I = 0.035\text{m}^4$$

$$\tau_v = \frac{V \cdot Q}{I \cdot t_w}$$



$$Q := b_m \cdot t_f \cdot \left(h_w - \frac{t_f}{2} - y_c \right)$$

$$V = 502.544\text{kN}$$

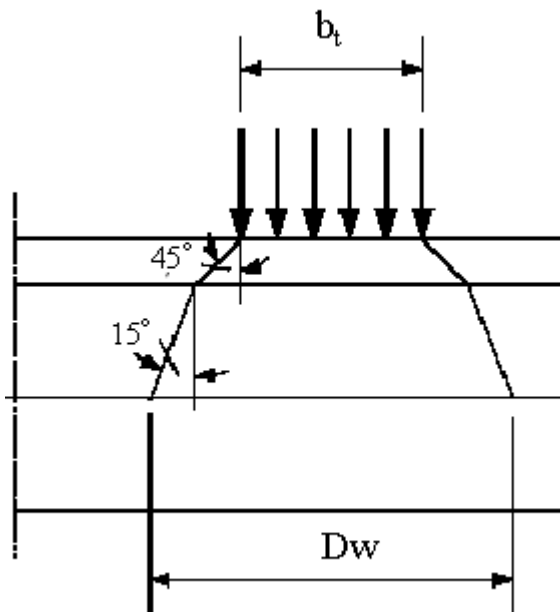
$$\mu_s := 0.35 \quad \text{coefficient of friction for moisture content between 12\% and 16\%}$$

$$f_p := 0.55\text{MPa}$$

$$\tau_v := \frac{V \cdot Q}{I \cdot t_w} \quad \tau_v = 1.2\text{MPa}$$

$$\tau_v = 1.2\text{MPa} > f_{vd} = 2.88\text{MPa} \quad \text{OK}$$

9.4 Maximum punching shear - local analysis



$$P = 187.5 \text{ kN}$$

one wheel load in combination IV:A (BRO 2004)

$$b_w := 0.72 \text{ m}$$

width of a tyre

$$b_t := 0.72 \text{ m} + 2 \cdot 0.088 \text{ m}$$

tyre width according to BRO 2004 after going through asphalt

$$t = 0.045 \text{ m}$$

width of one lamella

$$t_f = 0.215 \text{ m}$$

thickness of the deck

$$V_p := \frac{P}{b_t + 2 \cdot \frac{t_f}{2} \cdot \tan(15 \text{ deg})} \cdot t$$

$$V_p = 8.848 \text{ kN}$$

$$V_{res} = f_p \cdot b_l \cdot t_f \cdot \mu_s$$

resisting frictional force

$$f_p := 0.55 \cdot \text{MPa}$$

operational prestress level

$$\mu_s := 0.35$$

coefficient of friction for moisture content between 12% and 16%

$$b_l := 0.5 \text{ m}$$

tyre contact length in the direction of span

$$V_{res} := f_p \cdot b_l \cdot t_f \cdot \mu_s$$

$$V_{res} = 20.694 \text{ kN}$$

$$V_p = 8.848 \text{ kN}$$

<

$$V_{res} = 20.694 \text{ kN}$$

OK

10.0 Global deflection

Variable actions due to passage of traffic should be regarded as short-term actions. $k_{\text{def}} := 0$

in last combination V:C according to BRO2004 $\psi\gamma_{\text{def}} = 0.8$

$M_t := 1875\text{kNm}$ maximum moment due to 3x250kN

$M := M_t \cdot \psi\gamma_{\text{def}} + \frac{q_{\text{def}} \cdot L^2}{8}$ maximum moment due to 3x250kN + distributed traffic load

$W_f := 1.6 \cdot W_f$ $W_f = 0.534$ wheel factor multiplied by 1.6 in case of one lane bridge

$P_e := M \cdot \frac{4}{L}$ $P_e = 472\text{kN}$ equivalent concentrated load

$P_d := W_f \cdot P_e$ $P_d = 252.135\text{kN}$ design concentrated load

$\delta_{\text{II}} := \frac{P_d \cdot L^3}{48 \cdot E_{LW} \cdot I_{\text{ex}}}$ $\delta_{\text{II}} = 39.82\text{mm}$

according to EC5 $\delta_{\text{lim}} := \frac{L}{400}$ $\delta_{\text{lim}} = 37.5\text{mm}$

11.0 Vibrations (BRO 2004)

$$a_{\text{RMS}} = \frac{4 \cdot F \cdot v}{3.14 \cdot \sqrt{2 \cdot m \cdot E \cdot l}}$$

$$A_{\text{bridge}} := [2 \cdot b_x + (n_w - 1) \cdot (S - t_w)] \cdot t_f + n_w \cdot t_w \cdot h_w \quad A_{\text{bridge}} = 1.848 \text{m}^2$$

cross section of the bridge

$$\text{mass}_{\text{bridge}} := \frac{6 \frac{\text{kN}}{\text{m}^3} \cdot A_{\text{bridge}}}{9.81 \cdot \frac{\text{m}}{\text{s}^2}} \quad \text{mass}_{\text{bridge}} = 1.13 \times 10^3 \frac{\text{kg}}{\text{m}}$$

$$\text{mass}_{\text{surface}} := \frac{g_2 \cdot W}{9.81 \cdot \frac{\text{m}}{\text{s}^2}} \quad \text{mass}_{\text{surface}} = 875.173 \frac{\text{kg}}{\text{m}}$$

$$\text{mass} := \text{mass}_{\text{bridge}} + \text{mass}_{\text{surface}} \quad \text{mass} = 2.005 \times 10^3 \frac{\text{kg}}{\text{m}}$$

$$v := 15 \frac{\text{m}}{\text{s}} \quad \text{velocity of a vehicle}$$

$$F := 240 \text{kN}$$

$$E := E_{\text{LW}} \quad E = 1.3 \times 10^4 \text{MPa}$$

calculation modulus of inertia of the whole cross-section of the bridge

$$A := [b_x \cdot 2 + (n_w - 1) \cdot 2 \cdot B] \cdot t_f + n_w \cdot h_w \cdot t_w \quad A = 1.848 \text{m}^2$$

$$S_x := [b_x \cdot 2 + (n_w - 1) \cdot 2 \cdot B] \cdot t_f \cdot \left(h_w - \frac{t_f}{2} \right) + n_w \cdot h_w \cdot t_w \cdot \frac{h_w}{2} \quad S_x = 1.258 \text{m}^3$$

$$y_c := \frac{S_x}{A} \quad y_c = 0.681 \text{m}$$

$$I_{\text{tot}} := \frac{W \cdot t_f^3}{12} + W \cdot t_f \cdot \left(h_w - y_c - \frac{t_f}{2} \right)^2 + n_w \cdot \frac{t_w \cdot D^3}{12} + n_w \cdot t_w \cdot D \cdot \left(y_c - \frac{D}{2} \right)^2$$

$$I_{\text{tot}} = 0.177 \text{m}^4 \quad \text{the influence of railings is not included}$$

$$a_{\text{RMS}} := \frac{4 \cdot F \cdot v}{3.14 \cdot \sqrt{2 \text{mass} \cdot E \cdot l_{\text{tot}}}} \quad a_{\text{RMS}} = 1.511 \frac{\text{m}}{\text{s}^2}$$

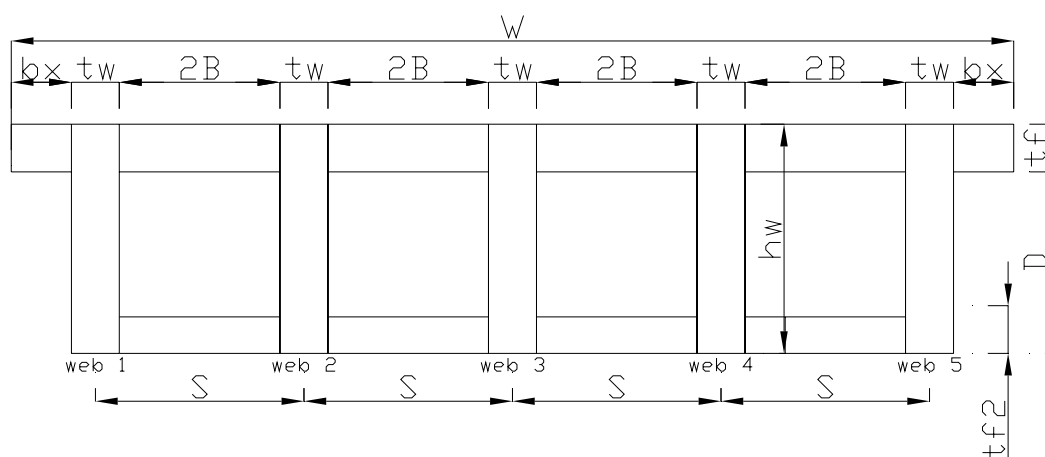
$$f_n := \frac{3.14}{2 \cdot L^2} \cdot \sqrt{\frac{E \cdot l_{\text{tot}}}{\text{mass}}} \quad f_n = 7.465 \text{Hz}$$

Appendix B – Mathcad file to perform an analysis of a box-beam bridge deck

1. Define Material Properties

$E_{LW} := 13000\text{MPa}$		mean value of longitudinal modulus of elasticity of the beams
$E_{Lf} := 13000\text{MPa}$		mean value of longitudinal modulus of elasticity of the deck
$E_{TW} := 0.03 \cdot E_{LW}$	$E_{TW} = 390\text{MPa}$	mean value of transverse modulus of elasticity of the beams
$E_{Tf} := 0.02 \cdot E_{Lf}$	$E_{Tf} := 260\text{MPa}$	mean value of transverse modulus of elasticity of the deck
$G_{of} := 0.04 \cdot E_{Lf}$	$G_{of} = 520\text{MPa}$	mean value of shear modulus
$\nu_0 := 0.025$		Poisson's ratio
Transverse modulus of elasticity and shear modulus calculated according to EC5		

2. Define Bridge Geometry

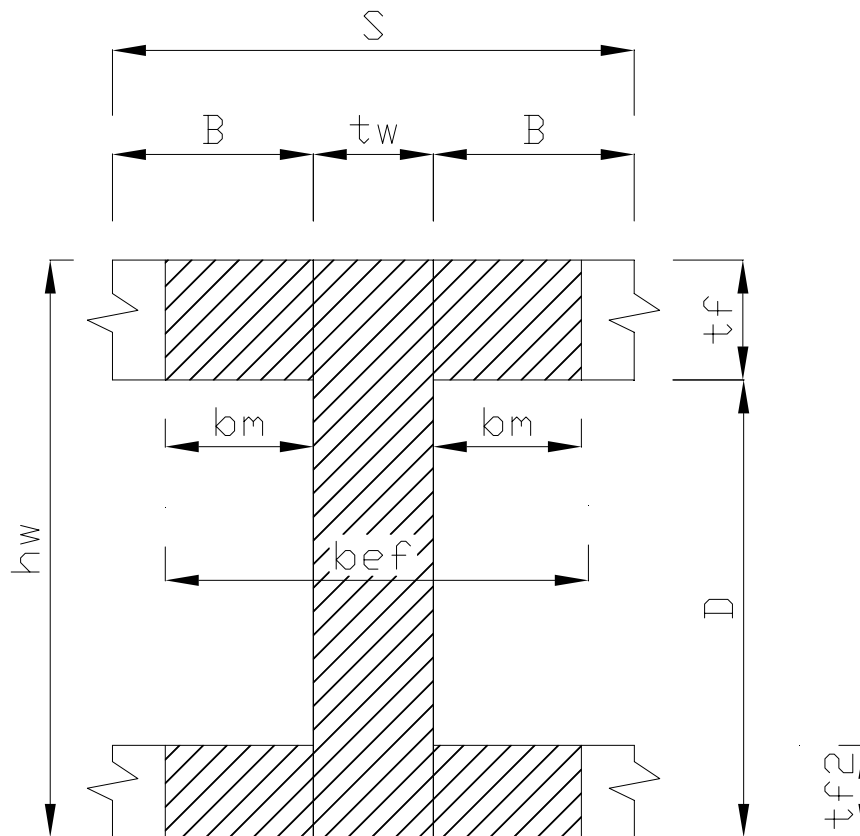


$L := 15\text{m}$	span of the bridge
$W := 4.495 \cdot \text{m}$	width of the bridge
$n_w := 5$	number of webs
$t_f := 215\text{mm}$	thickness of the upper flange
$t_{f2} := 165\text{mm}$	thickness of the bottom flange
$t_w := 215\text{mm}$	width of the web
$S := 935\text{mm}$	spacing
$h_w := 1035\text{mm}$	height of the web
$N_L := 1$	number of lanes

$t := 45\text{mm}$		width of one lamella
$D := h_w - t_f$	$D = 0.82\text{m}$	depth of portion of stringer that is outside the deck
$B := \frac{(S - t_w)}{2}$	$B = 0.36\text{m}$	one half clear spacing of webs
$b := (n_w - 1) \cdot S$		center to center distance between exterior stringers
$\alpha := \frac{b}{L}$		aspect ratio
$bx := \frac{W - b - t_w}{2}$	$bx = 0.27\text{m}$	width of exterior flange

2.1 Effective flange

2.2.2 Effective flange WVU2 (Taylor 2000)



$$b_m = \frac{2B}{2} \cdot \left[\frac{1 + \nu_{xz} \cdot \left(\frac{2B}{L}\right)^2}{1 + \frac{E_{Lw}}{G_{xz}} \cdot \left(\frac{2B}{L}\right)^2} \right]$$

$$v_{xz} := 0.025$$

$$G_{xz} := 520 \text{MPa}$$

$$\frac{E_{LW}}{G_{xz}} = 25$$

$$b_m := \frac{2B}{2} \cdot \left[\frac{1 + v_{xz} \cdot \left(\frac{2B}{L}\right)^2}{1 + \frac{E_{LW}}{G_{xz}} \cdot \left(\frac{2B}{L}\right)^2} \right] \quad b_m = 0.34 \text{m} \quad \text{the effective over-hanging flange-widht}$$

$$b_{ef1} := 2 \cdot b_m + t_w \quad b_{ef1} = 0.896 \text{m}$$

$$b_{ef2} := \frac{2B}{3} + t_w \quad b_{ef2} = 0.455 \text{m}$$

$$b_{ef} := \max(b_{ef1}, b_{ef2}) \quad b_{ef} = 0.896 \text{m}$$

2.2.1. Moment of inertia of interior box-section

$$A := b_{ef} \cdot t_f + (D - t_{f2}) \cdot t_w + b_{ef} \cdot t_{f2} \quad A = 4812.3884 \text{cm}^2$$

Location of the neutral axis

$$S_x := t_w \cdot \frac{D^2}{2} + b_{ef} \cdot t_f \cdot \left(h_w - \frac{t_f}{2}\right) + (b_{ef} - t_w) \cdot t_{f2} \cdot \frac{t_{f2}}{2} \quad S_x = 2.601896 \times 10^5 \text{cm}^3$$

$$y_c := \frac{S_x}{A} \quad y_c = 54.067 \text{cm}$$

$$I := t_w \cdot \frac{D^3}{12} + t_w \cdot D \cdot \left(y_c - \frac{D}{2}\right)^2 + b_{ef} \cdot \frac{t_f^3}{12} + b_{ef} \cdot t_f \cdot \left(h_w - \frac{t_f}{2} - y_c\right)^2 + \left[\frac{(b_{ef} - t_w) \cdot t_{f2}^3}{12} + (b_{ef} - t_w) \cdot t_{f2} \cdot \left(y_c - \frac{t_{f2}}{2}\right)^2 \right] \quad I = 0.066 \text{m}^4$$

2.2.2. Moments of inertia of exterior box-section

$$b_{ef.ex} := \min \left[b_{ef}, \frac{[W - [(n_w - 1) \cdot S + t_w]]}{2} + 0.5t_w + 0.5b_{ef} \right]$$

$$b_{ef.ex} = 0.825m$$

effective flange width of the exterior beam

$$A_{ex} := b_{ef.ex} \cdot t_f + D \cdot t_w + \frac{b_{ef} - t_w}{2} \cdot t_{f2}$$

$$A_{ex} = 4099.3192cm^2$$

Location of the neutral axis

$$S_{x.ex} := t_w \cdot \frac{D^2}{2} + b_{ef.ex} \cdot t_f \cdot \left(h_w - \frac{t_f}{2} \right)$$

$$S_{x.ex} = 2.368807 \times 10^5 cm^3$$

$$y_{c.ex} := \frac{S_{x.ex}}{A_{ex}}$$

$$y_{c.ex} = 57.785cm$$

$$I_{ex} := t_w \cdot \frac{D^3}{12} + t_w \cdot D \cdot \left(y_{c.ex} - \frac{D}{2} \right)^2 + b_{ef.ex} \cdot \frac{t_f^3}{12} + b_{ef.ex} \cdot t_f \cdot \left(h_w - \frac{t_f}{2} - y_{c.ex} \right)^2 + \frac{\left(\frac{b_{ef} - t_w}{2} \right) \cdot t_{f2}^3}{12} + \left(\frac{b_{ef} - t_w}{2} \right) \cdot t_{f2} \cdot \left(y_{c.ex} - \frac{t_{f2}}{2} \right)^2$$

$$I_{ex} = 0.051m^4$$

3.0. Define Loading

All the loads according to Bro 2004

3.1. Loads

3.1.1. Permanent load

Self weight of the bridge $g_{1k} := 6 \cdot \frac{kN}{m^3}$

Surfacing:

		Width	Density	Load
		mm	kN/m ³	kN/m ²
Asfaltmastix på isolmatta		18	17,2	0,31
HABT11		25	24	0,60
ABS>16		45	22,2	1,00
		88		1,91

$h_s := 88 \cdot \text{mm}$ height of the surfacing

$$g_{2k} := 1.91 \cdot \frac{\text{kN}}{\text{m}^2}$$

3.1.2. Traffic load

Ekvivalentlast typ 1

3 equivalent axle loadings of 250 kN each

$$q_{1Ak} := 3 \cdot 250 \cdot \text{kN}$$

$$q_{1Ak} = 750 \text{ kN}$$

(one wheel load $P_k := 125 \text{ kN}$)

uniformly distributed load

$$q_{1Bk} := 12 \cdot \frac{\text{kN}}{\text{m}}$$

3.2 Load combinations

3.2.1 ULS

For calculating in ULS according to BRO 2004 the load combination IV:A is calculated as follows:

Self weight	$\psi \gamma_{g1} := 1.0$	$g_1 := \psi \gamma_{g1} \cdot g_{1k}$	$g_1 = 6 \frac{\text{kN}}{\text{m}^3}$
Surfacing	$\psi \gamma_{g2} := 1.0$	$g_2 := g_{2k} \cdot \psi \gamma_{g2}$	$g_2 = 1.91 \frac{\text{kN}}{\text{m}^2}$
Traffic load	$\psi \gamma_{q1} := 1.5$	$q_{1A} := q_{1Ak} \cdot \psi \gamma_{q1}$	$q_{1A} = 1.125 \times 10^3 \text{ kN}$
		$q_{1B} := q_{1Bk} \cdot \psi \gamma_{q1}$	$q_{1B} = 18 \frac{\text{kN}}{\text{m}}$
(one wheel load)		$P := P_k \cdot \psi \gamma_{q1}$	$P = 187.5 \text{ kN}$

3.2.2 SLS

one wheel load	$\psi \gamma_{\text{def}} := 0.8$	$P_{\text{def}} := \psi \gamma_{\text{def}} \cdot P_k$	$P_{\text{def}} = 100 \text{ kN}$
uniformly distributed traffic	$\psi \gamma_{\text{def}} := 0.8$	$q_{\text{def}} := q_{1Bk} \cdot \psi \gamma_{\text{def}}$	$q_{\text{def}} = 9.6 \frac{\text{kN}}{\text{m}}$

4.0 Allowable design values

According to BKR2003

bending parallel to grain

$$f_{mk} := 33 \cdot \text{MPa}$$

(In bending with the moment vector perpendicular to the plane of the glue joint, the value of f_{mk} may be not more than 26 MPa)

tension parallel to grain

$$f_{tk} := 23 \text{MPa}$$

tension perpendicular to grain

$$f_{t90k} := 0.5 \text{MPa}$$

compression parallel to grain

$$f_{ck} := 36 \text{MPa}$$

compression perpendicular to grain

$$f_{c90k} := 8 \text{MPa}$$

longitudinal shear

$$f_{vk} := 4 \text{MPa}$$

According to EC5 (2004) Table 2.1 partial factor for material properties for glued laminated timber is:

$$\gamma_M := 1.25$$

For short term action for glued laminated timber $k_{mod} := 0.9$

$$f_{md} := f_{mk} \cdot \frac{k_{mod}}{\gamma_M} \quad f_{md} = 23.76 \text{MPa}$$

$$f_{td} := f_{tk} \cdot \frac{k_{mod}}{\gamma_M} \quad f_{td} = 16.56 \text{MPa}$$

$$f_{t90d} := f_{t90k} \cdot \frac{k_{mod}}{\gamma_M} \quad f_{t90d} = 0.36 \text{MPa}$$

$$f_{cd} := f_{ck} \cdot \frac{k_{mod}}{\gamma_M} \quad f_{cd} = 25.92 \text{MPa}$$

$$f_{c90d} := f_{c90k} \cdot \frac{k_{mod}}{\gamma_M} \quad f_{c90d} = 5.76 \text{MPa}$$

$$f_{vd} := f_{vk} \cdot \frac{k_{mod}}{\gamma_M} \quad f_{vd} = 2.88 \text{MPa}$$

5.0 Design the deck for local effects

5.1 The maximum local deflection

$$\delta_{\max} = \frac{P_{\text{def}} \cdot S^3}{4 \cdot K_{\delta} \cdot \frac{E_{\text{Tf}}}{1 + k_{\text{def}}} \cdot t^4}$$

$$k_{\text{def}} := 0$$

for glue laminated timber for short term actions

$$P_{\text{def}} = 100\text{kN}$$

one wheel load in combination V:C (Bro 2004)

$$K_{\delta} := -10.9 + 7.8 \left(\frac{S}{t_f} \right) + 0.27 \left(\frac{E_{\text{Lf}}}{E_{\text{Tf}}} \right)$$

$$K_{\delta} = 36.521$$

$$\delta_{\max} := \frac{P_{\text{def}} \cdot S^3}{4 \cdot K_{\delta} \cdot E_{\text{Tf}} \cdot t_f^4}$$

$$\delta_{\max} = 1.007\text{mm}$$

$$\delta_{\text{lim}} := 2.54\text{mm} \quad (\text{GangaRao 1992})$$

$$\delta_{\max} = 1.007\text{mm} <$$

$$\delta_{\text{lim}} := 2.54\text{mm} \quad \text{OK}$$

5.2 The maximum local transverse stress

$$\sigma_{\max} = \frac{3 \cdot P \cdot S}{2 \cdot K_{\sigma} \cdot t^3}$$

$$P = 187.5\text{kN}$$

one wheel load in combination IV:A (Bro 2004)

$$K_{\sigma} := 3 + 3.1 \cdot \left(\frac{S}{t_f} \right) + 0.15 \left(\frac{E_{\text{Lf}}}{E_{\text{Tf}}} \right)$$

$$K_{\sigma} = 23.981$$

$$\sigma_{\max} := \frac{3 \cdot P \cdot S}{2 \cdot K_{\sigma} \cdot t_f^3}$$

$$\sigma_{\max} = 1.103\text{MPa} <$$

$$f_{c90d} = 5.76\text{MPa} \quad \text{OK}$$

The value of σ_{\max} should be increased by the value of initial prestress

6.0 Maximum moment calculations

6.1 Maximum dead load moment

$$A_{ex} = 0.41\text{m}^2$$

$$A = 0.481\text{m}^2$$

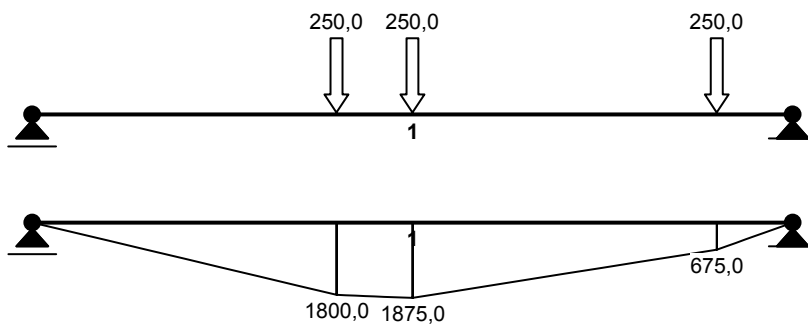
$$S_{ex} := 0.5 \cdot S + 0.5 \cdot t_w + bx \quad S_{ex} = 0.845\text{m}$$

$$S = 0.935\text{m}$$

$$M_{g,ex} := \frac{(g_1 \cdot A_{ex} + g_2 \cdot S_{ex}) \cdot L^2}{8} \quad M_{g,ex} = 114.568\text{kNm}$$

$$M_g := \frac{(g_1 \cdot A + g_2 \cdot S) \cdot L^2}{8} \quad M_g = 131.436\text{kNm}$$

6.2 Maximum live load moment



$$M_t := 1875 \text{ kNm}$$

maximum moment due to 3x250kN

$$\psi \gamma_{q1} = 1.5$$

partial factor

$$M := M_t \cdot \psi \gamma_{q1} + \frac{q_{1B} \cdot L^2}{8}$$

$$M = 3.319 \times 10^3 \text{ kNm}$$

sum of the moment due to concentrated load and uniformly distributed

$$W_f := \frac{3 \cdot N_L}{2.64 \cdot n_w - 0.64}$$

$$W_f = 0.239$$

$$M_l := W_f \cdot M$$

$$M_l = 792.695 \text{ kNm} \quad \text{moment in the most used web}$$

7.0 Maximum bending stresses

7.1 Maximum tensile stress in interior the web

$$\sigma_t := \frac{M_l + M_g}{I} \cdot y_c$$

$$\sigma_t = 7.538 \text{ MPa}$$

<

$$f_{md} = 23.76 \text{ MPa}$$

OK

7.2 Maximum tensile stress in the web

$$\sigma_{t.ex} := \frac{M_l + M_{g.ex}}{I_{ex}} \cdot y_{c.ex}$$

$$\sigma_{t.ex} = 10.253 \text{ MPa}$$

<

$$f_{md} = 23.76 \text{ MPa}$$

OK

7.3 Maximum compressive stress in the deck above interior web

$$\sigma_c := \frac{M_l + M_g}{I} \cdot (h_w - y_c)$$

$$\sigma_c = 6.892 \text{ MPa}$$

<

$$f_{cd} = 25.92 \text{ MPa}$$

OK

7.4 Maximum compressive stress in the deck above exterior web

$$\sigma_{c.ex} := \frac{M_l + M_{g.ex}}{I_{ex}} \cdot (h_w - y_{c.ex})$$

$$\sigma_{c.ex} = 8.111 \text{ MPa}$$

<

$$f_{cd} = 25.92 \text{ MPa}$$

OK

8.0 Maximum shear stresses

8.1 Maximum shear force due to dead load

$$V_g := (g_1 \cdot A + g_2 \cdot S) \cdot \frac{L}{2} \quad V_g = 35.05 \text{ kN} \quad \text{maximum shear force in the interior beam}$$

$$V_{g,ex} := (g_1 \cdot A_{ex} + g_2 \cdot S_{ex}) \cdot \frac{L}{2} \quad V_{g,ex} = 30.552 \text{ kN} \quad \text{maximum shear force in the exterior beam}$$

8.2 Maximum shear force due to traffic load

$$V_{t1} := 587.3 \text{ kN} \quad \text{maximum shear force due to } 3 \times 250 \text{ kN}$$

$$V_{LU} := V_{t1} \cdot \psi \gamma q_1 + q_{1B} \cdot \frac{L}{2}$$

$$V_{LU} = 1.016 \times 10^3 \text{ kN} \quad \text{maximum shear force due to concentrated traffic load } 6 \times 187,5 \text{ kN} \\ \text{and uniformly distributed traffic load } 18 \text{ kN/m (design values),} \\ \text{without load distribution}$$

$$V_{LD} := N_L \cdot W_f \cdot V_{LU}$$

$$V_{LD} = 242.735 \text{ kN} \quad \text{maximum shear force due to concentrated traffic load } 6 \times 187,5 \text{ kN} \\ \text{and uniformly distributed traffic load } 18 \text{ kN/m,} \\ \text{with load distribution}$$

$$V_t := 0.5 \cdot (0.6 \cdot V_{LU} + V_{LD}) \quad V_t = 426.242 \text{ kN}$$

9.0 Maximum shear stress

9.1 Maximum shear stress in the interior beam

$$V := V_t + V_g \quad V = 461.292 \text{ kN}$$

$$\tau := \frac{1.5 \cdot V}{t_w \cdot h_w} \quad \tau = 3.109 \text{ MPa}$$

maximum shear stress carried by the beam alone (conservative)

$$\tau = 3.109 \text{ MPa} \quad > \quad f_{vd} = 2.88 \text{ MPa} \quad \text{NOT OK}$$

9.2 Maximum shear stress in the exterior beam

$$V := V_t + V_{g,ex} \quad V = 456.794 \text{ kN}$$

$$\tau := \frac{1.5 \cdot V}{t_w \cdot h_w} \quad \tau = 3.079 \text{ MPa}$$

maximum shear stress carried by the beam alone (conservative)

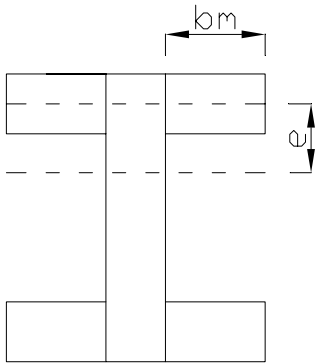
$$\tau = 3.079 \text{ MPa} \quad > \quad f_{vd} = 2.88 \text{ MPa} \quad \text{NOT OK}$$

The height of the web should be increased in order to take shear stress

9.3 Maximum shear stress at the interface between the web and the flange

$$V = 456.794\text{kN} \quad I = 0.066\text{m}^4$$

$$\tau_v = \frac{V \cdot Q}{I \cdot t_w}$$



$$Q := b_m \cdot t_f \cdot \left(h_w - \frac{t_f}{2} - y_c \right)$$

$$V = 456.794\text{kN}$$

$$\mu_s := 0.35 \quad \text{coefficient of friction for moisture content between 12\% and 16\%}$$

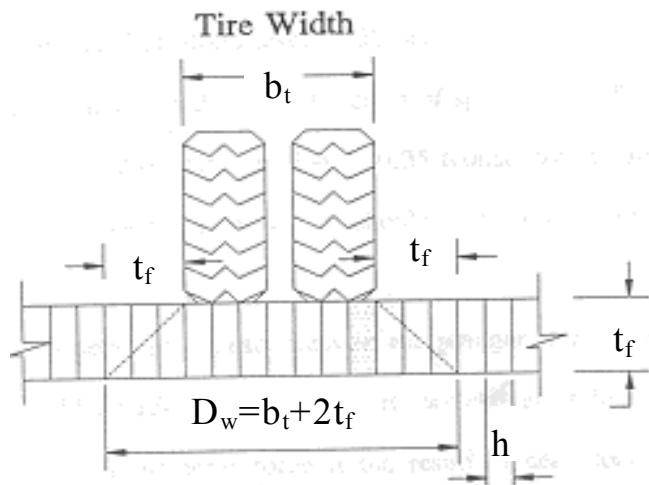
$$f_p := 0.55\text{MPa}$$

$$\tau_v := \frac{V \cdot Q}{I \cdot t_w} \quad \tau_v = 0.907\text{MPa}$$

$$V_{res} := f_p \cdot \mu_s \quad V_{res} = 0.193\text{MPa}$$

$$\tau_v = 0.907\text{MPa} > f_{vd} = 2.88\text{MPa} \quad \text{OK}$$

9.4 Maximum punching shear - local analysis



$$P = 187.5\text{kN}$$

one wheel load in combination IV:A (BRO 2004)

$$b_t := 0.72\text{m} + 2 \cdot 0.088\text{m}$$

tyre width according to BRO 2004+asphalt

$$t = 0.045\text{m}$$

width of one lamella

$$V_p := \frac{P}{b_t + 2 \cdot \frac{t_f}{2} \cdot \tan(15\text{deg})} \cdot t$$

$$V_p = 8.848\text{kN}$$

$$V_{\text{res}} = f_p \cdot b_l \cdot t_f \cdot \mu_s$$

resisting frictional force

$$f_p := 0.55 \cdot \text{MPa}$$

operational prestress level

$$\mu_s := 0.35$$

coefficient of friction for moisture content between 12% and 16%

$$b_l := 0.5\text{m}$$

tyre contact length in the direction of span

$$V_{\text{res}} := f_p \cdot b_l \cdot t_f \cdot \mu_s$$

$$V_{\text{res}} = 20.694\text{kN}$$

$$V_p = 8.848\text{kN}$$

<

$$V_{\text{res}} = 20.694\text{kN}$$

OK

10.0 Global deflection

Variable actions due to passage of traffic should be regarded as short-term actions. $k_{\text{def}} := 0$

in last combination V:C according to BRO2004 $\psi\gamma_{\text{def}} = 0.8$

$M_t := 1875 \text{ kNm}$ maximum moment due to 3x250kN

$M := M_t \cdot \psi\gamma_{\text{def}} + \frac{q_{\text{def}} \cdot L^2}{8}$ maximum moment due to 3x200kN + distributed traffic load

$W_f := 1.6 \cdot W_f$ $W_f = 0.382$ wheel factor multiplied by 1.6 in case of one lane bridge

$P_e := M \cdot \frac{4}{L}$ $P_e = 472 \text{ kN}$ equivalent concentrated load

$P_d := W_f \cdot P_e$ $P_d = 180.382 \text{ kN}$ design concentrated load

$\delta_{\parallel} := \frac{P_d \cdot L^3}{48 \cdot E_{LW} \cdot I_{ex}}$ $\delta_{\parallel} = 19.08 \text{ mm}$

according to EC5 $\delta_{\text{lim}} := \frac{L}{400}$ $\delta_{\text{lim}} = 37.5 \text{ mm}$

11.0 Vibrations (Bro 2004)

$$a_{\text{RMS}} = \frac{4 \cdot F \cdot v}{3.14 \cdot \sqrt{2} \cdot m \cdot E \cdot I}$$

$A_{\text{bridge}} := [2 \cdot b_x + (n_w - 1) \cdot (S - t_w)] \cdot t_f + n_w \cdot t_w \cdot h_w$ $A_{\text{bridge}} = 1.848 \text{ m}^2$ cross section of the bridge

$\text{mass}_{\text{bridge}} := \frac{6 \cdot \frac{\text{kN}}{\text{m}^3} \cdot A}{9.81 \cdot \frac{\text{m}}{\text{s}^2}}$ $\text{mass}_{\text{bridge}} = 294.336 \frac{\text{kg}}{\text{m}}$

$\text{mass}_{\text{surface}} := \frac{g_2 \cdot W}{9.81 \cdot \frac{\text{m}}{\text{s}^2}}$ $\text{mass}_{\text{surface}} = 875.173 \frac{\text{kg}}{\text{m}}$

$\text{mass} := \text{mass}_{\text{bridge}} + \text{mass}_{\text{surface}}$ $\text{mass} = 1.17 \times 10^3 \frac{\text{kg}}{\text{m}}$

$v := 15 \frac{\text{m}}{\text{s}}$ velocity of a vehicle

$$F := 240\text{kN}$$

$$E := E_{LW} \quad E = 1.3 \times 10^4 \text{MPa}$$

modulus of inertia of the whole cross-section of the bridge

$$A := [bx \cdot 2 + (n_W - 1) \cdot 2 \cdot B] \cdot t_f + n_W \cdot h_W \cdot t_W \quad A = 1.848\text{m}^2$$

$$S_X := [bx \cdot 2 + (n_W - 1) \cdot 2 \cdot B] \cdot t_f \cdot \left(h_W - \frac{t_f}{2} \right) + n_W \cdot h_W \cdot t_W \cdot \frac{h_W}{2} \quad S_X = 1.258\text{m}^3$$

$$y_C := \frac{S_X}{A} \quad y_C = 0.681\text{m}$$

$$I_{\text{tot}} := \frac{W \cdot t_f^3}{12} + W \cdot t_f \cdot \left(h_W - y_C - \frac{t_f}{2} \right)^2 + n_W \cdot \frac{t_W \cdot D^3}{12} + n_W \cdot t_W \cdot D \cdot \left(y_C - \frac{D}{2} \right)^2$$

$$I_{\text{tot}} = 0.177\text{m}^4$$

$$a_{\text{RMS}} := \frac{4 \cdot F \cdot v}{3.14 \cdot \sqrt{2 \text{mass} \cdot E \cdot I_{\text{tot}}}} \quad a_{\text{RMS}} = 1.979 \frac{\text{m}}{\text{s}^2}$$

$$f_n := \frac{3.14}{2 \cdot L^2} \cdot \sqrt{\frac{E \cdot I_{\text{tot}}}{\text{mass}}} \quad f_n = 9.776\text{Hz}$$

Appendix C – Comparison of maximum values of stress and deflection of the bridge for different configurations of Model 1

Table 1 Comparison of maximum values of stress and deflection of the bridge Config. 1 (5 webs, deck 215mm), beff calculated according to WVU1.

		FEM max results	Single beam		WVU conservative		WVU new approach	
			Hand calc.	Δ_1 [%]	Hand calc.	Δ_2 [%]	Hand calc.	Δ_3 [%]
Surface + self- weight + vehicle	Bending stress in the beam [MPa]	15,82	22,23	+40	16,46	+4	13,46	-15
	Shear force in the beam [kN]	286.01	353,56	+24	344,68	+21	321,08	+13
	Shear stress in the beam [MPa]	2.06	2,38	+16	2,32	+13	2,16	+5
	Compressive stress in the deck-Top [MPa]	-9,59	-11,98	+25	-8,87	-8	-7,25	-24
Vehicle	Deflection [mm]	33,8	43,12	+28	49,40	+46	39,11	+16

Table 2 Comparison of maximum values of stress and deflection of the bridge Config. 1 (5webs, deck 215mm), beff calculated according to WVU2.

		FEM max results	Single beam		WVU conservative		WVU new approach	
			Hand calc.	Δ [%]	Hand calc.	Δ [%]	Hand calc.	Δ [%]
Surface + self- weight + vehicle	Bending stress in the beam [MPa]	15,82	22,23	+40	16,50	+4	13,50	-15
	Shear force in the beam [kN]	286.01	353,56	+24	344,37	+21	320,89	+12
	Shear stress in the beam [MPa]	2.06	2,38	+16	2,32	+13	2,16	+5

	Compressive stress in the deck-Top [MPa]	-9,59	-11,98	+25	-9,00	-6	-7,37	-23
Vehicle	Deflection [mm]	33,8	43,12	+40	49,77	+47	39,44	+17

Table 3 Comparison of maximum values of stress and deflection of the bridge Config. 2A (4 webs, deck 215mm), beff calculated according to WVU1.

		FEM max results	Single beam		WVU1 conservative		WVU2 new approach	
			Hand calc.	Δ [%]	Hand calc.	Δ [%]	Hand calc.	Δ [%]
Surface + self-weight + vehicle	Bending stress in the beam [MPa]	18,42	22,38	+21	20,96	+14	16,46	-10
	Shear force in the beam [kN]	303.94	360,82	+18	385,35	+27	349,11	+15
	Shear stress in the beam [MPa]	2,22	2,43	+9	2,6	+17	2,353	+6
	Compressive stress in the deck-Top [MPa]	-10,4	-11,13	+7	-10,42	+0,2	-8,18	-21
Vehicle	Deflection [mm]	39,4	41,57	+6	62,48	+59	47,45	+20

Table 4 Comparison of maximum values of stress and deflection of the bridge Config. 2A (4 webs, deck 215mm), beff calculated according to WVU2.

		FEM max results	Single beam		WVU1 conservative		WVU2 new approach	
			Hand calc.	Δ [%]	Hand calc.	Δ [%]	Hand calc.	Δ [%]
Surface + self-weight + vehicle	Bending stress in the beam [MPa]	18,42	22,38	+21	21,07	+14	16,58	-10
	Shear force in the beam [kN]	303.94	360,82	+18	384,38	+26	348,55	+15
	Shear stress in the beam [MPa]	2,22	2,43	+9	2,6	+17	2,35	+6

	Compressive stress in the deck-Top [MPa]	-10,4	-11,13	+7	-10,84	+4	-8,53	-18
Vehicle	Deflection [mm]	39,4	41,57	+6	63,66	+62	48,48	+23

Table 5 Comparison of maximum values of stress and deflection of the bridge Config. 3B (3 webs, deck 280mm), beff calculated according to WVU1.

Belka pierwsza		FEM max results	Single beam		WVU1 - conservative		WVU2	
			Hand calc.	Δ [%]	Hand calc.	Δ [%]	Hand calc.	Δ [%]
Surface + self-weight + vehicle	Bending stress in the beam [MPa]	21,47	23,492	+9	23,61	+10	22,16	+3
	Shear force in the beam [kN]	401,23	389,08	-3	417,71	+4	405,7	+1
	Shear stress in the beam [MPa]	3,10	2,623	-25	2,816	-9	2,735	-11
	Compressive stress in the deck-Top [Mpa]	-9,91	-9,884	-0,3	-9,934	+0,2	-9,324	-6
Vehicle	Deflection [mm]	46,00	40,455	-12	65,1	+41	60,508	+32

Table 6 Comparison of maximum values of stress and deflection of the bridge Config. 3B (3 webs, deck 280mm), beff calculated according to WVU2.

		FEM max results	Single beam		WVU1 - conservative		WVU2	
			Hand calc.	Δ [%]	Hand calc.	Δ [%]	Hand calc.	Δ [%]
Surface + self-weight + vehicle	Bending stress in the beam [MPa]	21,47	23,335	+9	23,541	+10	22,02	+3
	Shear force in the beam [kN]	401,23	390,22	-3	419,60	+5	406,84	+1
	Shear stress in the beam [MPa]	3,10	2,63	-25	2,828	-9	2,74	-12

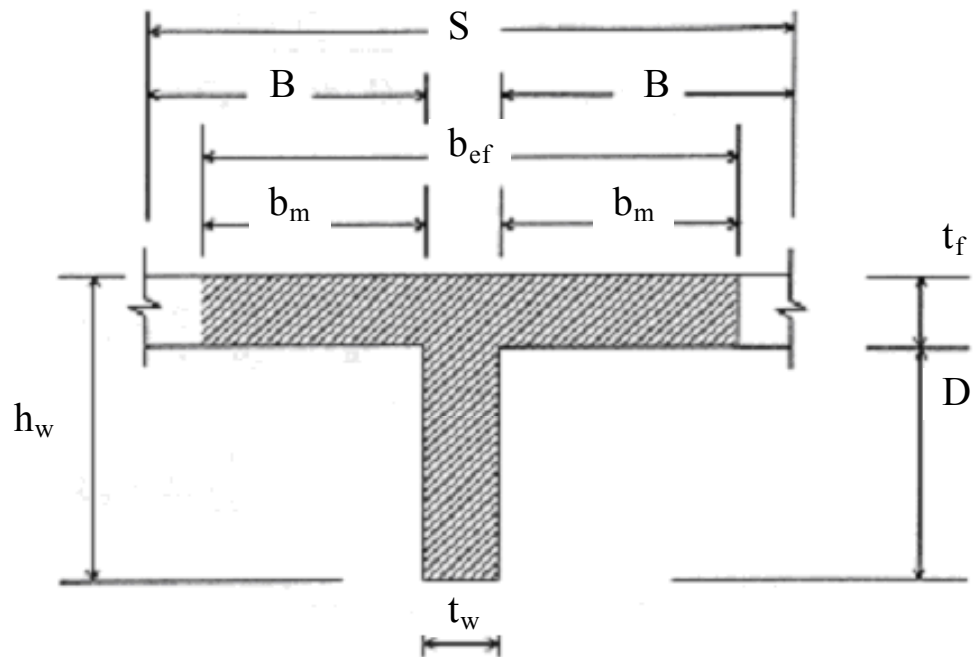
	Compressive stress in the deck-Top [MPa]	-9,91	-9,459	-0,3	-9,543	-4	-8,925	-10
Vehicle	Deflection [mm]	46,00	39,616	-12	64,032	+40	59,254	+29

$$\Delta_i = \frac{FEM_{result} - Hand.calc.}{FEM_{result}} \cdot 100\%$$

Appendix D – MathCAD file to calculate shear stresses in a T-beam bridge deck

1.0 T-beam bridge

1.1 Geometry



$t_f := 215\text{mm}$		thickness of the flange
$t_w := 215\text{mm}$		width of the web
$S := 935\text{mm}$		spacing
$h_w := 1035\text{mm}$		height of the web
$L := 15\text{m}$		span of the bridge
$D := h_w - t_f$	$D = 0.82\text{m}$	depth of portion of stringer that is outside the deck
$B := \frac{(S - t_w)}{2}$	$B = 0.36\text{m}$	one half clear spacing of webs
$n_w := 5$		number of webs
$b := (n_w - 1) \cdot S$		center to center distance between exterior stringers
$\alpha := \frac{b}{L}$		aspect ratio
$W := 4.495\text{m}$		width of the bridge

$N_L := 1$		number of lanes
$t := 45\text{mm}$		width of one lamella
$w := \frac{W - b - t_w}{2}$	$w = 0.27\text{m}$	width of exterior flange
$b_{\text{ef}} := 910\text{mm}$		effective flange width according to FEM, see Chapter 8.2
$b_{\text{ef.ex}} := 832.5\text{mm}$		

1.2 Moments of inertia

1.2.1. Moment of inertia of interior T-section

$$A := b_{\text{ef}} \cdot t_f + D \cdot t_w \quad A = 0.372\text{m}^2$$

Location of the neutral axis

$$S_{x1} := t_w \cdot \frac{D^2}{2} + b_{\text{ef}} \cdot t_f \left(h_w - \frac{t_f}{2} \right) \quad S_{x1} = 0.253748\text{m}^3$$

$$y_c := \frac{S_{x1}}{A} \quad y_c = 0.682\text{m}$$

$$S_x := t_w \cdot \frac{(D - y_c)^2}{2} + b_{\text{ef}} \cdot t_f \left(h_w - \frac{t_f}{2} - y_c \right) \quad S_x = 0.05\text{m}^3$$

$$I := t_w \cdot \frac{D^3}{12} + t_w \cdot D \cdot \left(y_c - \frac{D}{2} \right)^2 + b_{\text{ef}} \cdot \frac{t_f^3}{12} + b_{\text{ef}} \cdot t_f \left(h_w - \frac{t_f}{2} - y_c \right)^2$$

$$I = 0.035\text{m}^4$$

1.2.2. Moments of inertia of exterior T-section

$$A_{\text{ex}} := b_{\text{ef.ex}} \cdot t_f + D \cdot t_w \quad A_{\text{ex}} = 0.3553\text{m}^2$$

Location of the neutral axis

$$S_{x.\text{ex}1} := t_w \cdot \frac{D^2}{2} + b_{\text{ef.ex}} \cdot t_f \left(h_w - \frac{t_f}{2} \right) \quad S_{x.\text{ex}1} = 0.238294\text{m}^3$$

$$y_{c.\text{ex}} := \frac{S_{x.\text{ex}1}}{A_{\text{ex}}} \quad y_{c.\text{ex}} = 0.671\text{m}$$

$$S_{x,ex} := t_w \cdot \frac{(D - y_c)^2}{2} + b_{ef,ex} \cdot t_f \left(h_w - \frac{t_f}{2} - y_c \right) \quad S_{x,ex} = 0.046m^3$$

$$I_{ex} := t_w \cdot \frac{D^3}{12} + t_w \cdot D \cdot \left(y_{c,ex} - \frac{D}{2} \right)^2 + b_{ef,ex} \cdot \frac{t_f^3}{12} + b_{ef,ex} \cdot t_f \left(h_w - \frac{t_f}{2} - y_{c,ex} \right)^2$$

$$I_{ex} = 0.034m^4$$

1.3 Calculation of the shear stresses

$$V_1 := 27.6kN \quad \tau_1 := \frac{V_1 \cdot S_{x,ex}}{I_{ex} \cdot t_w} \quad \tau_1 = 0.172MPa$$

$$V_2 := 26.9kN \quad \tau_2 := \frac{V_2 \cdot S_x}{I \cdot t_w} \quad \tau_2 = 0.176MPa$$

$$V_3 := 25.5kN \quad \tau_3 := \frac{V_3 \cdot S_x}{I \cdot t_w} \quad \tau_3 = 0.167MPa$$

$$V_4 := 12kN \quad \tau_4 := \frac{V_4 \cdot S_x}{I \cdot t_w} \quad \tau_4 = 0.079MPa$$

$$V_5 := -1.94kN \quad \tau_5 := \frac{V_5 \cdot S_{x,ex}}{I_{ex} \cdot t_w} \quad \tau_5 = -0.012MPa$$

The value of the shear force was taken from FEM analysis, see Section 7.4.2.2.